Schweizerische Eidgenossenschaft
Confédération suisse
Confederazione Svizzera
Confederaziun svizra

Eidgenössisches Departement für Umwelt, Verkehr, Energie und Kommunikation UVEK
Département fédéral de l'environnement, des transports, de l'énergie et de la communication DETEC
Dipartimento federale dell'ambiente, dei trasporti, dell'energia e delle comunicazioni DATEC

Bundesamt für Strassen
Office fédéral des routes
Ufficio federale delle Strade

Modelling the corrosion initiation of reinforced concrete exposed to deicing salts

Modellierung der Initiierung von Korrosion bei chloridbelasteten Stahlbetonbauten

Modélisation de l'initiation de la corrosion due aux chlorures dans le béton armé

TFB AG - Technik und Forschung im Betonbau, Wildegg
Dr. Jan Bisschop
Dr. Yves Schiegg
Dr. Fritz Hunkeler

Forschungsprojekt AGB 2011/002 auf Antrag der Arbeitsgruppe Brückenforschung (AGB)

February 2016 **676**

Schweizerische Eidgenossenschaft
Confédération suisse
Confederazione Svizzera
Confederaziun svizra

Eidgenössisches Departement für Umwelt, Verkehr, Energie und Kommunikation UVEK
Département fédéral de l'environnement, des transports, de l'énergie et de la communication DETEC
Dipartimento federale dell'ambiente, dei trasporti, dell'energia e delle comunicazioni DATEC

Bundesamt für Strassen
Office fédéral des routes
Ufficio federale delle Strade

Modelling the corrosion initiation of reinforced concrete exposed to deicing salts

Modellierung der Initiierung von Korrosion bei chloridbelasteten Stahlbetonbauten

Modélisation de l'initiation de la corrosion due aux chlorures dans le béton armé

TFB AG - Technik und Forschung im Betonbau, Wildegg
Dr. Jan Bisschop
Dr. Yves Schiegg
Dr. Fritz Hunkeler

Forschungsprojekt AGB 2011/002 auf Antrag der Arbeitsgruppe Brückenforschung (AGB)

February 2016 **676**

Impressum

Forschungsstelle und Projektteam

Projektleitung
Dr. Yves Schiegg

Mitglieder
Dr. Jan Bisschop
Dr. Fritz Hunkeler

Begleitkommission

Präsident
Dr. Martin Käser

Mitglieder
Prof. Dr. Walter Kaufmann
Prof. Dr. Albin Kenel
Dr. Heidi Ungricht

Antragsteller

Arbeitsgruppe Brückenforschung (AGB)

Bezugsquelle

Das Dokument kann kostenlos von http://www.mobilityplatform.ch heruntergeladen werden.

Contents

Zusammenfassung

In diesem Bericht wird ein empirisches Modell für die Vorhersage der Initiierung von Korrosion der Bewehrung bei chloridbelasteten Stahlbetonbauten vorgeschlagen. Chloridinduzierte Korrosion ist eine Folge des Eindringens von Chloriden in den Beton, der in Kontakt mit Tausalzen oder Meerwasser kommt. In der Schweiz ist der Einsatz von Tausalzen weitverbreitet und Betonbauteile an Strassen, wie z.B. Brückenplatten, Stützen, Tunnelwänden oder Parkdecks können Chloride aufnehmen. Der Chloridgehalt in solchen Betonstrukturen steigt langsam an und nach Jahren oder Jahrzehnten wird ein Punkt erreicht, an dem der Betonstahl mit der kleinsten Bewehrungsüberdeckung zu korrodieren beginnt. Die Ansammlung von Korrosionsprodukten auf der Stahloberfläche führt im Laufe der Zeit zu Rissbildung oder Abplatzen des Überdeckungsbetons. Solche Schäden können umfangreiche Instandsetzungsmassnahmen oder sogar den vollständigen Rückbau des Bauteils zur Folge haben.

Chloridinduzierte Korrosion ist noch immer eine der Hauptursachen von Schäden an Betonbauten. Das Risiko einer Schädigung kann durch die Anwendung von Lebensdauermodellen, die unter Berücksichtigung der eingesetzten Werkstoffe und Strukturparameter den Zeitpunkt der Initiierung der Korrosion vorhersagen, teilweise verringert werden. Für bestehende Strukturen entspricht dies per Definition einer Vorhersage der Nutzungsdauer bis zum Korrosionsbeginn. Es ist klar, dass die effektive Nutzungsdauer eines Bauteils mit dem Beginn der Korrosion noch keineswegs erreicht ist. Da der Schadensfortschritt i.d.R. relativ langsam zunimmt, kann das Bauteil auch ohne Instandsetzung meist noch etliche Jahre bis Jahrzehnte genutzt werden. Wenn die Korrosion voraussichtlich noch vor dem Ende der erforderlichen Nutzungsdauer startet, kann die Lebensdauermodellierung helfen, einen Überwachungs- und Massnahmenplan zur Erhaltung der Betonstruktur zu entwickeln. Beim Neubau werden Lebensdauermodelle verwendet, um die Eigenschaften des Betons im Hinblick auf die Korrosionsbeständigkeit so effizient wie möglich zu verbessern. Es existieren zurzeit aber noch keine einfachen Rezepte, welche Beton- und Struktureigenschaften für das Erreichen einer bestimmten Lebensdauer unter Chloridbelastung erforderlich sind.

Aufgrund der hohen Bedeutung der Dauerhaftigkeit von Betonbauwerken sind in den letzten Jahrzehnten viele Vorhersagemodelle für den Chloridtransport und die Korrosionsinitiierung entwickelt worden. Es kann zwischen mechanistischen und empirischen Modellen unterschieden werden. Mechanistische Modelle enthalten Gleichungen für alle relevanten physikalischen und chemischen Reaktionen des Chloridtransports im Beton. Der umfangreiche Satz von Gleichungen erfordert in der Regel die Anwendung numerischer Modellierungen. Empirische Modelle basieren auf einer Gleichung, welche die primäre Transportphysik des Chloridtransports (z.B., Fick‘sches Gesetz) berücksichtigt. Allerdings sind detaillierte Mechanismen und deren Auswirkungen nicht explizit modelliert, sondern fliessen in die Ausgleichsrechnung (Fitting) mit ein. Empirische Modelle werden oft auf bestimmte Datensätze unter bestimmten Bedingungen abgestimmt, was die Anwendbarkeit solcher Modelle begrenzen kann. Auf der anderen Seite haben empirische Modelle den Vorteil, dass sie auch für Ingenieure leicht verständlich sind und mit handelsüblichen Tabellenkalkulationen berechnet werden können. Ausserdem erfordern sie die Eingabe von einer minimalen Anzahl von Parametern, die relativ einfach zu bestimmen sind.

Mechanistische Modelle beschreiben den Chloridtransportprozess genauer. Allerdings bedeutet dies nicht automatisch, dass sie genauere Vorhersagen ermöglichen als empirische Modelle, weil die Zuverlässigkeit der Vorhersage von der Repräsentativität der Eingabeparameter abhängig ist. Die Qualität der Vorhersageergebnisse kann nur durch den Vergleich mit Resultaten von Langzeitfeldmessungen überprüft werden. Die vorliegende Arbeit zeigt, wie langfristige Feldversuche genutzt werden, um Lebensdauermodelle zu validieren und anschliessend zu verbessern.

Das in diesem Bericht vorgeschlagene Vorhersagemodell basiert auf der bekannten Fehlerfunktionslösung (ERFC) des zweiten Fick‘schen Diffusionsgesetzes. Das Modell ist

sehr ähnlich zu bestehenden ERFC-Modellen, insbesondere dem DuraCrete-Modell. Es unterscheidet sich vom DuraCrete-Modell in der Weise, wie mit der Chloridoberflächenkonzentration und den sogenannten Transformationskonstanten umgegangen wird. Darüber hinaus sind einige der Eingangsparameter (vor allem der Alterungsfaktor), wie sie in der Literatur für DuraCrete erwähnt werden, für die (untersuchten) schweizerischen Verhältnisse und andere Situationen ungeeignet. Dies ist z.T. eine Folge der verschiedenen Modellabstimmungsverfahren, die in dieser Studie verwendet wurden.

Die Eingangsparameter des vorgeschlagenen Modells wurden unter Verwendung der Daten vom Feldversuch im Naxbergtunnel abgestimmt. Diese Untersuchungen wurden im Jahr 2000 im Naxberg Tunnel bei Göschenen im Kanton Uri (Höhe ca. 1000 Meter ü. M. und eine durchschnittliche Jahrestemperatur von 7°C) gestartet. In diesem Experiment wurden instrumentierte Betonplatten mit einer Abmessung von 60 x 50 x 10 cm hergestellt und in einer ca. 50 m vom Tunnelportal entfernten Nische der Tunnelwand (Spur Süd) montiert. Das Ziel dieses Feldversuches war die Untersuchung des Wasser- und Chlorideintrags bei unterschiedlichen Betonsorten, der Einfluss der Bewehrungsüberdeckung auf die Initiierung und den Korrosionsfortschritt sowie das Korrosionsverhalten unterschiedlicher Stahlqualitäten in verschiedenen Betonen unter realen Expositionsbedingungen. Zusammen mit den Betonplatten wurden zusätzliche Betonwürfel zur Überwachung der Entwicklung von verschiedenen Eigenschaften (Druckfestigkeit, Porosität und Transporteigenschaften) hergestellt.

Die untersuchten Betonsorten (Typ A bis H) enthalten Portlandzement oder eine Kombination aus Portlandzement und Zusatzstoffen (Silikastaub, Flugasche oder Hüttensand). Einzelne Platten wurden hydrophobiert. Pro Mischung wurden jeweils vier Platten übereinander am Tunnelgewölbe montiert. Durch die variable Höhenlage der Platten variiert die Expositionsklasse möglicherweise von unten (Platte 1) nach oben (Platte 4) zwischen XD3 (Spritzwasser) und XD1 (Sprühnebel). Insgesamt wurden 65 Bohrkerne aus den Betonplatten genommen, hauptsächlich zur Bestimmung von Chloridprofilen nach unterschiedlicher Expositionsdauer (1.5; 2.5; 3.5; 4.4; 12 und 12.8 Jahre).

Die gemessenen Chloridprofile zeigen einen kontinuierlichen Chlorideintrag über die Zeit. Nach 12 Jahren zeigen die meisten Profile einen maximalen Chloridgehalt im Betoninnern. Diese Spitzen (maximale Chloridkonzentration) treten häufig in einer Tiefe von etwa 20 mm auf. Dies ist ein typisches Phänomen bei Bauteilen, die salzhaltigem Spritzwasser ausgesetzt sind. Das Maximum wird vermutlich durch Trocknung, Auslaugung und Karbonatisierung des oberflächennahen Betons verursacht. Es gibt einen signifikanten Effekt von der Betonzusammensetzung auf die Geschwindigkeit und Tiefe der Chloridpenetration. Die Platten mit CEM I und einem w/z-Wert von 0.5 (Betone B, C und H) zeigen den stärksten Chlorideintrag, gefolgt von den Betonen mit Hüttensand (Beton D) und Flugasche (Beton E) mit dem gleichen w/z-Wert. Beton mit Silikastaub (Beton F) und CEM I Beton mit w/z-Wert von 0.35 (Beton G) zeigen die niedrigsten Eindringraten.

Nach 12 Jahren zeigen die Platten mit der grössten Porosität eine ‘Sättigung‘ des Betons mit Chloriden über die gesamte Plattenstärke von 10 cm. Ein einfaches Diffusionstyp-Modell kann diese hohe Konzentration von Chloriden in einer Tiefe von 70 bis 100 mm nicht prognostizieren. Ausgeprägtes kapillares Saugen und die relativ geringe Plattenstärke (10 cm) dürften die Ursache für diese Sättigung sein. Sonstige Beobachtungen aus den Chloridprofilen waren eine Abnahme der Chloridkonzentration und Eindringtiefe mit zunehmender Höhe über dem Bankett und ein stark reduzierter Chlorideintrag bei hydrophobierten Platten.

Mittels Regressionsverfahren an den gemessenen Chloridprofilen wurde der sogenannte scheinbare (‘apparant‘) Chloriddiffusionskoeffizient (D_{app}) der Feldbetone bestimmt. Dabei wurde festgestellt, dass die Betonzusammensetzung einen grossen Einfluss auf D_{app} hat. Der Unterschied von D_{app} zwischen dem Beton mit der höchsten Porosität/Permeabilität (H) und den dichteren Betonen (G und F) beträgt nach 12.8 Jahren Exposition einen Faktor 6 bis 7. Alle Betone zeigen eine Abnahme von D_{app} in den ersten 2.5 Jahren, die wahrscheinlich auf eine dichter werdende Struktur durch anhaltende Zementhydratation zurückzuführen ist. Die langfristige Veränderung von D_{app} unterscheidet sich bei den verschiedenen Betonen. Betone mit reinem Portlandzement erreichen einen praktisch

stabilen D_{app}-Wert nach 2.5 Jahren. Für Betone mit Zusatzstoffen nimmt D_{app} über die Zeit exponentiell ab, wobei D_{app} für die Platten 1 (Höhe 0-60 cm) in der Regel höher ist als D_{app} für die Platten 3 (Höhe 120-180 cm). Die höchste gemessene Chloridkonzentration (C_{max}) und die durch das Regressionsverfahren erhaltene Oberflächenkonzentration zeigen während der gesamten Versuchsdauer von 12 Jahren für alle Betonsorten einen allmählichen Anstieg.

Eine erste empirische Modellierung wurde mit den gemessenen Chloridprofilen und den scheinbaren Diffusionskoeffizienten (D_{app}) durchgeführt. Ein Ausgangsprofil das nach 2.5 bzw. 4.4 Jahren gemessen wurde, diente als Grundlage für die Berechnung der zukünftigen Profile nach 4.4 bzw. 12.8 Jahren. Die vorhergesagten Chloridprofile wurden anschliessend mit den entsprechenden, gemessenen Profilen verglichen. Das Ergebnis dieses Vergleichs war zufriedenstellend und zeigte, dass die Entwicklung der Naxberg Chloridprofile dem Fick'schen Diffusionsgesetz folgt. Dieses Ergebnis bedeutet jedoch nicht, dass der Chlorideintrag in jedem Fall ein reiner Diffusionsprozess ist. Es zeigt lediglich, dass die Entwicklung von Chloridprofilen (empirisch) durch eine mathematische Gleichung zweiter Ordnung wie das zweite Diffusionsgesetz beschrieben werden kann.

Für das vorgeschlagene Vorhersagemodell werden zwei weitere Eingangsparameter benötigt: (i) der Chloridmigrationskoeffizient von Beton im Alter von 28 Tagen (M_{28d}), und (ii) der kritische Chloridgehalt (C_{crit}). Im Labor wurde M_{28d} mit einem Standardverfahren (Norm SIA 262/1: Anhang B) gemessen und C_{crit} mit einer neu entwickelten Methode bestimmt. Der Parameter C_{crit} ist definiert als Chloridkonzentration im Beton, bei der die Depassivierung bzw. die Korrosion von Bewehrungsstahl beginnt. Dies ist einer der entscheidenden Input-Parameter zur Modellierung von Stahlbetonkorrosion. Unsere Messungen zeigten, dass es einen deutlichen Einfluss von Stahlsorte und Oberflächenbearbeitung auf C_{crit} gibt und, dass die gemessenen C_{crit}-Werte für normalen Betonstahl im Bereich von in der Literatur oder in den Normen publizierten Werte liegen.

Das in diesem Bericht vorgeschlagene Prognosemodell für den Chloridtransport beruht auf der Lösung des zweiten Fick'schen Gesetzes unter der Annahme eines konstanten Diffusionskoeffizienten (D) und einer konstanten Chlorid-Oberflächenkonzentration (C_s):

$$C(x,t) = C_{s,app} \cdot erfc\left(\frac{x}{2\sqrt{D_{app} \cdot t}}\right)$$

Im DuraCrete Ansatz wird D_{app} für eine bestimmte Expositionsdauer unter Verwendung der folgenden Gleichung berechnet:

$$D_{app} = K \cdot M_{28d} \cdot \left(\frac{t_0}{t}\right)^n$$

Dabei ist M_{28d} der Chloridmigrationskoeffizient, der im Labor bei einem Alter von 28 Tagen gemessen wird. Der Zeitpunkt t_0 ist die Referenzzeit (in Jahren), bei dem M gemessen wird, oder das Alter der ersten Chloridexposition (z.B. t_0 = 28 Tage). Die Zeit t ist die Chloridexpositionsdauer in Jahren. Der Korrelationsfaktor K ist eine Konstante, die den experimentell gemessenen M_{28d} mit dem aus den Felddaten bestimmten D_{app} verbindet. Der Alterungsfaktor n beschreibt, wie sich der Diffusionskoeffizient des Betons im Laufe der Zeit ändert.

Die Inputparameter K und n wurden mittels eines 'Tuning'-Verfahrens für jede Betonart separat bestimmt. Die Werte von K und n wurden so gewählt, dass die erhaltenen Chloridprofile mit den gemessenen Naxberg-Chloridprofilen bestmöglichst übereinstimmen. Die benötigten Migrationskoeffizienten (M_{28d}) wurden im Labor mit denselben Betonen wie im Naxbergtunnel gemessen. Für die Entwicklung der Chloridoberflächenkonzentration (C_{s_app}) wurde angenommen, dass diese der empirischen Gleichung aus den Naxberg-Messungen folgt. Es wurde festgestellt, dass K einen "universellen" Wert

von 0.5 für alle Betonarten darstellt, während der Alterungsfaktor n zwischen den verschiedenen Betonarten variiert.

Die Modellparameter K und n aus den Naxberg-Daten wurden für andere Feldexperimente in der Schweiz und in Schweden validiert. Bei dieser Validierung wurde festgestellt, dass die Chloridprofile aus anderen Feldexperimenten nicht mit den Naxberg-Parametern vorhergesagt werden können. Nur wenn die Chloridoberflächenkonzentration und Alterungsfaktoren angepasst wurden, war die Übereinstimmung der vorhergesagten mit den gemessenen Profilen gut. Die Chloridoberflächenkonzentration (C_{s_app}) ist abhängig vom Angebot an Chloriden für bestimmte Expositionsbedingungen und dieser Parameter kann darum nicht ohne weiteres vorhergesagt werden. Im Naxbergtunnel waren die Chloridoberflächenkonzentration viel höher als in den anderen beiden untersuchten Feldexperimenten. Der Alterungsfaktor n ist ebenfalls keine Materialkonstante, die nur von der Betonsorte abhängig ist. Umwelteinflüsse wie die Trocknungs- und Karbonatisierungsraten beeinflussen den Alterungsfaktor n. Demzufolge kann sich n mit den Expositionsbedingungen ändern.

Aufgrund der Validierung wurde klar, dass die Entwicklung der Chloridprofile am genauesten durch die Verwendung eines Alterungsfaktors n von 0.45 beschrieben werden kann, falls die Chloridoberflächenkonzentration mit dem gemessenen Wert übereinstimmt. Dies konnte für einen Beton mit reinem Portlandzement und für einen Beton mit einer Zugabe von 5% Silikastaub gezeigt werden. In einer nachfolgenden Variante wurde getestet, ob n = 0.45 in Kombination mit der vorhandenen Chloridoberflächenkonzentration auch zur Vorhersage der Naxberg-Profile verwendet werden kann. Für Betonsorten mit einer geringen Porosität waren diese Prognosen gut. Für die beiden Betonarten mit einer deutlich höheren Porosität und stärkeren Chlorideinträgen war es hingegen nicht möglich, einen n-Wert von 0.45 zu verwenden, um die gemessenen Chloridprofile rechnerisch zu bestätigen. Der Grund dafür dürfte darin liegen, dass der Chlorideintrag in den meisten, poröseren Naxberg-Betonen nicht überwiegend durch Diffusion gesteuert ist. Ein Beitrag vom variablen, kapillaren Saugen kann die Alterungsfaktoren in diesen relativ porösen Betonen beeinflusst haben.

Im abschliessenden Teil des Berichts werden einige Beispiele von Lebensdauerberechnungen erläutert. Diese zeigen, wie verschiedene Faktoren wie z.B. die Bewehrungsüberdeckung, Chloridoberflächenkonzentration und die Betonzusammensetzung die korrosionsfreie Nutzungsdauer von Stahlbetonbauteilen beeinflussen. In einigen dieser Berechnungen wurden Input-Parameter aus der Norm SIA 262 verwendet um zu testen, ob mit den Vorgaben dieser Norm eine ausreichende Dauerhaftigkeit sichergestellt werden kann. Für die Expositionsklasse XD3 konnte gezeigt werden, dass die Norm SIA 262 eine korrosionsfreie Lebensdauer von mindestens 25 Jahren garantiert, wenn die Lebensdauer auf eine deterministische Weise (d.h. ohne Streuung der Input-Parameter) berechnet wird. Die Lebensdauerberechnungen weisen darauf hin, dass eine Anpassung der Grenzwerte für M_{28d} für die Expositionsklasse XD3 und/oder die Bewehrungsüberdeckung in der Norm SIA 262 Betonbauten geprüft werden sollte. Relativ geringe Änderungen, z.B. $M_{28d} = 8 \cdot 10^{-12}$ m²/s anstelle von $10 \cdot 10^{-12}$ m²/s, oder eine Bewehrungsüberdeckung von 50 mm anstatt 45 mm kann die Initiierungszeit unter XD3 Exposition um rund 25 Jahre verlängern.

Der Bericht schliesst mit einem Leitfaden, in dem Schritt für Schritt aufgezeigt wird, wie die Nutzungsdauer von neuen oder bestehenden Bauwerken ermittelt werden kann.

Résumé

Ce rapport propose un modèle empirique pour la prédiction du processus d'initiation de la corrosion des aciers d'armature, dans les ouvrages en béton armé contaminés en chlorures. La corrosion induite par les chlorures est une conséquence de la pénétration des ions chlorures dans le béton exposé à l'eau de mer ou aux produits de déverglaçage. En Suisse, l'utilisation des sels de déverglaçage est très répandue et les éléments de construction en béton au voisinage des chaussées, comme par ex. tabliers de ponts, murs de soutènement, parois de tunnels ou dalles de parkings peuvent absorber des chlorures. La contamination en chlorures dans des structures de ce genre augmente très lentement et ce n'est qu'après des années, voire des décennies qu'elle atteint un seuil critique où le béton armé avec un enrobage d'armature minimal commence à corroder. Au fur et à mesure du temps, l'accumulation des produits de corrosion à la surface de l'acier mènent à des fissurations ou à des éclatements du béton d'enrobage. Ces dégradations peuvent occasionner d'importants travaux de remise en état ou même la destruction complète de l'élément de structure.

La corrosion induite par les chlorures reste l'une des raisons majeures de la détérioration des ouvrages en béton. Le risque de dégradation peut en partie être réduit par l'application de modèles de durabilité qui, compte tenu des matériaux utilisés et des paramètres structuraux, peuvent prédire la durée d'initiation du processus de corrosion. Pour les structures existantes, ceci correspond par définition à une prédiction de la durée de service jusqu'à l'amorçage de la corrosion. Il est clair que la durabilité effective d'un élément de structure n'est encore atteinte en aucune façon avec l'initiation de la corrosion. Comme l'évolution de la dégradation est en général assez lente, l'élément de structure peut encore rester en usage pendant des années ou même des décennies sans nécessité de remise en état. Si la corrosion semble s'amorcer avant la fin de la durée de vie prévue, la modélisation de la durabilité peut contribuer à développer un plan de surveillance et de mesures pour la maintenance de la structure en béton. Dans le projet de nouvelles constructions, les modèles de durabilité sont appliqués pour améliorer le plus efficacement possible les propriétés du béton à l'égard de la résistance à la corrosion. Mais pour l'instant, il n'existe pas encore de recette toute prête, à savoir quelles sont les propriétés du béton et des structures exigibles pour obtenir une durabilité définitive sous la charge des chlorures.

En raison de l'importance majeure de la durabilité des ouvrages d'art en béton, de nombreux modèles de prédiction pour le transport des ions chlorures et l'initiation du processus de corrosion ont été développés au cours des dernières décennies. Il y a lieu de distinguer entre les modèles mécaniques et les modèles empiriques. Les modèles mécaniques contiennent des équations pour toutes les réactions physico-chimiques significatives pour le transport des chlorures dans le béton. La multitude d'équations nécessite généralement le recours à une modélisation numérique. Les modèles empiriques se basent sur une équation qui tient compte de la physique de transport primaire pour le mouvement des ions chlorures (par ex. la loi de Fick). Toutefois, les mécanismes détaillés et leurs effets ne sont pas explicitement modélisés, mais s'intègrent dans le calcul d'optimisation (fittage). Les modèles empiriques sont conformés à des bases de données déterminées sous des conditions déterminées, ce qui peut limiter l'application de tels modèles. D'autre part, les modèles empiriques ont l'avantage d'être aisément compréhensibles également pour les ingénieurs et peuvent être calculés au moyen de tableurs d'usage. En outre, ils ne nécessitent qu'un nombre restreint de paramètres d'entrée pouvant être déterminés de manière relativement simple.

Les modèles mécaniques décrivent le phénomène de transport des ions chlorures plus précisément. Ce qui ne veut pas dire automatiquement qu'ils permettent des prédictions plus précises que les modèles empiriques, car la fiabilité de la prédiction dépend de la représentativité des paramètres d'entrée. La qualité des résultats prédictifs ne peut être vérifiée qu'avec des résultats de mesures comparatifs, recueillis à long terme sur le terrain. Le présent travail montre l'utilité des mesures de champ à long terme, pour valider les modèles de durabilité et les améliorer par la suite.

Le modèle de prédiction proposé dans ce document repose sur la fonction erreur complémentaire bien connue (ERFC) de la seconde loi de diffusion selon Fick. Ce modèle est très semblable aux modèles ERFC existants, en particulier le modèle DuraCrete. Il se distingue du modèle DuraCrete dans la manière de traiter l'accumulation des ions chlorures à la surface et les nommées constantes de transformation. Qui plus est, certains paramètres d'entrée (avant tout le facteur de vieillissement) cités dans la littérature propre à DuraCrete, ne se prêtent pas aux conditions (investiguées) qui règnent en Suisse ou à d'autres situations. Ceci est une conséquence partielle des différents procédés de conformité des modèles utilisés dans cette étude.

Les paramètres d'entrée du modèle proposé ont été adaptés à partir des données de l'essai de champ dans le tunnel du Naxberg. Ces investigations ont été lancées en l'an 2000 dans le tunnel du Naxberg, près de Göschenen dans le canton d'Uri (altitude env. 1000 m, température moyenne annuelle de 7°C). Dans cet essai, des plaques de béton instrumentées, d'une dimension de 60 x 50 x 10 cm ont été fabriquées et posées dans une niche de la paroi du tunnel située à env. 50 m de l'entrée du tunnel (voie sud). L'objectif de l'essai était d'examiner la pénétration de l'eau et des chlorures dans différentes sortes de béton, l'influence de l'enrobage d'armature sur l'initiation et la progression de la corrosion, ainsi que la tenue à la corrosion de différentes qualités d'acier dans différents bétons, sous des conditions d'exposition réelles. Outre les plaques en béton, on a fabriqué des cubes de béton pour la surveillance du développement de différentes propriétés spécifiées (résistance à la compression, porosité et propriétés de transport).

Les sortes de béton investiguées (types A à H) contiennent du ciment Portland ainsi que des additions (fumées de silice, cendres volantes ou laitiers de haut fourneau). Certaines plaques ont subit une imprégnation hydrofuge. Quatre plaques par mélange ont été superposées à la voûte du tunnel. Du fait de la variation en hauteur des plaques, la classe d'exposition varie de bas (plaque 1) en haut (plaque 4) entre XD3 (projections d'eau) et XD1 (embruns). Au total 65 carottes ont été extraites des plaques en béton, avant tout pour déterminer les profils de chlorures selon des durées d'exposition variables (1,5 ; 2,5 ; 3,5 ; 4,4 ; 12 ; et 12,8 années).

Les profils de chlorures mesurés indiquent une pénétration continue des ions dans le temps. Après 12 ans, la plupart des profils révèlent une contamination en chlorures maximale dans le cœur du béton. Ces pics (concentration de chlorures maximale) apparaissent souvent à une profondeur d'environ 20 mm. Ceci est un phénomène typique pour les éléments de structure exposés à la projection d'eau saline. Le maximum est probablement causé par la dessiccation, le délavage et la carbonatation du béton dans une zone proche de la surface. La composition du béton a un effet significatif sur la vitesse et la profondeur de pénétration des ions chlorures. Les plaques à base de CEM I et un rapport e/c de 0.5 (bétons B, C et H) révèlent la pénétration la plus forte, suivies des bétons avec laitiers (béton D) et cendres volantes (béton E) de même valeur e/c. Le béton avec fumées de silice (béton F) et le béton CEM I avec un rapport e/c de 0.35 (béton G) présentent les taux de pénétration les plus faibles.

Après 12 ans, les plaques présentant la plus grande porosité révèlent une saturation en chlorures de 10 cm sur toute l'épaisseur de la plaque. Un modèle de type de diffusion simple n'est pas en mesure de pronostiquer une concentration en chlorures aussi élevée à une profondeur de 70 à 100 mm. Une succion capillaire prononcée et l'épaisseur de la plaque (10 cm) pourraient être à l'origine de cette saturation. Les profils de chlorures ont fait observer en outre une diminution de l'accumulation et de la profondeur de pénétration des ions en fonction de l'augmentation de la hauteur depuis l'accotement, ainsi qu'une réduction accentuée de la pénétration des chlorures dans les plaques bénéficiant d'une imprégnation hydrofuge.

Au moyen de la méthode de régression à partir des profils de chlorures mesurés, on a déterminé le coefficient de diffusion apparent (D_{app}) des bétons étudiés. On a constaté que la composition du béton avait une grande influence sur le D_{app}. La différence du D_{app} entre le béton à plus grande porosité / perméabilité (H) et les bétons plus compacts (G et F) était d'un facteur de 6 à 7 après 12 années d'exposition. Tous les bétons révèlent une

réduction du D_{app} au cours des premiers 2.5 ans, due probablement à une structure devenant plus compacte grâce à l'hydratation permanente du ciment. La modification à long terme du D_{app} diffère d'un béton à l'autre. Les bétons qui contiennent uniquement du ciment Portland atteignent une valeur D_{app} pratiquement stable après 2.5 ans. Les bétons avec additions subissent une décroissance exponentielle du D_{app} dans le temps, D_{app} étant en général plus élevé dans les plaques 1 (hauteur 0-60 cm) que dans les plaques 3 (hauteur 120-180 cm). Le plus haut degré de concentration en chlorures mesuré (C_{max}) ainsi que la concentration à la surface obtenue par la méthode de régression, indiquent un accroissement progressif dans toutes les sortes de béton, au cours de l'ensemble des essais d'une durée totale de 12 ans.

Une première modélisation empirique a été effectuée au moyen des profils de chlorures mesurés et des coefficients de diffusion (D_{app}). Un profil de sortie mesuré après 2.5, resp. 4.4 ans a servi de base pour le calcul des profils futurs après 4.4 ou 12 ans. Les profils de chlorures ont ensuite été comparés aux profils mesurés correspondants. Le résultat de cette comparaison s'est avérée satisfaisant et a démontré que l'évolution des profils de chlorures du Naxberg suivait la loi de diffusion de Fick. Néanmoins, ce résultat ne signifie pas que la pénétration de chlorures soit un pur processus de diffusion dans chaque cas. Il indique uniquement que l'évolution des profils de chlorures (empirique) peut être décrite par une équation mathématique de deuxième ordre, comme la seconde loi de diffusion.

Le modèle de prédiction proposé nécessite encore deux autres paramètres d'entrée : (i) le coefficient de migration des chlorures dans un béton âgé de 28 jours (M_{28d}) et (ii) la teneur en chlorures critique (C_{crit}). M_{28d} a été mesuré en laboratoire avec un procédé standard (norme SIA 262/1 : annexe B) et C_{crit} à l'aide d'une nouvelle méthode développée depuis peu. Le paramètre C_{crit} est défini en tant que concentration des chlorures dans le béton à partir de laquelle s'amorce la dépassivation, resp. la corrosion des aciers d'armature. Ce paramètre d'entrée est des plus décisifs pour la modélisation de la corrosion du béton armé. Nos mesures ont montré que le type d'acier et le traitement des surfaces exerçaient une influence notable sur C_{crit} et que les valeurs C_{crit} mesurées pour un béton ordinaire, se situaient dans la zone des valeurs publiées dans les normes ou la littérature.

Le modèle de prédiction pour le transport des ions chlorures proposé dans ce rapport, repose sur la résolution de la seconde loi de Fick, supposant un coefficient de diffusion constant (D) et une concentration en chlorures à la surface constante (Cs) :

$$C(x,t) = C_{s,app} \cdot erfc\left(\frac{x}{2\sqrt{D_{app} \cdot t}}\right)$$

Dans le modèle DuraCrete, D_{app} est calculé pour un temps d'exposition déterminé en utilisant l'équation suivante :

$$D_{app} = K \cdot M_{28d} \cdot \left(\frac{t_0}{t}\right)^n$$

M_{28d} est le coefficient de migration des ions chlorures qui est mesuré en laboratoire à un âge de 28 jours. t_o est le temps de référence (en années) pendant lequel on mesure M ou l'âge de la première exposition aux chlorures (par ex. t_o = 28 jours). Le temps t est la durée d'exposition aux chlorures en années. Le facteur de corrélation K est une constante qui lie la mesure expérimentale M_{28d} au D_{app} déterminé à partir des données recueillies sur le terrain. Le facteur de vieillissement n décrit la modification du coefficient de diffusion du béton au fur et à mesure du temps.

Les paramètres d'entrée K et n ont été déterminés séparément pour chaque sorte de béton au moyen d'un procédé « Tuning ». Les valeurs K et n ont été choisies en sorte

que les profils de chlorures obtenus correspondent autant que possible aux profils de chlorures du Naxberg. Les coefficients de migration M_{28d} nécessités ont été mesurés en laboratoire avec des bétons identiques à ceux du tunnel du Naxberg. Pour l'évolution de la concentration de chlorures à la surface (C_{s_app}), il a été admis que celle-ci suivait l'équation empirique issue des mesures du Naxberg. On a constaté que K représentait une valeur « universelle » de 0.5 pour toutes les sortes de béton, tandis que le facteur de vieillissement n variait selon les sortes de béton.

Les paramètres de modélisation K et n à base des données du Naxberg, ont été validées pour d'autres essais sur le terrain en Suisse et en Suède. Lors de cette validation, il a été constaté que les profils de chlorures provenant d'autres essais de champ ne pouvaient pas être prédits par les paramètres du Naxberg. Un bon état de conformité entre les profils prédits et les profils mesurés n'a été obtenu qu'après avoir adapté la concentration en chlorures à la surface et le facteur de vieillissement. La concentration en chlorures à la surface (C_{s_app}) est dépendante de la teneur en chlorures pour une classe d'exposition définie et ce paramètre ne peut pas être prédit d'emblée. Dans le tunnel du Naxberg, les concentrations en chlorures à la surface étaient beaucoup plus élevées que dans les deux autres essais effectués sur le terrain. Le facteur de vieillissement n n'est pas non plus une constante propre aux matériaux et qui ne dépend que de la sorte de béton. Les influences environnementales comme la dessiccation et la carbonatation influencent également le facteur de vieillissement n. Par conséquent, n peut se modifier suivant la classe d'exposition.

En considération de la validation, il est devenu évident que l'évolution des profils de chlorures ne peut être décrite de manière précise qu'en utilisant un facteur de vieillissement n de 0.45, pour autant que la concentration en chlorures à la surface concorde avec la valeur mesurée. Ceci a pu être démontré en présence d'un béton contenant du pur ciment Portland et d'un béton avec une addition de 5% de fumées de silice. Dans une autre variante, il a été testé si n = 0.45, en combinaison avec l'accumulation de chlorures présente à la surface, pouvait également être utilisé pour la prédiction des profils du Naxberg. Pour les sortes de béton de faible porosité, les prédictions furent bonnes. Par contre, pour les deux sortes de béton de porosité nettement plus élevée et des pénétrations de chlorures plus intenses, il n'a pas été possible d'utiliser la valeur n de 0.45 pour confirmer par calcul les profils de chlorures mesurés. Ceci pourrait être attribué au fait que la pénétration des chlorures dans la plupart des bétons du Naxberg plus poreux, ne se fait pas seulement par diffusion. L'absorption capillaire variable pourrait avoir influencé partiellement les facteurs de vieillissement dans ces types de béton relativement poreux.

La dernière partie de ce rapport est illustrée par quelques exemples de calculs de la durée de vie. Ceux-ci montrent l'influence exercée par différents facteurs, par ex. l'enrobage de l'armature, l'accumulation des chlorures à la surface et la composition du béton, sur la durée de vie exempte de corrosion des éléments de structure en béton armé. Des paramètres tirés de la norme SIA 262 ont été utilisés dans certains calculs, dans le but de tester si les recommandations de la norme étaient à même d'assurer une durabilité des ouvrages suffisante. Concernant la classe d'exposition (XD3), il a pu être démontré que la norme SIA 262 garantissait une durée de vie à l'abri de la corrosion de 25 ans au moins, si la durabilité était calculée de manière déterministe (c.-à-d. sans dispersion des paramètres d'entrée). Les calculs d'évaluation de la durabilité indiquent qu'il conviendrait d'examiner un ajustement des valeurs limites M_{28d} pour la classe d'exposition XD3 et/ou de l'enrobage d'armature faisant foi dans la norme 262 « Construction en béton ». De petites modifications comme par ex. $M_{28d} = 8 \cdot 10^{-12}$ m²/s au lieu de $10 \cdot 10^{-12}$ m²/s ou un enrobage de l'armature de 50 mm au lieu de 45 mm pourraient prolonger le temps d'initiation de 25 ans sous XD3.

Le rapport se termine par un fil conducteur qui dépeint pas à pas comment déterminer la durée de vie d'ouvrages neufs ou déjà existants.

Summary

In this report an empirical model for the prediction of the onset of chloride-induced corrosion of steel reinforcement in concrete is proposed. Chloride-induced corrosion is a result of the ingress of dissolved chloride salts into concrete that is in contact with seawater or deicing salts. In Switzerland deicing salts are widely used, and concrete structures near roads, such as bridge decks, overpass supports, tunnel walls or parking floors, may take up chlorides. In such environments, the chloride content of the concrete slowly increases and after years or tens of years the point is ultimately reached at which the reinforcement steel with the smallest distance from the concrete surface will start to corrode. The builtup of corrosion products around the steel in concrete, leads to cracking or spalling of the cover concrete. The damage may proceed to a stage that requires large-scale rehabilitation or complete demolition of a concrete element or structure.

Chloride-induced corrosion still is a major cause of damage of concrete structures. The problem can partly be avoided by applying a service life model that predicts the onset of corrosion from a number of material and structure parameters. For existing structures this means predicting the remaining lifetime until corrosion starts. If the corrosion is expected to start before the ending of the required service lifetime, then service life modelling helps to develop a concrete structure monitoring and renovation plan. For new concrete structures, service life models are used to make concrete structure design as efficient as possible with regard to corrosion resistance. Which concrete and structure properties are required for achieving a given lifetime in a given environment with chloride ingress? Note that in cases of a slow development of corrosion-induced damage, the practical service life of concrete structures may be significantly longer than the predicted service life.

Because of its high importance, many prediction models for chloride transport and corrosion initiation in concrete have been developed in the last decades. A distinction can be made between mechanistic and empirical models. Mechanistic models contain equations for all relevant physical and chemical reactions in the chloride transport. The extensive set of equations usually requires finding solutions by means of numerical modelling. Empirical models are based on an equation that captures the primary transport physics of the chloride transport (e.g., Fick's law). However, detailed mechanisms are not explicitly modelled, and their effects may end up in the fitting constants. Empirical models are often tuned towards certain data sets under certain conditions, and this may limit the applicability of such models. A clear advantage of empirical models is that they are easily available to construction engineers, i.e., are applicable in commercially available spreadsheets. Moreover, they require the input of a minimum number of parameters that are relatively easy to obtain.

Mechanistic models may describe the chloride transport process in more detail. This does, however, not imply that they lead to more accurate predictions than empirical models do. This is because the reliability of a prediction outcome depends on the representativeness of the input parameters. The quality of the prediction results can be tested be means of comparing them to the results of long-term field measurements. An objective of this study is to show how long-term field experiments help to tune, validate and improve service life models.

The prediction model proposed in this report is based on the well-known error-function (ERFC) solution of Fick's second law of diffusion. The model is very similar to existing ERFC-models, particularly the DuraCrete model. It differs from DuraCrete in the way it deals with chloride surface concentration and the so-called transformation constants. Some of the input parameter (most notably the ageing factors) prescribed for DuraCrete in particular environments were found to be unsuitable for the Swiss and other situations that were investigated. This may be partly a result of the different model tuning method used in this study.

The input parameters of the proposed model were tuned by using the data of the Naxberg field (and laboratory) experiment. The Naxberg field experiment was started in

the year 2000 in the Naxberg tunnel near Göschenen in the Kanton of Uri (altitude of ca. 1000 meters), with an average annual temperature of 7°C. In this experiment, plates with a dimension of 60 x 50 x 10 cm were prepared of different types of reinforced concretes and placed in the tunnel wall, ca. 50 m from the tunnel entrance. The purpose of this field experiment was to study the effect of concrete type, reinforcement type, cover thickness, height from road, and hydrophobic impregnation on the rate of chloride ingress and reinforcement corrosion under natural road conditions. Together with the Naxberg-plates, additional concrete cubes were cast for monitoring the development of various properties (compressive strength, porosity, and transport properties) as a function of time.

The studied concrete types (called A to H) contained Portland cement or a combination of Portland cement and a mineral addition (slag, fly ash or silica fume) in order to simulate modern concretes that contain such additions. Four plates per concrete type were placed on top of each other (numbered 1 to 4) for studying the effect of height on chloride ingress rate. The exposure class from bottom (plate 1) to top (plate 4) was expected to vary from merely salty spray water contact (XD3) to salty mist water contact (XD1). In this study, a total of 65 cores have been taken from the concrete plates, mainly with the purpose of measuring the chloride profiles at different chloride exposure times (1.5; 2.5; 3.5; 4.4; 12; and 12.8 years).

The measured chloride profiles showed ongoing chloride ingress with time. After 12 years chloride exposure, most profiles show a mountain-shaped profile with the peak chloride concentration occurring at depth of around 20 mm. This is a typical phenomenon for field concretes exposed to salty spray water, and can be explained by chloride binding and by drying, leaching and/or carbonation of the concrete surface layers. There was a significant effect of concrete type on the rate and depth of chloride penetration. The plates consisting of CEM I concrete with a w/c-ratio of 0.5 (concretes B, C, and H) showed the strongest chloride ingress, followed by the concretes with slag (concrete D) and fly ash (concrete E) having the same w/-ratio. Concrete with silica fume (concrete F) and CEM I concrete with a w/c-ratio of 0.35 (concrete G) showed the lowest ingress rate.

After 12-year chloride ingress some of the concrete plates with plain Portland cement and a w/c-ratio of 0.5 were apparantly saturated with chlorides, i.e., showed horizontal chloride profiles over the entire 10 cm thickness of the plate. A simple diffusion-type model could not predict these high concentrations of chlorides at a depth of 70-100 cm. Capillary suction effects and the relative low plate thickness (10 cm) could have caused this ‘early’ chloride saturation. Other observations from the profiles were that the chloride concentrations and ingress rate decreased with increasing height from road, and that hydrophobic impregnation strongly reduced chloride ingress rate.

By means of regression of the measured chloride profiles, the so-called apparent chloride diffusion coefficient (D_{app}) and chloride surface concentration (C_{s_app}) of the field concretes were determined. It was found that concrete type had a large effect on D_{app}. There is a factor of 6-7 times difference in D_{app} between the concrete (H) with apparantly the highest porosity/permeability and the least porous concretes (G and F) after 12 years exposure. All concretes show an initial (0-2.5 years) decrease in D_{app}, probably due to material densification caused by ongoing cement hydration. The long-term change in D_{app} differs between the different concretes: Concretes with plain Portland cement paste seem to reach a stable D_{app} value after 2.5 years exposure. For concretes with supplementary cement materials D_{app} can roughly be described by an expontial decay function of time. The D_{app} calculated for the plates 1 (0-60 cm) is generally higher than D_{app} for plates 3 (120-180 cm). The C_{s_app} and maximum measured chloride concentration (C_{max}) show a clear increase with time for all concrete types up to at least 12 years.

A trial empirical modelling exercise was initially carried out with the obtained chloride profiles and diffusion coefficients (D_{app}). A starting profile as measured after 2.5 or 4.4 years was the basis of the calculation of a subsequent profile after 4.4 or 12 years using the error-function simplification of Fick’s second law of diffusion. The predicted chloride profile was then compared to the measured profile after 4.4 or 12 years. The results of the exercise were satisfactory and showed that the evolution of Naxberg chloride profiles follows Fick’s law of diffusion in the majority of cases. This result does however not

necessarily imply that chloride ingress occurred by a pure diffusion mechanism. It only showed that the development of chloride profiles could (empirically) be described by second-order mathematical equation such a Fick's second law of diffusion.

For the prediction model proposed in this report two other input parameters are needed: (i) the migration coefficient of concrete at an age of 28 days (M_{28d}), and (ii) the critical chloride content (C_{crit}). Both parameters were measured in the laboratory using a standard method for M_{28d} (Standard SIA 262/1: Annex B) and using a newly developed method for C_{crit}. The parameter C_{crit} is defined as the total internal chloride concentration in concrete at which depassivation or corrosion of reinforcement steel starts. This is one of the decisive input parameters for lifetime modelling of reinforced concrete in contact with salt. Our measurements show that there is strong effect of steel type and processing method on C_{crit}, and that the measured C_{crit}-value for ordinary rebar steel was close to (but higher than) the values prescribed in national and international standards.

The prediction model proposed in this report is as follows: The basis of the proposed model is the solution of Fick's second law under the assumption of constant diffusion coefficient (D) and chloride surface concentration (C_s), i.e., the error-function solution:

$$C(x,t) = C_{s,app} \cdot erfc\left(\frac{x}{2\sqrt{D_{app} \cdot t}}\right)$$

In the DuraCrete-approach, D_{app} is calculated for a given exposure duration using the following expression:

$$D_{app} = K \cdot M_{28d} \cdot \left(\frac{t_0}{t}\right)^n$$

With M_{28d} being the chloride migration coefficient measured in the laboratory at a concrete age of 28 days. The time t_0 is the reference time (in years) at which M is measured (t_0 = 28 days) or the age of first chloride exposure. The time t is the exposure period in years. The correlation factor K is a constant that links the experimentally measured M to field performance (D_{app}). The factor n is the ageing factor, describing how the diffusion coefficient of the concrete changes with time.

The input parameters K and n were obtained by a fitting procedure separately for each concrete type. The values of K and n were chosen in a way to obtain chloride profiles that best matched the measured Naxberg chloride profiles. The required migration coefficients (M_{28d}) were measured in the laboratory on the same concretes. The evolution of the chloride surface concentration (C_{s_app}) was assumed to follow the empirical equation obtained from Naxberg measurements. It was found that K could be held constant at a 'universal' value of 0.5, while the ageing factor n varied between the concrete types.

The model parameters K and n obtained with the Naxberg field experiment data were tested for other road settings in Switzerland and Sweden. In this validation exercise it was found the chloride profiles measured in these other settings could not be predicted with the Naxberg parameters. Only if the chloride surface concentration and ageing factors were adjusted a good match of predicted and measured profiles could be obtained. The chloride surface concentration (C_{s_app}) depends on the supply of chlorides to the surface in a particular setting, and this parameter is hard to predict. In Naxberg the chloride surface concentrations were much higher than in the other two studied settings. The ageing factor n is also not a material constant that depends on concrete type only: environmental influences like the rate of concrete drying and carbonation affect n. Thus, n obtained in one setting may not be valid in another one.

From the validation exercise it became clear that if the chloride surface concentration was set equal to the measured value, then the evolution of chloride profiles can be best

described by using an aging factor n = 0.45. This was found for concrete with plain Portland cement and for concrete with a 5% addition of silica fume. In a subsequent exercise, it was tested if n = 0.45 could also be used for predicting the Naxberg profiles if the chloride surface concentration was adjusted. This was found to also produce good predictions for the three Naxberg concrete types with the lowest porosity. For the two concrete types with apparently the highest porosity and chloride ingress rate, an n-value of 0.45 was unable to reproduce the measured chloride profiles. The interpretation here is that in these Naxberg concretes, the chloride ingress was not predominantly controlled by diffusion. A (variable) contribution of capillary suction may have had an influence on the ageing factors in these concretes.

In the final part of this report a large number of example lifetime calculations are given that show how different factors, such as cover thickness, chloride surface concentration and concrete type affect the corrosion-free lifetime of reinforced concrete structures. In some of these calculations, the input parameters were given the values as required by Swiss standards in order to test if Swiss standards guarantee enough durability with regard to chloride-induced corrosion. For the exposition class (XD3) it was shown that Swiss standards appear to guarantee a corrosion-free lifetime of at least 25 years, if lifetime is calculated in a deterministic manner with zero standard deviation of the input parameters. The deterministic and probabilistic lifetime calculations presented in the report suggest that XD3 limit values for M_{28d} and/or cover thickness in Swiss standards need to be discussed. Relative small changes, e.g., M_{28d} = 8 instead of $10 \cdot 10^{-12}$ m^2/s, or a minimum cover thickness of 50 instead of 45 mm, can increase lifetime under XD3 exposure by 25 years.

The report concludes with step by step guidelines that explain how to make actual lifetime predictions for existing or new concrete structures.

1 Introduction

1.1 Problem description: chlorides in concrete

The ingress of dissolved chloride salts into concrete is a major cause of damage in reinforced concrete structures. Durability problems due to chloride ingress may occur in concrete structures in contact with sea water, or in road environments in which the use of deicing salts is common. In Switzerland deicing salts are widely used, and concrete structures near roads, such as bridge decks, overpass supports, tunnel walls or parking floors, may uptake chlorides. Some typical chloride-induced damage cases as they commonly occur in Switzerland are illustrated in Fig. 1.

Dissolved chloride salts penetrate into concrete by diffusion in the pore fluid, or move along with water that is sucked into concrete by capillary forces. When chlorides reach the depth of the first reinforcement steel in concrete (usually around 3-5 cm), and exceed a critical content, the so-called depassivation of steel will occur and it can start to corrode. The built-up of corrosion products around the steel in concrete, leads to cracking or spalling of the cover concrete. Ongoing corrosion also leads to a reduction of the rebar cross-section, which eventually reduces the load-carrying capacity of a concrete element. The damage may proceed to a stage that requires large scale rehabilitation or demolition of a concrete element or structure.

Chloride-induced corrosion in marine environments is a well-known and widely studied problem. A distinction between 4 marine microclimates for concrete can be made [Nanukuttan 2006]: (1) completely immersed in sea water; (2) fluctuating immersion in sea water due to tidal movements; (3) in contact with spray sea water (splash zone); and (4) in contact with sea water mist. Since the chloride concentration in sea water is relatively constant throughout the world, the driving force of chloride ingress in marine microclimates is relatively well known, and can therefore be predicted. In road environments the amount of chlorides (from deicing salts) that will reach a concrete surface depends on many factors and will vary seasonally. These rather undefined boundary conditions make it difficult to develop reliable service life prediction models for road environments.

Most existing service life prediction models for concrete in salty environments are based on the same principle: The calculation of the time required to reach the critical chloride content at the surface of the first reinforcement layer. At chloride levels above the critical chloride content the steel in concrete will depassivate or start to corrode. The duration to corrosion onset depends on the availability of chlorides at the concrete surface; the transport distance (= cover thickness), and the density and chemical properties of the concrete which determine the chloride transport coefficient of the material. Larger cover depth or denser concrete usually leads to higher expected lifetime (durability) of concrete. A conservative design of a concrete structure for worst-case scenario chloride ingress is likely to be much more expensive than a structure that is designed for a given lifetime in a specific microclimate. Moreover, an over-conservative design may require the use of more concrete and concrete that is less eco-friendly, which would increase the carbon-footprint of the concrete structure. Service life models help with the effective and efficient design of durable concrete structures.

The objective of this study was to propose a user-friendly model for predicting the corrosion-free lifetime of concrete structures with ingress of deicing salts. The proposed empirical model is based on the same principle as other existing empirical models. The focus of this project is on obtaining representative model input parameters relevant for road environments as they occur in Switzerland. As will be shown in this report, empirical models are not necessarily less reliable than sophisticated (mechanistic) prediction models. The reliability of a prediction model is primarily determined by its capability to predict results of long-term field experiments.

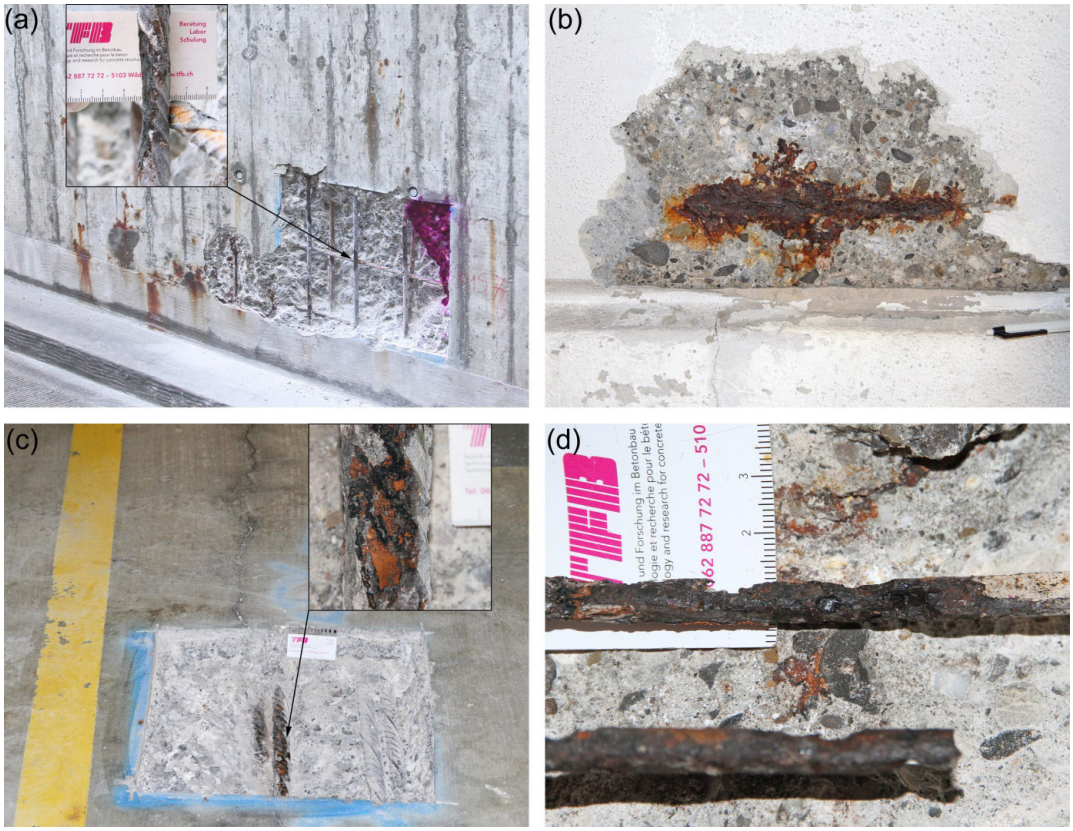

Fig.1: *Chloride-induced corrosion in reinforced concrete structures in road environments. (a) Corrosion in concrete wall adjacent to road led to a 3 mm reduction in reinforcement bar diameter (cover thickness is 25 mm); (b) Spalling of concrete wall due to rebar corrosion; (c) Localized corrosion in concrete parking floor due to presence of a crack. (d) Chloride-induced corrosion in a parking floor that led to extreme reinforcement diameter reduction.*

1.2 The Naxberg field experiment

In the year 2000 the Naxberg field experiment was started in the Naxberg tunnel near Göschenen in the Kanton of Uri (altitude of ca. 1000 meters), with an average annual temperature of 7°C. In this experiment, plates with dimensions of 60 x 50 x 10 cm were prepared of different types of reinforced concretes and placed in the tunnel wall, ca. 50 m from the tunnel entrance (Fig. 2). The purpose of this field experiment was to study the effect of concrete type, reinforcement type, cover thickness, height from road, and hydrophobic impregnation on the rate of chloride ingress and reinforcement corrosion under natural road conditions. A number of sensors were embedded in the concrete plates for the *in-situ* measurement of electrical resistance (water content), chloride content, corrosion initiation properties, and temperature. Together with the Naxberg-plates additional concrete cubes were cast for monitoring the development of various properties (compressive strength, porosity, and transport properties) as a function of time.

The studied concrete types (called A to H) contained Portland cement or a combination of Portland cement and a mineral addition (slag, fly ash or silica fume) in order to simulate modern concretes that contain such additions (see Table 1). Four plates per concrete type were placed on top of each other (numbered 1 to 4) for studying the effect of height on chloride ingress rate. The exposure class from bottom (plate 1) to top (plate 4) was expected to gradually change from salty spray water contact (XD3) to salty mist water contact (XD1). There is gap of ca. 5 cm between back side of the concrete plates and the tunnel wall, but no air circulation took place behind the plates. A cross-section image of the experimental set-up can be found in Ungricht [2004].

Tab.1: *Composition of studied concretes in the Naxberg experiment.*

Plate:	**A, B, C, H***	**D**	**E**	**F**	**G**
Cement type	CEM I 42.5 N	CEM I + slag	CEM I + fly ash	CEM I + silica fume	CEM I 42.5 N
Cement (kg/m^3)	300	249	269	277	367
Min. addition (kg/m^3)	-	50	40	19	-
Min. addition (% of CEM I)	-	20.1%	14.9%	6.9%	-
w/b	0.5	0.5	0.5	0.5	0.35
Concrete density (kg/m^3)	2452	2441	2428	2397	2371

* Concretes A, B, C, and H, are equal in composition, but differ in the types of reinforcement steel used or other factors. In plates A the effect of hydrophobic impregnation (plate A1-A4) and mixed-in chlorides (plates A3, A4, B3, B4 + 2% chlorides) were tested.

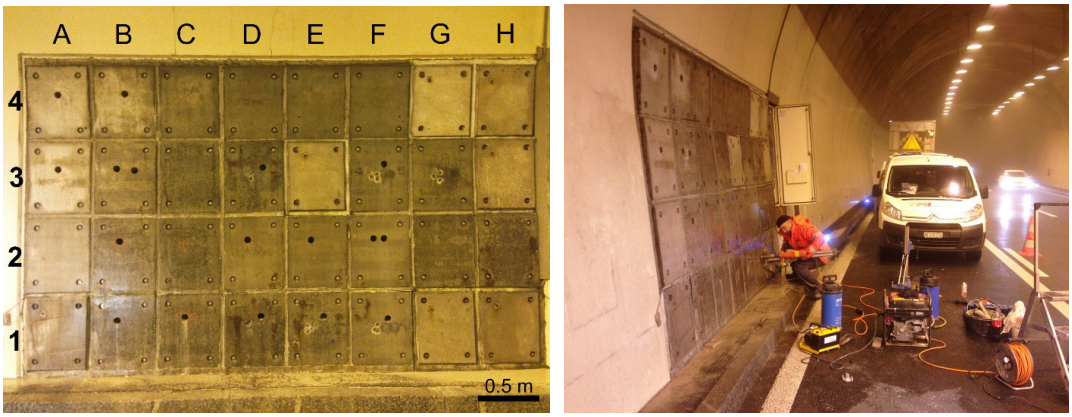

Fig.2: *The Naxberg field experiment: (a) arrangement of concrete plates A to H (see Table 1) at height levels 1 to 4; (b) Setting of the experimental panel in the west-side tunnel wall, ca. 50 m from tunnel entrance.*

A total of 65 cores have been taken from the concrete plates in the last 14 years, mainly with the purpose of measuring the chloride profiles at different chloride exposure times (1.5; 2.5; 3.5; 4.4; 12; and 12.8 years). Some oversampled plates have been taken out of the test panel in 2013, and were replaced by new ones. These old plates were studied in the laboratory to determine the corrosion degrees and carbonation depths.

Most of the first results collected after 3 years were part of the Dissertation of Dr. Heidi Ungricht [Ungricht 2004; Ungricht 2008]. These results can be summarized as follows: The *in-situ* moisture measurements showed that water content in the concrete top layer fluctuated due to capillary water uptake and drying by water evaporation. The net water uptake varied with the time of the year, and was much determined by the magnitude of 'single' water-uptake events. The nature of the water ingress had a large effect on chloride ingress rate during winter time when deicing salts were applied. The chloride entered the concrete relatively rapidly with smaller or larger events of capillary water uptake. Long-term penetration or redistribution of chlorides occurred by a diffusion process [Ungricht 2004, Ungricht 2006].

In a recent publication on the Naxberg experiment [Schiegg 2014], the corrosion state of the reinforcement in the concrete after 12 years chloride exposure is evaluated. A selected number of plates were taken from the wall, and crushed in the laboratory to expose the steel. The reinforcement closer to the surface started to corrode earlier as those at larger depth, as expected. The reinforcement made of normal rebar steel (500B) showed much more corrosion than the ones out of 'stainless' steels (types 1.4003 and 1.4401/1.4462). In concretes with mineral additions (slag, fly ash and silica fume), the corrosion initiation at 3 cm depth occurred around 8 years. In ordinary Portland cement

concrete (with equal w/c-ratio) corrosion already started after 3-4 years at this depth level. In the ordinary PC concrete, hydrophobic treatment was very efficient in delaying the rate of chloride ingress and avoiding initiation of steel corrosion.

1.3 Structure of report

In Chapter 2 a literature review is presented about all the aspects of chloride ingress into concrete. There are different fundamental mechanisms by which chlorides enter the concrete (diffusion, migration or capillary suction), and the transport coefficient that define these transport modes are measured with different testing methods. It is important to understand what the different laboratory transport coefficients mean, how they relate to each other, and how they relate to chloride ingress under natural conditions. The essential factors that influence the rate of chloride ingress, such as temperature, moisture content, and concrete composition, are described. Furthermore, Chapter 2 gives a brief introduction into the topic of corrosion of steel in concrete, and the concept of critical chloride content. In the final part of Chapter 2, and overview of existing service life models and their performances is given.

In Chapter 3 all the measured chloride profiles at exposure times of 1.5; 2.5; 3.5; 4.4; 12; and 12.8 years will be presented and described. They show a clear effect of concrete type, height from road, and exposure time on the rate of chloride ingress. The so-called 'apparent diffusion coefficient' is determined from each chloride profile by means of a regression method. A set of empirical equations is deduced from the complete Naxberg chloride profile database, in order to test if chloride ingress in Naxberg follows systematic rules and obeys Fick's law of diffusion. The purpose of this trial exercise was to see if an empirical prediction model based on Fick's law could function for the Naxberg chloride ingress conditions. Finally, an overview of the measurements (mainly migration coefficients) on the Naxberg laboratory cubes is presented.

In Chapter 4 a new experimental method is described to measure the critical chloride content of concrete. The results of a first series of experiments on different types of steels with different surface treatments show the performance of this technique.

In Chapter 5 an empirical prediction model for engineers is proposed. The basis of the model is the widely used DuraCrete-model. It differs in terms of the magnitudes of the input-parameters, and in the way it deals with concrete surface effects. The performance of the model is tuned and tested against the Naxberg-results, and other long-term field experiments in Switzerland and Sweden. The empirical prediction results are also compared with the outcome of a mechanistic prediction model (TransChlor). The chapter concludes with some example lifetime calculations using the proposed model and measured critical chloride contents.

In Chapter 6, various implications of this study will be outlined. Most notable the question if Swiss standards guarantee enough concrete durability in salty environments, will be addressed. Practical guidelines for making lifetime predictions for either new and old concrete structures are given. The chapter ends with some research recommendations that could lead to improved reliability of empirical lifetime prediction modelling in Switzerland.

2 Literature review

2.1 Chloride transport: definitions and experimental methods

2.1.1 Transport mechanisms of chloride ingress

The starting time for chloride-induced corrosion of reinforcement in concrete is initially determined by the chloride transport rate in concrete. Corrosion can start when chlorides reach the depth of the first reinforcement bars (X_{cover}) and exceed a critical concentration (C_{crit}) that will depassivate the steel (Fig. 3). The rate of ingress depends on three main factors: (1) the amount of chlorides at the surface (= the driving force); (2) the concrete permeability or density; and (3) environmental conditions. Environmental conditions determine the moisture state and temperature of concrete, at least in the surface layers, which affect the transport mechanism (diffusion or capillary suction) and rate of chloride ingress.

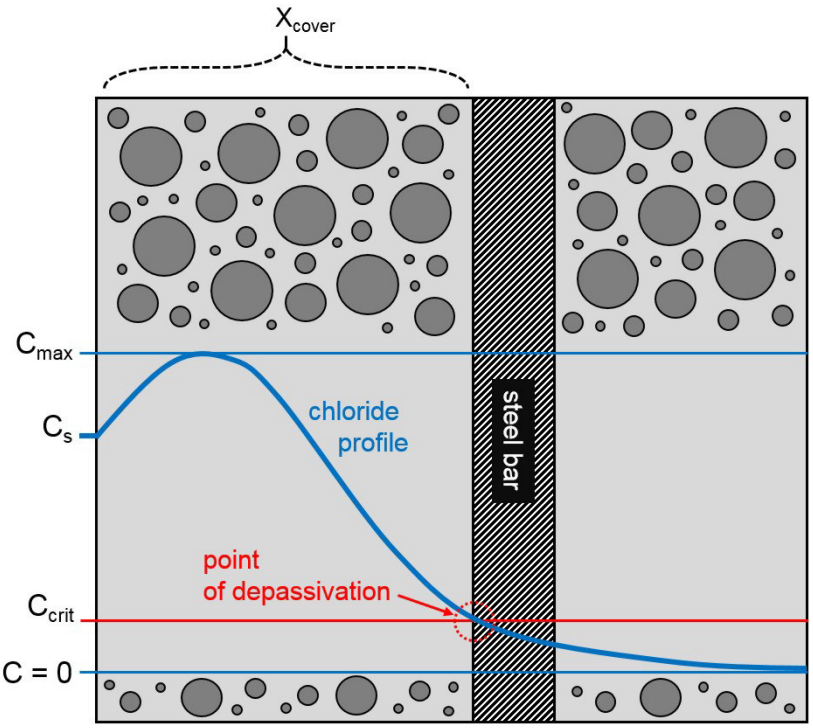

Fig.3: *Schematic illustration of the process of initiation of chloride induced corrosion in reinforced concrete.*

Diffusional transport of chloride into concrete is defined by Fick's laws of diffusion (see Section 2.1.3 for formulations). It occurs under a chloride concentration gradient, i.e., a difference in chloride concentration between the outer surface and inside of the concrete. The rate of diffusional transport is determined by the magnitude of the concentration gradient and by the concrete's resistance to chloride ingress, i.e., the chloride diffusion coefficient of the concrete. The chloride diffusion coefficient does not only depend on concrete density, but also on the temperature, moisture state and some chemical characteristics of concrete.

Macroscopically, the transport of chlorides through concrete in a gradient field may be considered to be diffusion and follow Fick's laws. However, on a microscale, the diffusional transport of chlorides in concrete is more complicated, because of chemical interactions exist between the chlorides and other ions in the pore solution, and physical interactions with the pore walls. When such interactions are strong, the transport of chlorides in concrete may no longer be described accurately by Fick's law.

Migration is the transport of chlorides through concrete under an applied electrical field, and does not occur under normal (natural) conditions in concrete structures before corrosion. Electrically-forced chloride transport is often used in experiments with the purpose to accelerate the chloride transport in concrete. A concrete migration coefficient can be obtained in matters of days, while the measurement of a diffusion coefficient lasts a number of weeks. Chloride migration is described by the Nernst-Planck equation.

Capillary suction is a third transport mechanism by which chlorides can enter the concrete. This occurs in a dry or partly saturated concrete when water with dissolved chloride ions at the concrete surface permeates into concrete by the suction force of capillary pores in concrete. This type of chloride transport occurs in concrete under alternating dry and wet conditions, in the so-called spray zone, and potentially can occur at much higher rates than diffusional ingress.

Extended reviews about the transport mechanisms in concrete and their formulations can be found in literature [Ungricht 2004, Tang 2005, Lay 2006, Conciatori 2008, Kapteina 2011, Spiesz 2013].

2.1.2 Experimental methods

Different methods exist for the measurement of the diffusion (D) or migration (M) coefficient of concrete. The aim of measuring D or M is to determine if a concrete complies with durability requirements as defined for various environments in national or international standards. Moreover, when D or M are known, service lifetime predictions can be made for concretes in specific environments. For the characterisation of a concrete with regard to its capacity to resist ingress of chlorides by capillary suction, no standard testing methods exist.

The measurement of the diffusion (D) or migration (M) coefficient is carried out under either steady-state (ss) or non-steady-state (nss) conditions. In a steady-state (ss) experiment, the concentration gradient across a specimen is held constant and Fick's first law (or equivalent) is used to calculate D (or M). In a non-steady-state experiment, D or M are determined under transient concentration conditions using the second order laws for diffusion or migration. As will be seen later, D or M obtained under steady-state or non-steady-state conditions are fundamentally different and cannot be used interchangeably.

Here we will briefly mention two standard tests as examples: (1) A test to measure migration coefficient according to Swiss standard SIA 262/1 [SIA 262/1], and (2) a test to measure a diffusion coefficient according to the proposed European standard CEN/EN 12390-11 [CEN/EN 12390]. Other testing methods to measure D or M, or other parameters to characterize chloride transport in concrete are described elsewhere [Andrade 1993, Delagrave 1996, Tang 1992; Tang 1996, Truc 2000, Castellote 2001, Tong 2001, Yang 2002, Climent 2002, Stanish 2003, Tang 2005, Dalen 2006, Castellote 2006, De Vera 2007, Guimarães 2011, Spiesz 2013, Olsson 2013].

Migration coefficient according to Swiss standard SIA 262/1 [SIA 262/1]:

The migration coefficient is measured on a concrete specimen with a diameter of 50 or 100 mm and a height of 50 mm. The concrete is prepared and cured according to standards and tested at an age of 28 days. It is also possible to measure the migration coefficient from cores taken out of existing concrete structures (not contaminated with chlorides). The specimen is placed in a migration cell that contains a 3% NaCl solution and a voltage of 20V is applied to the specimen. The test duration is 2 days after which the penetration depth of the chlorides into the specimen is determined. This is done by splitting the specimen in two halves, and spraying a silver nitrate solution on the surface to highlight the chloride ingress front. The migration coefficient M is calculated from average depth of the migration front by using a specific empirical formula.

This migration coefficient is obtained under non-steady-state (M_{nss}) and water-saturated conditions at room temperature. M_{nss} determined in the laboratory on a core from a

concrete structure is not equal to the actual in-situ diffusion coefficient (D_{nss}) of the concrete in that concrete structure, because of difference in transport mechanisms (migration vs. diffusion), temperature and moisture state. The migration coefficient changes with the age of the concrete (see Sections 2.2.6; 3.5).

Diffusion coefficient according to European standard CEN/EN 12390-11 [CEN/EN 2013]:

In this test there is some freedom with regard to specimen size and age and the way the concrete is in contact with the salt solution. A specimen can be prepared in the laboratory according to standard methods or taken from an existing concrete structure (not contaminated with chlorides). The concrete specimen is pre-saturated with water, and brought into contact with a 3% NaCl solution, either by complete or partial immersion or by so-called 'ponding'. The standard test duration is 90 days, after which the chloride distribution (profile) as a function of distance from surface is determined. This is done by a grinding procedure in which powder samples of at least 8 layers (with thickness of 5-10 mm) are collected and analysed for chloride content. The chloride content of each layer is plotted as a function of depth, and from this curve the diffusion coefficient is obtained by a regression procedure as explained in Section 2.1.3.

This diffusion coefficient is obtained under non-steady-state conditions (D_{nss}), and under water-saturated conditions at room temperature. D_{nss} determined in the laboratory on a core from an existing concrete structure is not equal to the actual *in-situ* diffusion coefficient (D_{nss}) of the concrete in that concrete structure, because of differences in temperature and moisture state. The diffusion coefficient changes with age of the concrete (see Section 2.2.6).

2.1.3 Regression method to determine the diffusion coefficient

The measurement of a diffusion coefficient (D_{nss}) in laboratory experiments (such as the one described above [CEN/EN 2013] or from chloride contaminated concrete in existing structure is based on the principle of regression of a measured chloride profile. The regression is based on the assumption that the ingress of chlorides followed Fick's second law of diffusion:

$$\frac{\partial C}{\partial t} = D_{nss} \cdot \frac{\partial^2 C}{\partial x^2} \qquad (1)$$

Under the assumptions of a time-independence of the chloride surface concentration, and a time-independent diffusion coefficient, Fick's second law has the following solution:

$$C(x,t) = C_0 \cdot erfc\left(\frac{x}{2\sqrt{D_{nss} \cdot t}}\right) \qquad (2)$$

Where x is the distance from surface (depth), t = time of exposure to chloride, and erfc() is the error function, a mathematical integral function used in statistics. The error function *erf* or *erfc* (= error function complement) can be solved in common computer spreadsheets and does not require numerical computations. The diffusion coefficient is determined by fitting equation (2) to the measured chloride profile. The fitting unknowns, D_{nss} and C_0, are selected in a way that will produce the best result in a non-linear least squares regression analysis such as described in [CEN/EN 2013]. In an Excel-spreadsheet the regression can be performed using the Solver-function.

Two different types of chloride profiles and the best-fit diffusion-type curve through the measured data points obtained by the regression method are shown in Fig. 4. These examples illustrate the two types of chloride profiles as they are often measured in field concretes: a normal chloride profile (Fig. 4a) and a 'mountain-shaped' chloride profile (Fig. 4b). Mountain-shaped profiles are a result of drying, carbonation or other types of processes that occur in the surface layer of concrete [Andrade 2015]. The fitting

parameters are the apparent diffusion coefficient (D_{app}) and apparent surface concentration (C_{s_app}) which correspond to D_{nss} and C_0, respectively. As will be explained later (see Section 2.4.2) the term 'apparent' is used here since the obtained parameters are not true Fickian diffusion parameters.

In the case of 'normal' chloride profiles, the apparent surface concentration (C_{s_app}) obtained by regression is close to the actual measured (maximum) surface concentration. In the case of the mountain-shaped profile, there are different ways to carry out the fitting procedure. The regression can be carried out with all data points, or with only those from the peak and deeper levels. In these cases, the apparent surface concentration is obtained by extrapolation, and C_{s_app} usually is much larger than the actual surface or peak concentration. C_{s_app} becomes a virtual fitting parameter with no physical meaning. The procedure described in [CEN/EN 2013] ignores the surface points with concentrations below the peak concentration in the regression, and requires the correlation coefficient (R^2) of the fit with the data points to be larger than 0.95. Alternative regression methods have also been proposed in which the peak point becomes the starting point of the regression i.e., $C_{max} = C_{s\_app}$ [Kapteina 2011, Andrade 2015]. This alternative procedure produces D_{app} with lower values since the total area under the chloride profile is smaller: less chloride ingress in the same amount of time is considered.

In this study, we used the regression procedure as described in [CEN/EN 2013] with an extrapolated surface concentration in case of mountain-shaped profiles. The alternative regression procedure as proposed by Andrade [Andrade 2015] is more cumbersome and might also introduce some bias in the results if the depth of the peak concentration is concrete-type dependent. Note that the correlation factors (K, n) in the ERFC prediction model proposed in this study are based on a fitting procedure described in [CEN/EN-2013]. These correlation factors (K, n) may change if another regression method is used to obtain D_{app} and C_{s_app}. The prediction model would then also require the input of lower chloride surface concentrations.

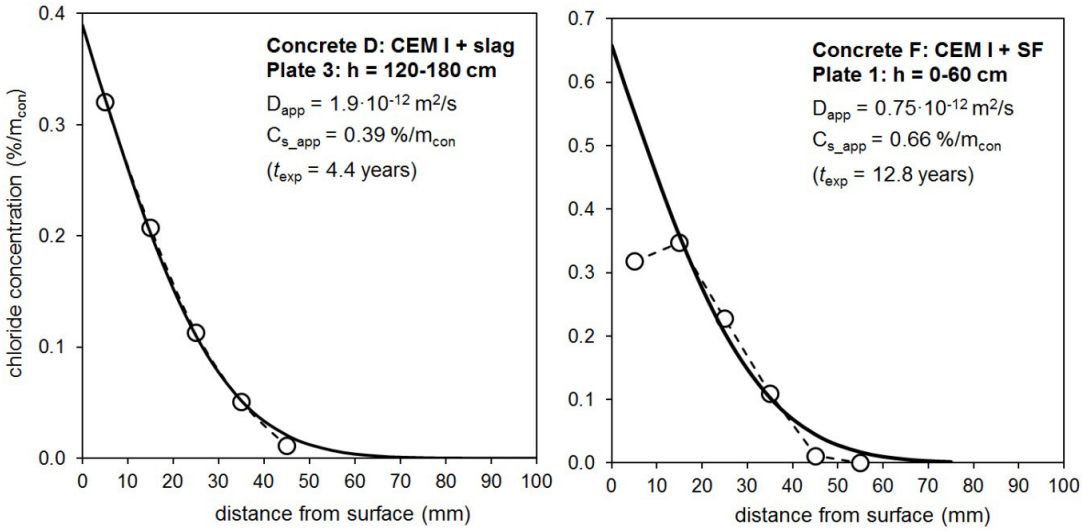

Fig.4: *Examples of chloride profiles from which D_{app} (=D_{nss}) and C_{s_app} (=C_s) are determined using the regression analyses described in text. (a) Example of a normal chloride profile, i.e., with the highest chloride content near the concrete surface. (b) Example of a so-called mountain-shaped profile with the maximum chloride concentration occurring at a particular depth into to the concrete.*

2.1.4 Relationships between chloride transport coefficients

A large round-robin test has been carried out on methods for determining chloride transport parameters of 4 different concrete types using up to 13 different methods in 27 different laboratories around the world [Castellote 2006]. A total of 7 different methods were used to measure diffusion (D) and migration (M) coefficients under steady-state (ss)

and non-steady-state (nss) conditions. The average values of each group (D_{ss}, Dn_{ss}, M_{ss}, and M_{nss}) for each concrete type is given in Table 2. For steady-state conditions the ratio D/M ranges between 0.63 and 0.96 depending on concrete type. For non-steady-state conditions it ranges between 0.97 and 1.43 depending on concrete type. D or M measured under non-steady-state conditions is a factor 3 to 10 times larger as the one measured under steady-state conditions.

Other studies on the relationship between different chloride transport parameters have shown varying results [Tang 1996, Delagrave 1996]. Tang (1996) showed that under non-steady-state conditions the chloride transport coefficient of natural immersion tests (D_{nss}) is very similar to those of a rapid migration test (M_{nss}). He states that this is a coincidence since in slow diffusion experiments the chloride binding effect must be much stronger than in fast migration tests, and that further research is needed to explain this 'coincidence'. Delagrave et al (1996) measured chloride transport coefficients using different methods and found varying correlations between the different measures.

It has been shown that for Portland cement concrete the diffusion/migration coefficient (D_{nss}/M_{nss}) is about a factor 10 larger than the so-called effective diffusion/migration coefficient [Tong 2001, Spiesz 2013]. The effective diffusion/migration coefficient is the coefficient obtained in steady-state experiments. It correlates with the flux of ions through a concrete specimen (per m^2 concrete surface), i.e., it refers to the total volume of concrete. The diffusion or migration coefficient obtained in non-steady-state tests only represents the diffusion/migration of chlorides in the pore solution of concrete [Spiesz 2013]. The correlation between D_{nss} (M_{nss}) and D_{ss} (M_{ss}) is therefore mostly defined by the porosity for water-saturated concretes. Since the amount of chloride binding may also differ between steady-state and non-steady-state experiments, this is a second factor for possible differences between transport coefficients obtained under these different conditions. The ratio ss/nss (last column of Table 2) is thus determined by the (permeable) porosity of the concretes and the difference in chloride binding between ss and nss-experiments.

***Tab.2**: Comparison of D and M under ss- and nss-conditions [Castellote 2006]. Transport coefficients ($\cdot 10^{-12}$ m^2/s) with total of n measurements in the round-robin test.*

Concrete mix with:	D_{ss} (n= 9)	M_{ss} (n= 206)	D_{ss}/M_{ss}	D_{nss} (n= 245)	M_{nss} (n= 309)	D_{nss}/M_{nss}	ss/nss (D+M)
plain CEM I	1.87	1.94	0.96	21.56	17.13	1.26	0.10
slag	0.54	0.85	0.63	3.79	2.65	1.43	0.20
fly ash	0.80	1.15	0.69	7.21	6.15	1.17	0.14
silica fume	0.96	1.10	0.87	2.97	3.08	0.97	0.34

2.2 Effects on chloride transport rate

2.2.1 Surface chloride concentration

When chloride ingress occurs by diffusion, the surface concentration has an important effect on the ingress rate, since the concentration gradient across the concrete surface layer determines the magnitude of the driving force of the ingress process. The driving force of chloride diffusion is strictly speaking the concentration gradient of dissolved chlorides in the pore solution, and not the gradient in total chloride content including the chlorides that precipitated in the concrete. Here we review how the total surface chloride concentration (C_s) has been observed to change with time in different environments, since most empirical models work with total chloride concentration as input parameter.

The surface chloride concentration (C_s) is the concentration in the uppermost concrete layer expressed as a weight fraction of the concrete or as a weight fraction of the binder. The surface concentration is to a first degree determined by the availability or supply of salt at the concrete surface. However, even when the salt concentration (supply) of the

environment is constant (e.g., as in sea water), the surface chloride concentration increases with time (years). This is a result of the slow, cumulative binding of chloride salts inside the concrete. Thus, when the surface concentration increases over a period of years, this does not mean that the availability of chlorides at the concrete surface increased.

In road environments, the situation is even more complicated because deicing salts are usually only supplied to the concrete in winter time. Thus, the availability of chlorides at the concrete surface fluctuates during the year. The amount of deicing salts used in winter time may fluctuate from year to year as well. Moreover, in summer time, chloride may be leached-out from the concrete surface layers by rain water followed by drying [Poulsen 2006]. Carbonation of concrete is another process known to reduce the chloride concentration in concrete [Meijers 2005, Andrade 2015]. In road environments, we can therefore expect all kinds of short and long-term changes in chloride surface concentration. After many exposure years, the maximum chloride concentration often occurs not at the surface, but at a particular depth free of carbonation and short-term wetting/drying effects (see Fig. 4b).

The concentration of chlorides in sea water is a relatively constant parameter with a subordinate effect on the chloride ingress rate into concretes submerged in sea water [Lindvall 2007]. Various researchers have shown that the surface chloride concentration of concrete permanently immersed in sea water or some kind of salt solution, increases slowly with time, and it may take 5-10 years to reach the maximum (end-) value [Costa 1999, Lindvall 2001, De Rooij 2006]. De Rooij et al [2006] showed that C_s for concrete submerged in seawater reaches a stable value after around 10 year exposure and then remains more or less constant until 40 years. The reported long-term (>10 year up to 25 years) surface concentrations of concrete in sea-water are in the range of 0.2-0.8 %/m_{con} [Helland 2010, Aldred 2014].

Much less data is available for C_s-development in road environments. Lindvall and Nilsson [2001] showed that for atmospheric zones there also is a continuous increase in the first 5 years or even longer. In the Naxberg-experiment described in this report, also a clear evolution of C_s has been observed (see Chapter 3). Arya et al [2014] showed that there is an increase in surface concentration with the number of wetting-drying cycles. On the contrary, Kapteina [2011] refers to experiments in which no clear increase in C_s in road environments was observed in the first 5 years, and in her service life model C_s is therefore considered to be a constant. The reported long-term (>8 year) surface concentrations of concrete in deicing road environments are commonly in the range of 0.15-0.3 %/m_{con} [Goltermann 2004, Tang 2010, Sika/SGK 2013].

From a modelling point of view it would be useful to know according to which expression the C_s grows with time. Firstly, this could be a matter of simply plotting a best fit empirical equation to the available experimental data (see for example Chapter 3.4). Secondly, an evolution expression may also be partly based on theoretical considerations. Some authors suggest that the surface concentration increases as a square root function of time [ACI 2000, Stewart 1998, Uji 1990], or that C_s increases linearly with exposure time, eventually reaching a maximum value that remains constant with time [Life-365 2013, Phurkhao 2005]. Sifeng [2012] showed that the evolution expression (either a complex exponential or hyperbola function) depends on cement type and solution salt concentration. Nilsson and Frederiksen [2011] give a general expression for the evolution of surface concentration with adjustable input parameters. Thus, there is no consensus about how surface concentration in road environments changes with time and how to deal with this issue in prediction models.

2.2.2 Moisture content and temperature

Internal moisture state or relative humidity (RH) of concrete has a significant effect on the chloride transport rate in concrete. The chloride ion transport only occurs through the liquid phase in concrete, and the rate of chloride transport is therefore directly controlled by the amount of liquid in the permeable pores in concrete. There have been surprisingly

few systematic studies on the (important) effect of moisture content on chloride transport in concrete. This partly has to do with the difficulty of measuring chloride transport in partly saturated concrete. In most standard experiments (see section 2.1.2), the concrete is first saturated with water, and all pores are filled with water. When the effect of internal RH is to be investigated, the chlorides cannot be easily introduced into the concrete by means of a solution.

Climent et al [2002] developed a method to supply a limited amount of Cl^- to the partly saturated concrete surface through gaseous hydrogen chloride which is a combustion product of polyvinyl chloride (PVC). They showed that the chloride diffusion coefficient follows a linear increasing expression as a function of water saturation in the range of 30 to 70%. Below 30% water saturation the diffusion coefficient became an order of magnitude lower than the D measured at 80% RH. Nielsen and Geiker [2003] studied the effect of saturation state on chloride diffusivity by applying chloride to the surface using a shock-exposure that did not affect the internal/overall moisture state. They showed that there is a strong increasing effect on internal RH in range from 0.6 to 1, i.e., the D_{app} measured at 65% RH is 20% of the one measured at 100% RH. Olsson et al [2013] showed that the conductivity of all the different types of concretes studies at 100% RH is almost an order of magnitude larger than the one at 50% RH. Guimarães et al [2011] also measured a drop in D by an order of magnitude going from 100 to 30% saturation degree.

Concretes exposed to outdoor atmosphere rarely have a uniform moisture distribution. Drying of concrete is a very slow process, and therefore the core of a thick concrete unit usually has larger internal RH than the surface layers. If a moisture gradient exists in a concrete we can thus expect a corresponding gradient in D, being low outside and higher inside. The rate of chloride ingress will be much affected by the D of the dried surface layer, since all chlorides needs to pass this layer.

Diffusive motion of ions in a fluid is also strongly affected by temperature, and temperature is therefore expected and known to have a large effect on diffusion coefficients. The temperature effect has been measured by various researches in the range of 5 to 80°C [Yuan 2006, Lindvall 2007, Yang 2009, Nguyen 2009, Weng 2012]. The effect of temperature is clear in diffusion coefficients obtained from natural profiles from sea-water [Lindvall 2007] and in migration experiments [Yuan 2006].

The temperature-dependence of the chloride diffusion coefficient can be described through the Arrhenius Equation (conf. [Nguyen 2009]):

$$D(T) = D(T_0)\exp\left[\frac{E_a}{R}\left(\frac{1}{T_0} - \frac{1}{T}\right)\right] \quad (3)$$

where, E_a is the energy of activation (J/mol), R is the gas constant (8.314 J/mol K), T is the temperature (K) and T_0 is the reference temperature (in K).

2.2.3 Other environmental effects

Apart from the effect of internal moisture and temperature state of the concrete on chloride diffusion, there are other environmental influences. The microclimatic setting affects the transport mechanisms. For concrete permanently submerged in salty sea water, diffusion is expected to be the main mechanism for chloride ingress [Nanukuttan 2006]. In microclimatic settings with strong wet-dry cycles, the so-called splash/spray zone, we can expect an effect of capillary suction on ingress rate. The splash zone occurs in concrete elements just above the sea level in marine environments (transition between submerged and atmosphere), but also in road environments. Salt spread out on road surfaces will be sprayed on adjacent concrete surfaces by passing traffic (see Fig. 2, 25). Experimental work shows that depending on the nature and length of the wet-dry cycles, an increase or decrease of chloride ingress rate may occur [Gang 2015]. Finally,

mist water may transport chlorides from sea water or wet roads, and lead to the diffusional ingress of chlorides into concrete elements that are above the splash zone.

The carbonation rate of concrete, that will vary with microclimatic conditions, will also affect chloride ingress, by affecting chloride binding [Meijers 2005, Andrade 2015], or by leading to a densification of the concrete surface layer.

2.2.4 Chloride binding

Part of the chloride ions that migrate into the concrete will not remain as free dissolved ions in the pore solution, but will absorb (physically bound) to the pore wall or will become chemically bound (e.g., as Friedel's salt). An excellent literature review on the topic of chloride binding in concrete can be found in Yuan et al [2009]. The amount of chlorides that is bound in the concrete depends, amongst others, on the following factors: chloride concentration, cement composition, type of introduced salt (cation type); temperature, supplementary cementing materials, and carbonation [Yuan 2009].

The amount of chloride binding is determined by measuring the total (acid-soluble) chloride content and the free (water-soluble) chloride content and subtracting the two measures. The relationship between the free and bound chlorides for a range of chloride concentrations will define the chloride binding isotherm. This isotherm can be compared to theoretical isotherms for absorption processes in porous media, such as Langmuir, BET and Freundlich binding isotherms.

The amount of C_3A and C_4AF in cement seems to have a significant impact on the degree of chloride binding, since the chlorides react with these cement compounds [Yuan 2009, Siegwart 2003, Sumranwanich 2004]. Depending on the C_3A-content (of up to 14% C_3A) and chloride concentration in the paste/solution, up to ca. 50% of the total chloride content can consist of bound chlorides [Yuan 2009]. Other binding chloride contents that have been reported in literature are 25% [Loser 2009] and 40% [Maes 2013] of the total chloride content in OPC-concrete.

Geiker et al [2007] found that chloride binding in Portland cement paste was highly dependent on the content of alkali metals; the higher the content of alkalis the lower the content of bound chloride at any given chloride content. Contrary to traditional views, they state that the content of alumina is possibly less important for binding than the alkalis content. Moreover, from their thermodynamic study they conclude that chlorides are probably more effectively bound in cement containing sufficient limestone filler (about 5%) in order to maximize the content of the monocarbonate AFM-phase.

An important issue is the effect of additions (silica fume, fly ash, slag) on chloride binding, since such effect may help to explain the effect of these additions on chloride transport rate and perhaps the effect of additions on the time to reinforcement corrosion. Yuan et al [2009] mention in their review paper that silica fume addition generally reduces chloride binding. On the contrary, fly ash and slag increase the chloride binding for typical replacement amounts, the main reasons probably are being that these additions contain alumina that promotes the formation of Friedel's salt [Kopecsko 2009, Yuan 2009]. Loser et al [2010] found that chloride binding in concrete with additions is strongly related to the hydration degree of the blended cements. However, the decisive parameter for chloride resistance for these blended concretes was the permeability and not the chloride binding.

2.2.5 Effect of concrete composition

There are a number of ways in which the concrete composition affects the ingress rate of chlorides. Perhaps the most important compositional factors are those that affect the permeability of the concrete matrix. Chlorides are only transported through the fluid phase in the pore space of cement paste, and not through the solid aggregates. Thus, the w/c-ratio [Chalee 2008, Bermudez 2010, Zheng 2010] of the concrete in combination with the binder content in the concrete are two prime factors controlling the rate of chloride ingress. The effect of binder/aggregate weight fraction on the flux of chlorides through

concrete is shown in steady-state experiments [Weng 2012). However, the effect of binder/aggregate fraction amount on D_{nss} or M_{nss} may be much smaller, because these parameters refer to transport of chloride through the fluid phase in concrete only.

In addition to the amount and dilution degree of binder in concrete, there is also an important effect on binder type on chloride transport properties. The cement type will determine the pore size distribution of the matrix and how it develops. This affects the magnitude and evolution of permeability [Loser 2010], and as a result the diffusive or capillary ingress of the chlorides. Pore size distribution also affects the amount of fluid that is retained in the pore space at given RH, and thus the moisture state of concrete and its effect on chloride transport. The chloride binding capacity is affected by cement type as well as described above [Loser 2010]. Another effect of concrete and cement type on chloride transport is caused by the effect of cement type on concrete carbonation which in turn affects the chloride permeability in the surface layers.

Some studies report the effect of concrete composition on D_{nss} and M_{nss} at a specific point in time (at relatively young age). Such results need to be considered with caution, since the observed trends in D_{nss} and M_{nss} at early ages may not be representative for long-term behaviour. Sandberg et al [1998] and Lindvall and Nilsson [2001] studied various types of concretes with Portland cement, fly ash and silica fume. These showed that after 5 years of salt exposure in sea water or road environments, 5% of silica fume addition reduced the diffusion coefficient by a factor 2 with respect to plain PC-concrete having the same w/c-ratio. An addition of 10% silica fume reduced the D_{nss} by a factor 3 relative to PC-concrete in both exposures regimes [Lindvall 2001]. The same behaviour was observed for the addition of fly ash to the concrete or fly-ash combined with silica fume. The effect of increasing amount of FA-addition on the lowering of D_{nss} has also been shown by Chalee and Jaturapitakkul [2008]: 50% FA produces a D_{nss} that is a 3-6 times smaller than the one for PC-concrete (depending on w/c-ratio and fly ash type) after 5 years. Also for slag cement it has been shown that additions of up to 70% slag reduced the D_{nss} and M_{nss} [Maes 2013].

2.2.6 Time-dependence of chloride transport coefficients

It is well-known that the chloride transport coefficients (D and M) are not constant in time. They generally tend to decrease with time, or in rare cases increase with time. The ageing of the concrete with regard to chloride resistance may last for many years, or perhaps even during the entire service life of a concrete structure. This chloride-related ageing of concrete can be characterized by the ageing factor (n), that is the time exponent of the (exponential) decay of D (or M) with time:

$$D = D_0 \cdot \left(\frac{t_0}{t} \right)^n \qquad (4)$$

Where, D is the transport coefficient at time t and D_0 is the chloride transport coefficient at a reference time t_0. The ageing factor is an important input-parameter in many service life prediction models.

There are a number of reasons for the time-dependence of D and M: Firstly, there is reduction of permeability/porosity with ongoing cement hydration. The specific kinetics of the hydration of a binder will therefore partly determine the ageing factor. Secondly, chloride binding may lead to a reduction in porosity with time, or becoming proportionally larger with time, and this will also slow down the chloride transport. Thirdly, drying and carbonation may lead to a gradual change of the surface concrete and lead to a slowing down of chloride ingress. Finally, depending on how the D or M is measured there might be additional factors contributing to the time-dependence of D and M. For example, part of the long-term ageing in D_{nss} obtained from concrete structures may be a mathematical effect caused by the applied regression method to obtain D_{nss}. Also, chloride ingress by capillary suction can have an effect on the ageing factor as will be discussed in section

3.6.2. Thus, the ageing factor is not a material parameter, but depends on how and under what conditions (e.g., cured in fresh or salt water) it is measured.

Table 3 lists a large number of ageing factors (n) for a variety of cement types measured from field concretes for different exposure classes, and for laboratory measurements. From the table it becomes clear that the ageing factor is not a robust parameter, but depends on measurement method or conditions (exposure class): for CEM I, slag, FA and

Tab.3: *Published aging factors (n) for field and laboratory concretes under different exposure conditions. DuraCrete-type ageing factors are highlighted in grey.*

cement type	add.-% / w/b-ratio	n	exposure time (y)	exposure class or experiment	reference
CEM I	0.5	**0.10**	12	XD3	this study
	0.5	**0.45**	12	XD3	this study
	0.35	**0.45-0.55**	12	XD3	this study
	0.4 - 0.6	**0.65**	?	XD1	[STRUREL 2012]
	0.4 - 0.5	**0.60**	40	XD1, XD3	[Kapteina 2011]
	0.4 - 0.6	**0.30**	?	XS2, XS3, XD3	[STRUREL 2012]
	0.4 - 0.6	**0.40**	?	XD2, XS2, XS3	[Wegen 2012]
	0.46 - 0.6	**0.22-0.40**	5	migration test	[Audenaert 2009]
	0.5	**0.32**	4	diffusion test	[Stanish 2003]
	0.5	**0.44**	4	XS2	[Costa 1999]
	0.5	**0.51**	3	XS3	
	0.5	**0.42**	4	XS1	
	0.3	**0.41**	4	XS2	
	0.3	**0.43**	3	XS3	
	0.3	**0.36**	4	XS1	
CEM I + slag	20% / 0.5	**0.20**	12	XD3	this study
	CEM III/B (25-50% slag) / 0.4 - 0.6	**0.65**	?	XD1	[STRUREL 2012] [Wegen 2012]
	CEM III/A or CEM III/B (50-80% slag)	**0.70**	?	XD1, XD3, XS1	[Wegen 2012]
	CEM III/B (25-50% slag) / 0.4 - 0.6	**0.45**	10	XD2, XS2, XS3, XD3	[STRUREL 2012] [Wegen 2012]
	CEM III/A / 0.4 - 0.6	**0.40**	?	XD2, XS2, XS3, XD3	[STRUREL 2012]
	CEM III/A or CEM III/B (50-80% slag)	**0.50**	?	XD2, XS2, XS3	[Wegen 2012]
	20% / 0.36	**0.2-0.3**	25	XS1, XS3	[Oslakovic 2010]
	CEM III/A / 0.46	**0.43**	5	migration test	[Audenaert 2009]
CEM I + fly ash	15% / 0.5	**0.30-0.45**	12	XD3	this study
	>20% / 0.4 - 0.62	**0.65**	?	XD1	[STRUREL 2012]
	21-30% / ?	**0.80**	?	XD1, XD3, XS1	[Wegen 2012]
	>20% / 0.4 - 0.62	**0.60**	?	XS2, XS3, XD3	[STRUREL 2012]
	21-30% / ?	**0.70**	?	XD2, XS2, XS3	[Wegen 2012]
	25% / 0.5	**0.66**	4	diffusion test	[Stanish 2003]
	56% / 0.5	**0.79**	4		
CEM I + silica fume	7% / 0.5	**0.45**	12	XD3	this study
	4% / 0.35	**0.40-0.45**	4	XS3	[Costa 1999]
	4% / 0.35	**0.38-0.59**	4	XS2	
	4 (8)% / 0.3 (0.4)	**0.6 (0.61)**	3	diffusion test	[Nokken 2006]
	12% / 0.4	**0.5**	3	diffusion test	

SF concretes the reported n-values range between 0.1-0.65; 0.2-0.65; 0.3-0.8, and 0.38-0.59, respectively. Van der Wegen et al [Wegen 2012] proposes ageing factors for atmospheric road conditions (XD1, XD3) that are systematically larger than for sea water exposure (XS2, XS3). STRUREL-software proposes larger n-values for mist conditions (XD1, XS1) compared to submerged/spray conditions (XD2, XS2, XS3). Note that ageing factors may also differ with the applied regression method and fitting procedures, and care should be taken when comparing the different n-values in Table 3.

2.3 Corrosion of reinforcement steel

2.3.1 Chloride induced corrosion mechanisms

In salt-free environments, steel reinforcement in concrete will not corrode if the internal pH of the concrete maintains a value above 11 - 11.5. Under these conditions, the steel is passivated and protected by a thin layer of ferric oxides against corrosion. Breakdown of the passivation layer may occur when the internal pH is reduced below a critical value (of 11 - 11.5), for example, as a result of concrete carbonation or leaching. In the case of chloride-induced corrosion, the pH of the concrete may largely remain unchanged (i.e., pH>12.5). The depassivation is then caused by the corrosive action of the chloride ions dissolved in the pore solution around the steel bar. The identification of chloride-induced corrosion is based on measuring the chloride content of the concrete and the depth of carbonation, and on the specific nature of the corrosion occurrence (corrosion pitting and products). Some chloride-induced corrosion phenomena in concrete are shown in Fig. 1.

A large number of papers and books are treating the mechanism of chloride-induced corrosion of steel in concrete [Bažant 1979, Tuutti 1982, Page 1982, Schiessl 1988, Berke 1990, Böhni 2005, Broomfield 2006, Raupach 2007, Angst 2011a, Bertolini 2013]. For the onset of corrosion (local breakdown of the passivation layer) a pH dependant threshold value in chloride concentrations needs to be exceeded. After corrosion initiation, the role of chlorides in the corrosion process may become less important, and the corrosion rate is mainly controlled by the availability of water and oxygen in the concrete, the effect of the macroelement (surface ratio cathodic to anodic area) and the resistivity of concrete [Langford 1987, Hunkeler 1996, Schiegg 2002, Andrade 2004, Hunkeler 2005, Hornbostel 2013].

The corrosion reaction is an electrochemical process with steel dissolution occurring at the anode surface:

$$Fe \rightarrow Fe^{2+} + 2\,e^{-} \qquad (5)$$

In the cathodic region, dissolved oxygen in pore water reacts with the incoming electrons from the steel bar in the presence of water to form hydroxyl ions (OH^-):

$$H_2O + ½O_2 + 2e^{-} \rightarrow 2OH^{-} \qquad (6)$$

The total cell reaction is as follows:

$$Fe + H_2O + ½O_2 \rightarrow Fe(OH)_2 \qquad (7)$$

The corrosion product iron hydroxide ($Fe(OH)_2$) reacts further with available oxygen and water to form red rust:

$$4Fe(OH)_2 + O_2 + 2H_20 \rightarrow 4\,Fe(OH)_3 \qquad (8)$$

$Fe(OH)_2$ and $Fe(OH)_3$ are not the only corrosion products that may form in the corrosion process. In saturated concrete (permanently immersed in water), oxygen supply is restricted, and black rust (Fe_3O_4) may form. This is also the type of rust observed in the so-called lollipop experiments to measure the critical chloride content (see Fig. 20). The type of rust forming is important with regard to corrosion induced cracking and spalling of

concrete [Hunkeler 2006]. Red rust has a volume four times larger as the one of steel [Bažant 1979, Liu 1998]. Black rust occupies twice as much space compared to steel.

2.3.2 Critical chloride content

The critical chloride content (C_{crit}) is defined as the total internal chloride concentration in concrete at which depassivation or corrosion of reinforcement steel starts. It is expressed as the chloride weight fraction with regard to the concrete or binder content. This is one of the decisive input parameters for lifetime modelling of reinforced concrete in contact with sea water or deicing salt. An excellent review of the available experimental data for C_{crit} in literature can be found in Angst et al [2009]. It shows that there is little precise consensus about how this parameter should be measured, and what its value is. For normal concrete with normal rebar steel, experimentally determined C_{crit}-values using a variety of techniques, ranges between 0.1 and 3% of binder content [Breit 2001, Angst 2009].

Critical chloride contents have been determined from: (i) theoretical considerations; (ii) directly from concrete structures showing the onset of corrosion; (iii) from experiments with steel bars immersed in a solution, and (iv) from experiments with a steel bar embedded in concrete. The latter experiments are generally considered to represent the practical situation best. In this project, a so-called lollipop experiment to measure C_{crit} was developed, which is broadly similar to other methods described in literature (see Chapter 4): A steel bar is embedded in a cylindrical mortar or concrete specimen with constant cover thickness. Before the introduction of chlorides, the specimen is cured in a lime bath in order to create a passive film on the steel bar. Then, the specimen is immersed in a NaCl-solution, and chlorides will enter the specimen by diffusion. To speed up the experiment, the cover thickness is held low and/or the chlorides are accelerated by dry-wetting cycles or by electrically forcing the diffusion process. Alternatively, the chlorides can be mixed with the concrete at given concentration. The corrosion state is usually monitored, non-destructively, by measuring the potential over the steel bar [Angst 2009, Angst 2011c].

At the point of depassivation, as indicated by a sharp drop in potential (or a raise in current in alternative experiments), the specimen is taken out of the solution followed by a measurement of the total chloride content in the concrete directly around the steel bar. There is no consensus about how to collect sample material from the specimen for the chloride content determination. Some researchers collect powder samples from the concrete around the steel bar by grinding. Others measure the chloride profile in the specimen with steel bar or on a duplicate specimen without steel bar, and obtain C_{crit} by means of interpolation. In case of powder sample collection, the actual paste content of the concrete adjacent the steel needs to be determined, as this significantly deviates from the bulk due to wall-effects (see Chapter 4). In the case of the interpolation-method, a too low value for C_{crit} may be obtained because of chloride enrichments effects at the steel bar surface [Oh 2003]. An important specimen size effect on C_{crit} is to be expected due to probabilistic effect as described by Angst et al [2011b]. The use of small specimens can therefore rapidly lead to large scatter in C_{crit} measurements.

A number of researchers have not observed a significant effect of cement type or mixture composition (w/c-ratio and cement content) on C_{crit}. [Hansson 1990, Petterson 1993, Breit 2001]. Yu et al [2011] found that higher cement alkalinity delayed rebar corrosion by increasing C_{crit}. Angst et al [2009] reviewed the effect of binder type, chloride binding capacity, and mineral admixtures on C_{crit}. Theoretically, the effects of cement type and mineral admixtures on chloride binding should also affect C_{crit}. However, there exist no systematic studies that really confirm these effects [Angst 2009]. Moreover, some reported effects on C_{crit} may be only apparent, since the results of different concrete types were not properly normalized to comparable conditions.

For service life modelling and standard specifications the most conservative values measured for C_{crit} are usually used, which are the lowest values measured for a certain type of steel in a certain type of concrete. Table 4 shows which maximum values of C_{crit} are prescribed by international standards or specifications.

Tab.4: *C_{crit}-values prescribed for normal rebar steel in various (inter)national specifications [Breit 1997, Ann 2007].*

Country	Document	year	max. C_{crit} (%/m_{bin})		
			pre-stressed (dry/wet)	not pre-stressed (wet)	not pre-stressed (dry)
Germany	EN 206	1995		0.4	
UK	BS 8110	1985	0.1	0.2	0.4
Norway	NS 3420	1986		0.4	
USA	ACI 201/222	2008	0.08	0.1	0.2
	ACI 318	1989		0.3	
	ACI 357	1997	0.06	0.1	
International /RILEM	TC 124-SRC	1994		0.3 – 0.5	

2.4 Chloride transport prediction models

2.4.1 General considerations

Because of its practical importance, many prediction models for chloride-induced corrosion have been developed in the last 40 years or so. In this chapter an overview of the existing 'chloride' service life models is given, which are mainly transport models. The concrete service life is often taken as the time to onset of corrosion of the first layer of reinforcement bars. This corrosion-free service life ends when the chloride concentration at the first reinforcements exceeds the critical chloride content (C_{crit}). Note that in cases of a slow development of corrosion-induced damage, the practical service-life of concrete structures may be significantly longer than the predicted service-life. Models that consider the kinetics of corrosion after initiation are not reviewed here. With regard to the chloride transport kinetics, a distinction can be made between two broad classes of transport models: (1) mechanistic models and (2) empirical models [Tang 2005, Angst 2012]:

Mechanistic models contain equations for all relevant physical and chemical reactions in the chloride transport. The extensive set of equations usually requires finding solutions by means of numerical modelling. The purpose of such models is to learn how certain factors affect the chloride transport process, or in others cases to make actual service life predictions. Mechanistic models reported in literature are usually not easily available to construction engineers. The reasons being that the codes are too complicated to use (i.e., a lack of user-friendly interface), or because they require input parameters that are difficult to obtain.

Empirical models are based on an equation that captures the primary transport physics of the chloride transport (e.g., Fick's law). However, many of the detailed mechanisms are not explicitly modelled, and may end up in certain fitting constants. These models are often tuned towards certain data sets under certain conditions, and this may limit the applicability of such models. Moreover, empirical models will never question the preciseness of a field measurement. A clear advantage of such models, though, is that they are easily available to construction engineers, i.e., are applicable in commercially available spreadsheets. Moreover, they require the input of a minimum number of parameters that are relatively easy to obtain.

Mechanistic models may describe better and in more detail the chloride transport process, however this does not automatically imply that they lead to more accurate predictions than empirical models do. This is because the reliability of a prediction outcome also depends on the representativeness of the input-parameters. The quality of the prediction results can be tested by means of comparing them to the results of long-term field measurements. This is one of the main objectives of this study: to show how

long-term field experiments such as Naxberg help to tune and validate service life models.

Some transport models produce probabilistic results, meaning that the prediction results are presented as corrosion initiation probabilities or as a reliability index (see [Gehlen 2000, STUREL 2012]). This makes sense because often the service life of large concrete units needs to be predicted, and these show significant spatial non-uniformity in material properties, cover thickness and availability of chlorides at the service [Goltermann 2004]. The probability can then be interpreted as the probability that corrosion will be initiated somewhere in the concrete element, or as a proportion of the reinforcement steel that may start to corrode after a certain amount of time. However, probabilistic results are difficult to validate, i.e., check against actual field performance. Therefore we will focus in this report on the deterministic output of prediction models, and compare those results to actual field performance. Models described in this report can be extended into a version producing probabilistic results. These probabilistic methods are well-described in literature [STRUREL 2012, Gehlen 2000] and are not repeated here.

2.4.2 ERFC-type prediction models

Empirical ERFC models for service life prediction are relatively simple models based on Fick's second law of diffusion under the assumption of time-independence of the diffusion coefficient (D) and chloride surface concentration (C_s). Under these assumptions the solution of Fick's second law is an error-function or error-function complement (ERFC) that can be computed non-numerically in commercially available spreadsheets. This model approach was first proposed by Collepardi et al [1970]. The error-function is also widely used in cases of a time-dependent diffusion coefficient and chloride surface concentration. Mathematically it is incorrect to replace D by a D(t)-equation and C_s by C_s(t)-equation in the error-function, since the error-function is no longer the solution of Fick's second-law when D and C_s become time-dependent [Tang, 2005]. However, since these diffusion-type models are used as empirical models, they do not necessarily have to be mathematically correct, as long as they produce results that are in agreement with field measurements. Other models deal with the time-dependence of input properties in a more sophisticated way, or by solving Fick's second law numerically [Maheswaran 2004, Poulsen 2006, Life-365 2008).

The error-function prediction model is as follows for the situation of concrete with no significant initial chloride content:

$$C(x,t) = C_{surface,app} \cdot erfc\left(\frac{x}{2\sqrt{D_{app} \cdot t}}\right) \qquad (9)$$

This equation was already introduced in chapter 2.1.3 since it can be used to determine the diffusion coefficient (D_{nss}) from a chloride profile. When the chloride diffusion coefficient is known then it can be used to predict the development of chloride profile with time. In this equation the non-steady-state diffusion coefficient (D_{nss}) is replaced by the apparent diffusion coefficient (D_{app}), both representing the same type of diffusion coefficient. The term 'apparent diffusion coefficient' is often used to express the two-fold apparent nature of this diffusion coefficient: (i) D_{app} represents an average diffusion coefficient for a given period (in which the transport properties of concrete may be changing/decreasing; (ii) D_{app} is not a pure diffusion coefficient, but a transport coefficient determined from a chloride profile that includes non-mobile (i.e., bound) chlorides, and chloride transport may occur by non-diffusive mechanisms.

The apparent diffusion coefficient (D_{app}) can be determined from a chloride profile from an existing concrete structure, with the purpose to predict how the chloride will develop further in future. In the case of a new concrete structure, the actual D_{app} is not known, and need to be determined from laboratory experiments on the to-be-used concrete. This is not straight forward because D_{nss} or M_{nss} determined in the laboratory may differ

significantly from the field-D_{app} for a number of reasons. Certain correlation factors are needed to calculate D_{app} from D_{nss} or M_{nss} as determined in the laboratory. In the DuraCrete model this is done as follows from measurements of the migration coefficient (M_{nss}) at an age (t_0) of 28 days [Gehlen 2000, Kapteina 2011, STRUREL, 2012]:

$$D_{app} = K \cdot M_{28d} \cdot \left(\frac{t_0}{t} \right)^n \tag{10}$$

This formulation contains two correlation factors, the correlation factor K and the ageing factor n. The correlation factor K is supposed to express the differences in temperature, moisture content, age at first chloride ingress, and other differences between the laboratory measurement and the actual field performance. The ageing factor n is supposed to express the time-dependence of the apparent diffusion coefficient (D_{app}) in the field. Aging factors determined (short-term) laboratory experiments may not be representatives for the field case. The values for K and n can be obtained by fitting the DuraCrete model to a set of chloride profiles from a field experiment when the M_{28d}-value is known.

The apparent chloride surface concentration (C_{s_app}) is an apparent parameter for the same reasons why D is apparent. Moreover, when C_s is obtained by regression of a chloride profile showing a mountain-shape, C_{s_app} represents a virtual, extrapolated surface concentration. In some cases a constant value for a particular setting may be assumed (conf. [Kapteina 2011]). In other cases, one of the time-dependent relationships of C_s such as described in Section 2.2.1 may be applicable.

2.4.3 Transport models with capillary suction effects

The ‘error-function’ diffusion models may not accurately describe chloride ingress in partly saturated concrete in road environments, since effects of capillary suction may contribute to the chloride ingress. Under spray water conditions, a partly-saturated concrete may come into sudden contact with water containing dissolved salts that will then penetrate the concrete by capillary suction. This type of ingress may occur much more rapidly than diffusion and lead to a chloride distribution (profile) that cannot be predicted by the error-function. In microclimates with large or irregular capillary effects, simple ERFC-models may therefore no longer function. However, when the contribution of capillary ingress is relatively small compared to diffusional ingress, and shows no large variations in time, the error-function approach may still be useable [Kapteina 2011]. The capillary effects then become an integral part of the apparent diffusion coefficient and ageing factor.

A number of mechanistic models consider capillary suction effects explicitly in addition to diffusional ingress. Examples of such models are the ones developed by Meijers et al [2005], Sleiman et al [2012]; and by Lay [2006]. The elaborated models for transport in partly saturated concrete including capillary effects can produce results in particular cases that are very similar to those produced by simple error-function models, i.e., with only minor differences in the shape of the chloride profiles [Meijers 2005, Lay, 2006]. Experiments have also shown that chloride ingress during wetting-drying cycles, i.e., under conditions in which capillary suction effects are expected, produces chloride profiles roughly similar to those obtained in saturated (pure diffusion) experiments [Gang 2015].

Finally, the STADIUM model (see e.g. [Conciatori 2015]) should be mentioned here. It is commercially available and therefore of particular interest to engineers: it is a prediction software package based on finite element model, with which the ingress of corrosive substances such as chlorides can be predicted. It is an elaborate model for coupled transport of water and ions based on the Nernst-Planck/Poisson equation, and considers moisture and heat convection effects. It includes a chemical equilibrium code for the chemical reactions that happens due to the ingress of water and ions, e.g., dissolution, precipitation, chloride binding, carbonation, etc, and their feedback effects on the transport properties of the material. Onset of reinforcement corrosion is predicted to occur

when the chloride concentration at the rebars exceeds a critical value, and a specific incubation time has passed.

2.4.4 TransChlor

TransChlor is a mechanistic chloride ingress model that has initially been developed in Switzerland (EPFL) and tested for various road settings (microclimates) in Switzerland [Denarie 2003, Conciatori 2008, 2010]. In this model capillary suction is also explicitly considered. In this project, the chloride ingress in the Naxberg experiment has been predicted with this model, and the results of these simulations will be presented in Section 5.5.

TransChlor is a comprehensive (numerical) model for moisture and chloride transport in the concrete cover layers, and considers most of the physical and chemical reactions relevant for the chloride transport process explicitly. Ingress of chlorides occurs by diffusion and/or capillary suction, and effects of carbonation and chloride binding, as well as thermal effects are considered [Conciatori 2008]. The dominant mode of moisture and chloride ingress will be determined by the microclimate or exposure class of the concrete ('submerged', spray water or mist conditions). Microclimate will have a significant effect on the chloride ingress rate, and the microclimate (exposure class) therefore needs to be correctly identified for a particular setting in order to obtain reliable prediction results.

The amount of salts at the surface is predicted from actual meteorological data and the amount of deicing salts used in a particular region. When the amount of the actual used deicing salts is not known, this parameter is predicted from the meteorological data: salt trucks are used on days with snow or on days with precipitation in combination with a certain threshold temperature. The mode of salt spraying (mechanical or automatic) is also an input parameter for the model to predict the chloride surface concentration [Conciatori 2008].

The moisture and chloride transport equations in the model have been validated by laboratory experiments. Under combined actions of chloride ingress, carbonation, chloride-binding and drying-wetting cycles, the models produces a mountain-shaped chloride profiles which is in agreement with those observed in field experiments [Conciatori 2008]. The model results have, however, not been compared to long-term field experiments before as will be done in this report (see Section 5.5).

2.4.5 Bench-marking of prediction models

In a number of studies the performance of various service life prediction models has been evaluated. In these studies, the chloride ingress was predicted for a particular concrete in a particular setting (mostly in sea water) and compared to the actual field performance (i.e., chloride profiles) after many years of chloride exposure.

Oslakovic et al [2010] compared the lifetime predictions made with North American Life-365, the Croatian CHLODIF model, and the DuraCrete model to chloride profiles in a marine bridge after 25 years in a sea-water environment (spray and atmospheric conditions). This study was only partly a bench-mark study since the actual measured chloride surface concentration in the bridge after 25 years chloride exposure, was used as input for the model predictions. For new concrete structures, the time-evolution of the surface concentration, and the maximum value reached are unknown, and also need to be predicted or assumed. Without fitting of C_s in this bench-marking study, the lifetime predictions could have significantly differed from the current results.

Since the ageing factor of the bridge concrete was not known (measured), they set this parameter to zero in the Life-365 model. For this case the Life-365 model produced too strong chloride ingress rates after 25 years. Only when the minimum measured D (obtained from Cl-profile regression) was used, a reasonable match between predicted and measured profiles was found. Alternatively, a match was found by 'manually' reducing the surface concentration or by setting the ageing factor to a value of 0.31 as

theoretically predicted by the Life-365 model. In the CHLODIF-model a default ageing factor of 0.1 was used, and this produced a reasonable agreement of predicted and measured chloride profiles in the atmospheric zone (XS1), but still too high chloride concentration for the spray exposure (XS3). Finally, the 'default' ageing factors of 0.65 and 0.85 used in DuraCrete for the given exposure classes, lead to predictions with a too large reliability (= too slow chloride ingress). Only when the ageing factor was set to values of 0.20 and 0.25 predictions with reasonable reliability could be obtained. This study showed that the three different types of error-function type prediction models produced similar and reasonable result if an ageing factor of 0.2-0.3 was used for the tested slag concrete, and the surface concentration was 'fitted' to the measured values.

Aldred and Castel [2014] tested the performance of the CSM-model, Life-365, and STADIUM for a concrete with slag or silica fume replacement in a splash zone sea water environment (XS1-3) with 600 cycles of wetting per year. In these predictions only initial information and model default values were used, i.e., input parameters that would have been available at the time that the marine concrete was prepared. All three models underestimated the chloride ingress at early exposure ages (2 and 6 years). At 19 years of chloride exposure the predictions of the three models varied; either similar, lower or higher chloride ingress rates compared to field behaviour were obtained. Unfortunately, no information is given in the paper about which default values were used in making these predictions, such that it remains unclear why the model predictions deviated from the field observations.

Another model validation study was carried out by Tang et al [2010] on basis of the results of a Swedish field experiment (Borås). The measured chloride profiles and model results are presented in Figures 5 and 6. The main source of disagreement between observations and predictions for the SRPC concrete is that the input C_s for all models does not match the actual surface or peak concentration. For the SRPC + 5% SF concrete, the model input C_s is closer to the one measured, and therefore better predictions were obtained. Furthermore it is seen that a simple ERFC model (with n = 0) overestimates the chloride profiles in all cases, and the DuraCrete models (with n = 0.65) tends to underestimate the chloride profiles if input-C_s would have been fitted to the observed C_s.

A large world-wide bench-marking exercise involving 18 modellers and a large variety of service life models was carried out in the framework of the EU-funded research project 'CHLORTEST' [Tang 2005]. In this exercise a number of measured chloride profiles were selected, and the 18 modelers were asked to predict these and future profiles. In one case the early age migration a coefficient of the concrete was provided in the other case is was not. The modelling results show a large scatter for a variety of reasons. In the CHLORTEST-report no detailed information is given about which model is linked to which modelled chloride profile, and therefore it is impossible to say something about the reliability of specific models. One measured weak chloride profile, due to e.g., chloride leaching in summer or due to some kind of blocking action, was significantly overestimated by all modelers. For the other chloride profiles the best predictions were generally obtained by models that (coincidently) used a chloride surface concentration that matched the measured surface concentration. The models with a constant C_s generally had lower prediction performance than those with a time-dependent C_s. No general conclusion about the effect of different ageing factors in the models was given.

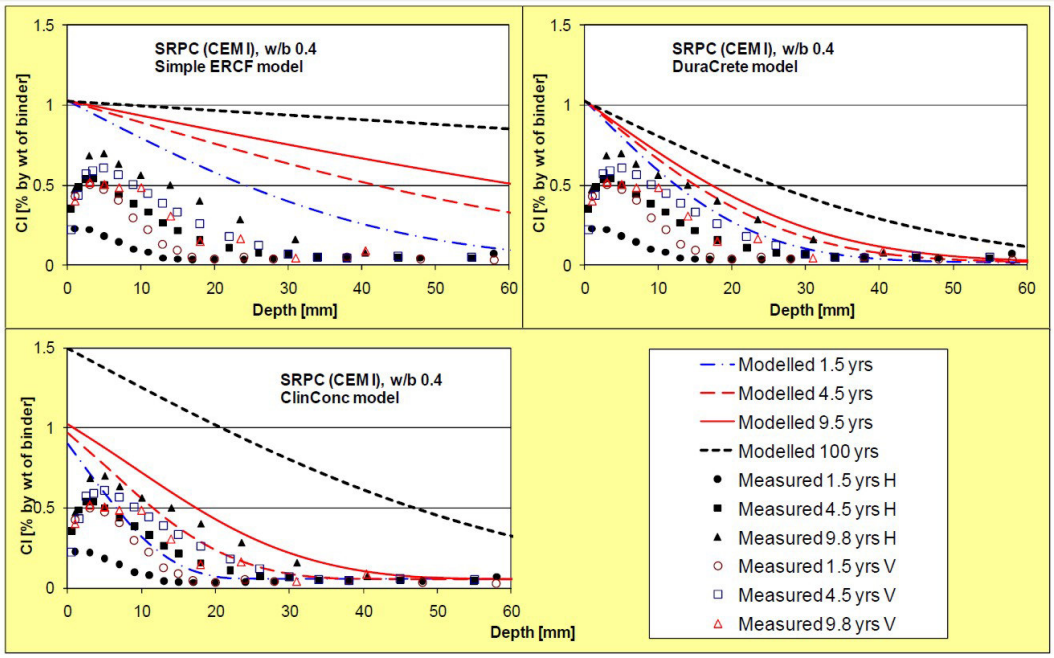

Fig.5: *Modelled and measured chloride profiles for SRPC concrete (from: [Tang 2010] – reprinted with kind permission).*

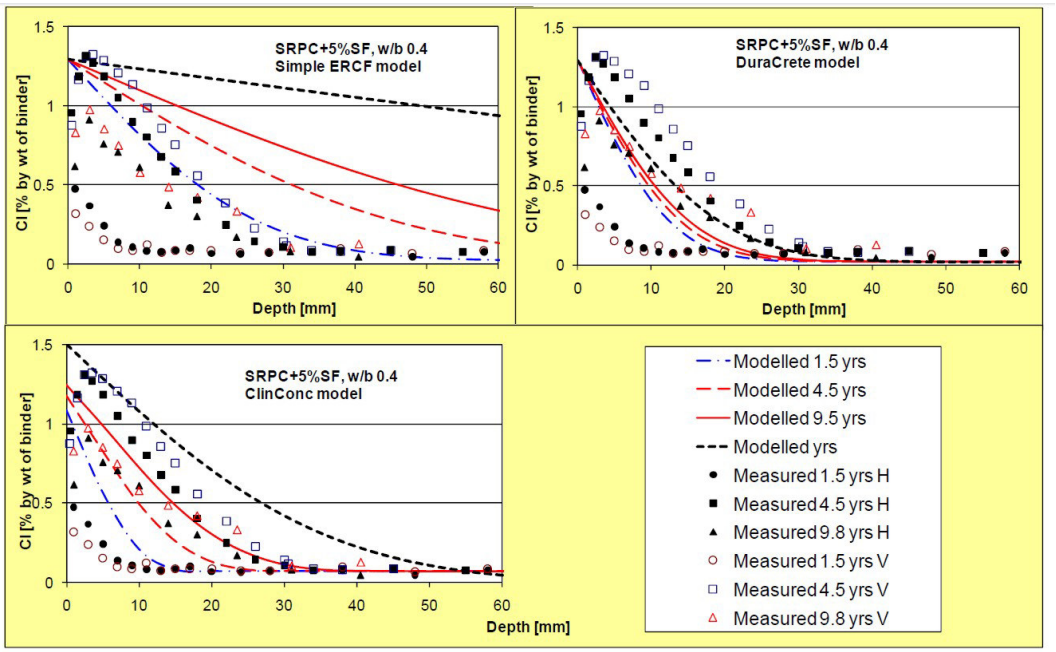

Fig.6: *Modelled and measured chloride profiles for SRPC + 5% SF concrete (from: [Tang 2010] – reprinted with kind permission).*

3 Results of the Naxberg experiment

3.1 Method to obtain chloride profiles

A description of the Naxberg field experiment and the studied concrete types is given in Chapter 1. A total of 65 cores (Ø 5 cm, l = 10 cm) have been drilled from the Naxberg plates for the measurement of chloride profiles at different ages (see Table 5). First exposure to chlorides (deicing salts) is assumed to have occurred at the start of the winter (01/12/2000), at which the concrete had an age of about 6 months. The plates were placed into the tunnel wall in the autumn of the year 2000. The cores were cut into slices with 10 mm thickness, and the total acid-soluble chloride content was measured in compliance with Swiss standard SN EN 14629 [SN EN 14629]. In this report, chloride concentrations are mostly expressed as a weight fraction (%) of the dried concrete. Calculating the concentration back to binder weight involves making an assumption of the hydration/reaction degree, which is not a straight-forward matter for blended cements. Moreover, gradients in cement content that usually occur near the concrete surface are to be considered, if a proper chloride profile expressed as weigth fraction of binder weight is to be obtained. Approximate chloride weigth fractions of cement can be calculated using the data in Table 1.

Only one core was taken from each plate at each sampling date, because of the limited sampling space. Due to the presence of the reinforcement grid and various types of embedded sensors, a maximum total of 6-8 cores could be taken from each plate (of 60 x 50 cm). Duplicate cores from the same or adjacent plates were taken in a few cases to check the reproducibility of the measurement of chloride profiles. The accuracy or representativeness of the chloride measurements depends mainly on the total volume of the concrete sample that is analysed, and not just on the number of analysed samples. The typical sample volume of a slice (Ø 5 cm, l = 1 cm) is relatively large compared to samples obtained by techniques involving powder drilling or core grinding.

Tab.5: *Concrete age and chloride ingress durations at moment of core sampling.*

Age (years)	Sample and measurement month & year	Chloride exposure duration (years from 01/12/2000)
2	April 2002	1.4
3	June 2003	2.5
4	June 2004	3.5
5	May 2005	4.4
12.5	November 2012	12
13.5	October 2013	12.8

3.2 Description of chloride profiles

All measured chloride profiles are shown in Fig. 7 and 8. In most cases there was an ongoing chloride ingress with time. The overlap or apparent retreat of chloride profiles in subsequent years that was measured in a few cases, may be either due to season-induced variations in the chloride contents, or be a result of sampling issues. Poulsen and Mejlbrom [2006] showed that chloride concentrations drop in the summer due to leaching of the concrete by spray water from traffic or rain, and the absence of deicing salt application. Reproducibility of the measurement of chloride profiles after longer exposure durations (12 or 12. 8 years) is suggested by: (i) the profiles from concrete B1, B2, and C1 measured at 12.8 years; (ii) the profiles H3 and H4 at 12 years; (iii) the profiles A3 and A4 measured at 12.8 years; (iv) the profiles E1 and E2 after 12.8 years; and (v) the profiles F1 and F2 after 12.8 years. In general the reproducibility of measurements from adjacent plates is very good after 12 or 12.8 years chloride exposure. An exception is

plate D1 and D2 that show strongly differing chloride profiles after 12.8 year. This height effect will be addressed in Section 3.3.

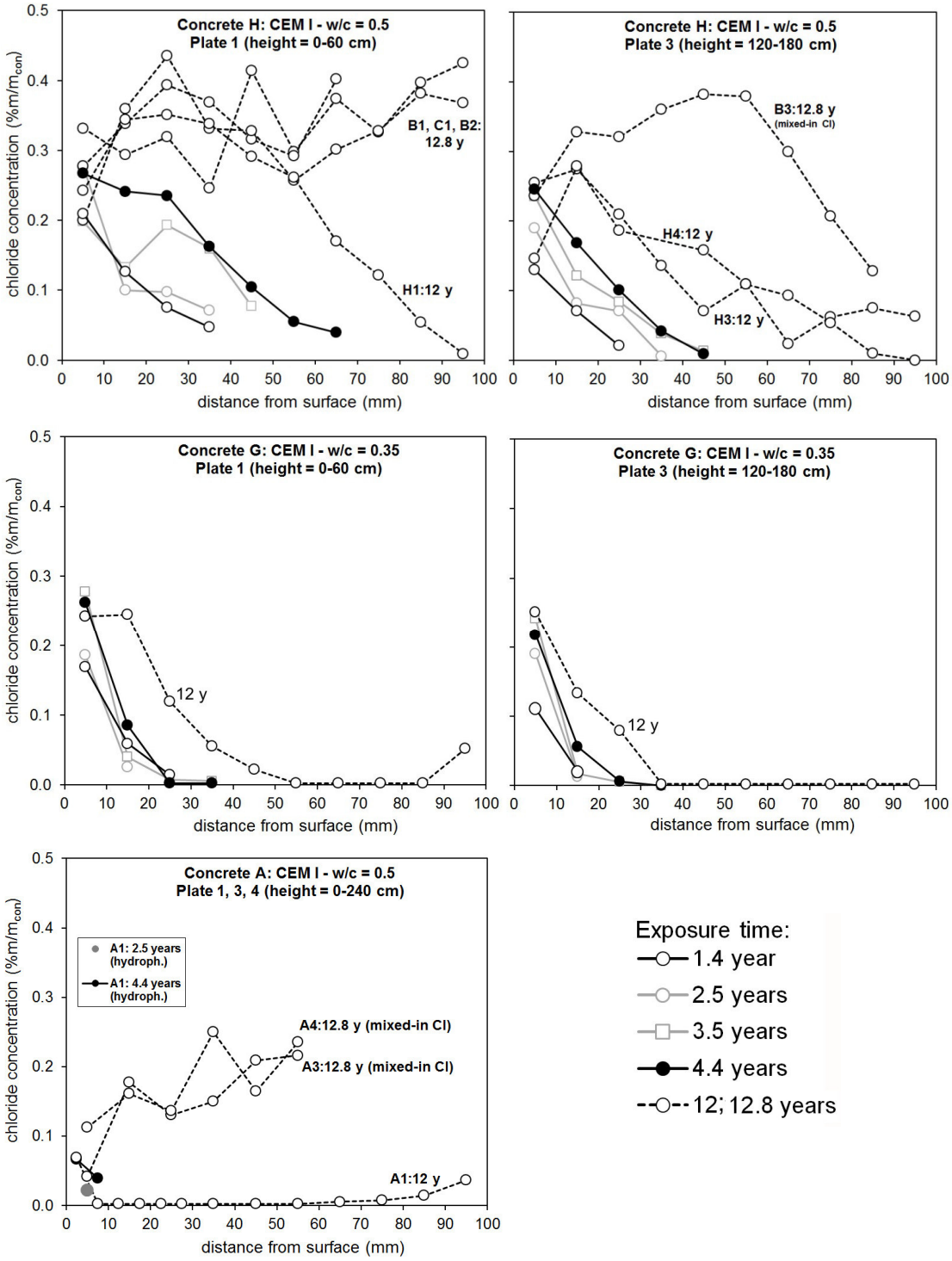

Fig.7: *Measured chloride profiles from the Naxberg plates 1 and 3 made out of CEM I concrete having a w/c-ratio of 0.5 (concrete H) or 0.35 (concrete G), and plates with hydrophobic impregnation (A1) or mix-in chlorides (concretes A3, A4 and B3).*

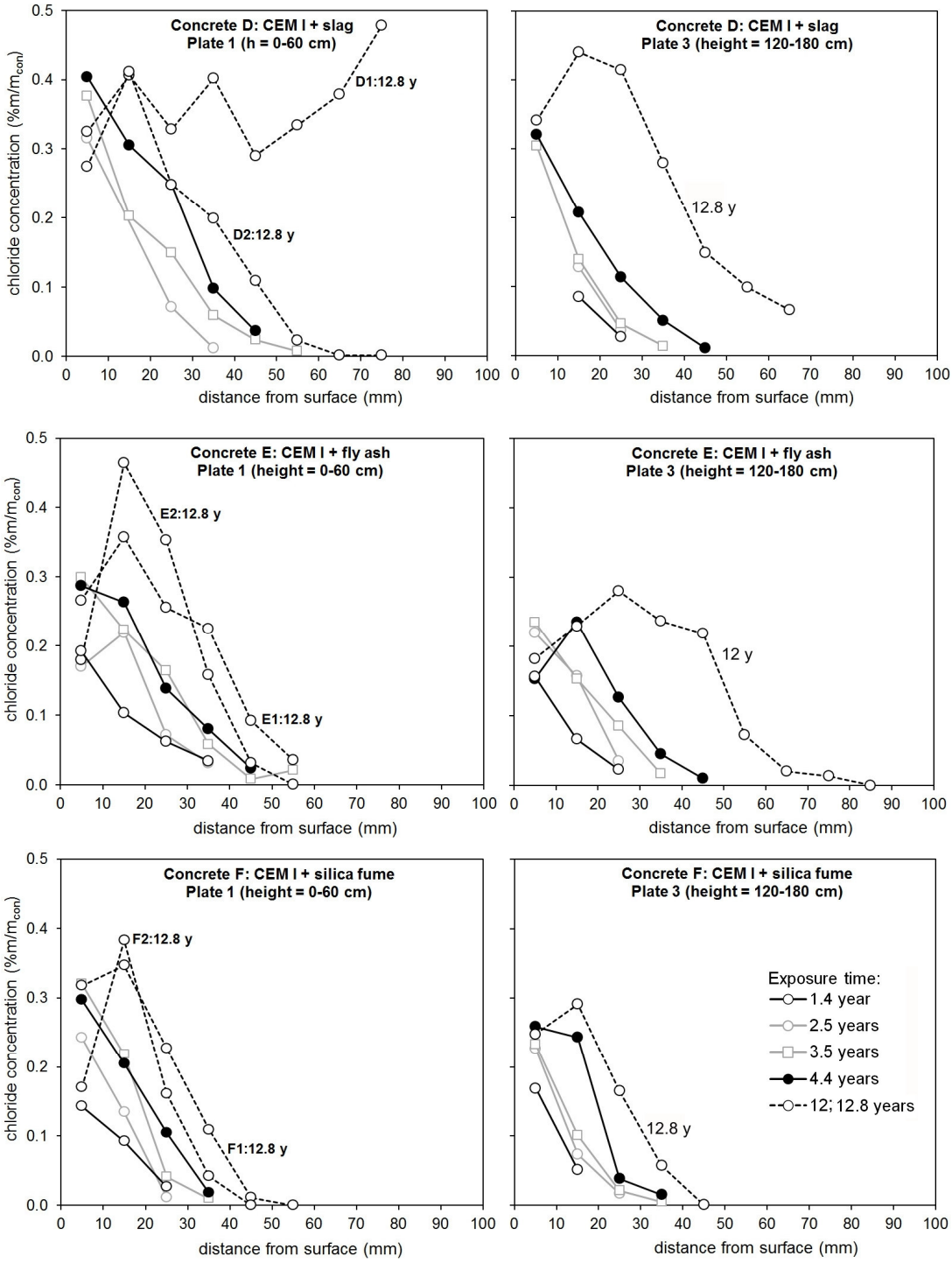

Fig.8: *Measured chloride profiles from the Naxberg plates 1 and 3 made out of concrete with slag (concrete D), fly ash (concrete E), or silica fume (concrete F).*

The progressive ingress of chloride with time is shown by the penetration of the chloride front, but also by an overall increase in chloride concentration at the shallower depth levels (ca. 10-20 mm). As explained in section 2.2.1, this is a result of cumulative chloride binding and not caused by a gradual temporal increase in chloride availability at the surface. After 12 years chloride exposure, most profiles show a mountain-shaped profile with the peak chloride concentration occurring at depth of around 20 mm. This is a typical phenomenon for field concretes exposed to salty spray water, that can be explained by

drying, leaching and/or carbonation of the concrete surface layers at 0-20 mm depth [Marchand 2009, Mejjers 2005, Andrade 2015].

There is significant effect of concrete type on the rate and depth of chloride penetration. The plates consisting of CEM I concrete with a w/c-ratio of 0.5 (concretes B, C, and H) show the strongest chloride ingress, followed by the concretes with slag (concrete D) and fly ash (concrete E) having the same w/-ratio. Concrete with silica fume (concrete F) and CEM I concrete with a w/c-ratio of 0.35 showed the lowest ingress rate. The lower plates of concrete H show horizontal profiles after 12.8 years and apparantly are then 'saturated' with chlorides. The maximum measured chloride concentrations after 12.8 years were less affected by concrete type and range between 0.3 and 0.45 %/m_{con} for concretes with a w/c-ratio of 0.5 (Fig. 7 and 8).

The effects of the height from road on the rate of ingress appears as relatively small from the profiles. Profiles of adjacent plates in the same concrete at the same time are similar. There are however, some systematic differences in chloride ingress rates as function of height that become clear after a quantitative analyses of the profiles (see Section 3.3). Another observation that can be made from the profiles is that the hydrophobic impregnation had a strong effect on the chloride ingress rate (see profiles A1 - Fig. 7).

3.3 Regression analyses to obtain D_{app} and C_{s_app}

By means of a regression method it is possible to obtain two parameters from the measured chloride profiles: the apparent diffusion coefficient (D_{app}) and the apparent surface concentration (C_{s_app}). The regression is based on the well-known error-function approach and is described in section 2.1.3 and below. The error-function is a solution of Fick's second law of diffusion, under the assumption of time-independence of the diffusion coefficient and the surface concentration. The diffusion coefficient obtained is called 'apparent' because: (i) D_{app} represents an average diffusion coefficient for a given period in which the transport properties of concrete is changing; (ii) D_{app} is not a pure diffusion coefficient, but a transport coefficient determined from a chloride profile that includes non-mobile chlorides bound to the material, and chloride transport may have occurred by non-diffusive mechanisms (e.g., by capillary suction). The apparent chloride surface concentration (C_{s_app}) is an apparent parameter for the same reasons why D is apparent. Moreover, when C_s is obtained by regression of a mountain-shaped chloride profile, C_{s_app} represents a virtual, extrapolated surface concentration.

The regression method as implemented in excel can be summarized as follows, and is described in detail in European standard CEN/EN 12390-11:2013 [CEN/EN 2013]:

(1) The measured chloride profile is plotted in a diagram.

(2) A theoretical chloride profile is then plotted in same diagram. It is calculated with the error-function using assumed input parameters D_{app} and C_{s_app}. D_{app} and C_{s_app} are chosen in a way such that the calculated profile is roughly similar to the measured one.

(3) The regression is then carried out using the 'solver'-function in excel. The solver finds a combination of D_{app} and C_{s_app} that produces the smallest deviation between the measured and calculated profile. This is done by calculating the deviation between the two profiles $(C_m-C_{regr})^2$ at each point und cumulating the deviations for all points.

The D_{app} obtained by regression for all Naxberg concrete types is plotted as function of time in Fig. 9. Note that these results for concretes H and D are biased at exposure duration of 12.8 years, since no regression could be carried out on the 'saturated' chloride profiles. A regression of these near horizontal profiles would produce an extremely high D_{app}. Thus, D_{app} obtained for concretes H and D at 12 or 12.8 years are based on profiles that showed lower than average chloride ingress.

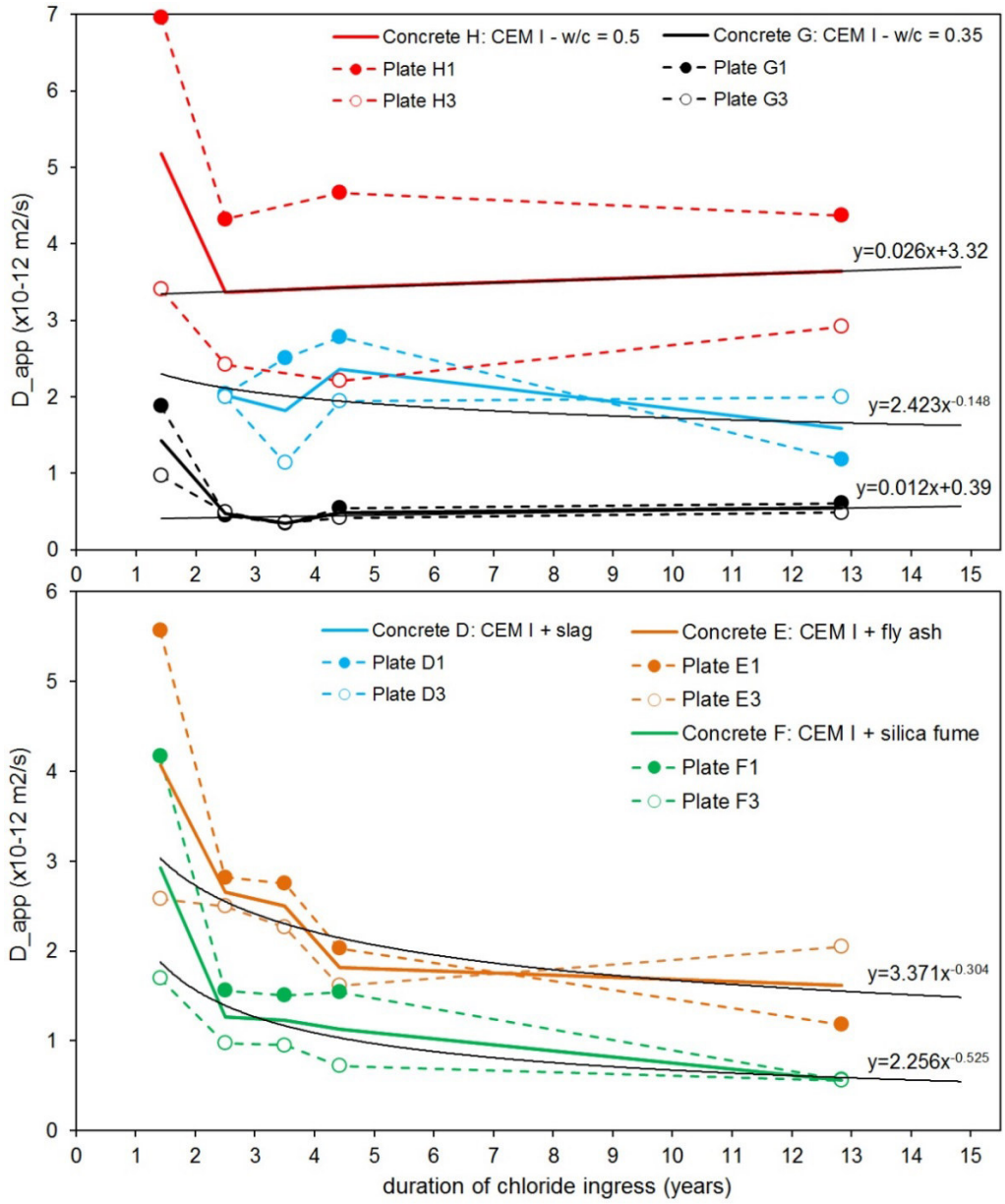

Fig.9: *Evolution of apparent diffusion coefficient (D_{app}) for all Naxberg concretes. The trend lines are given for the data sets (average) excluding the first measurement at 1.5 year exposure as explained in the text.*

It is clear that concrete type has a large effect on D_{app}. There is factor of 6-7 times difference in D_{app} between concrete H and concretes G and F (after 12 years exposure). For CEM I concretes (H und G) there was an initial (0-2.5 years) decrease in D_{app}, but then D_{app} remains more or less stable up to 13 years. As said, this trend is biased for the H-concretes. For concretes with fly-ash (E) or silica fume (F) there is a continuous decrease in D_{app} that can be approximated by an exponential decay function. For the concrete with slag (D), the decay trend is not clear, partly because of the abovementioned bias for the D_{app} after 12.8 years, and partly because of the measured 'irregularity' around 4 years.

The D_{app} calculated for the plates 1 (0-60 cm) is generally higher than D_{app} for plates 3 (120-180 cm). An exception occurs for concrete D after 12.8 years, which can be explained by the abovementioned bias caused by 'saturated' profiles. Another exception to the general trends occurs for concrete E after 12.8 years for which no obvious explanation can be given.

The development of the maximum measured chloride concentration (C_{max}) and C_{s_app} as obtained by regression as function of time and height from road is given in Fig. 10 and 11. Fig. 10 shows the average development for all concrete types individually, i.e., all plates of the same concrete averaged. Fig. 11 shows the average development of all concrete types, including the average effect of height. In all cases, a clear increase in time of both parameters can be seen.

The data points from 2.5 years exposure appear to show an exponential increase of C_{max} and C_{s_app} (Fig. 11). The fitted exponential functions shown in Fig. 11 are taken as describing the average increase in C_{s_app} in the Naxberg experiment. A clear effect of height from road on C_{max} and C_{s_app} exists: the average chloride concentration in the upper plates (nr. 3) is about 15% smaller than the one in the lower plates (nr. 1).

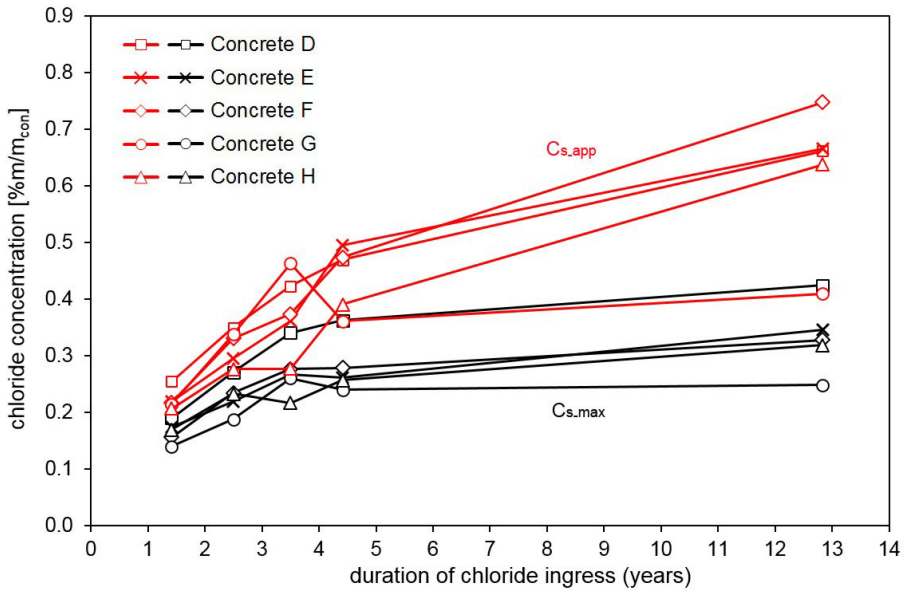

Fig.10: *Development of the maximum measured chloride concentration and C_{s_app} obtained by regression as function of time per mixture type (averages of all plates).*

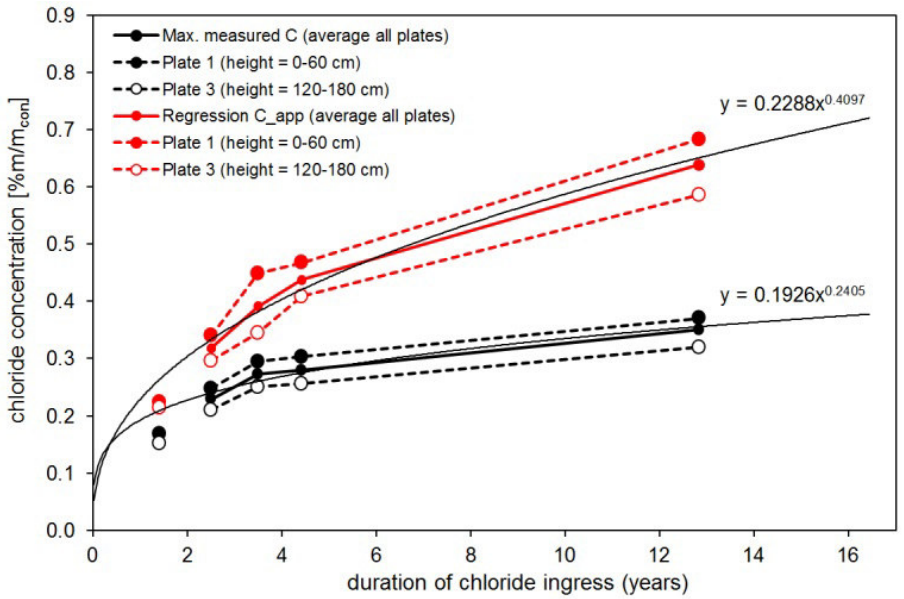

Fig.11: *Development of the maximum measured chloride concentration and C_{s_app} obtained by regression as function of time and height from road in Naxberg. The chloride measurements are averaged over all types of concrete. The trend lines are given for the data sets, excluding the first data point at 1.4 year exposure.*

3.4 Trial empirical prediction of Naxberg-profiles

The trend lines in Fig. 9 and 11 provide a set of equations that approximately describe the chloride transport behaviour of the different types of concrete in the Naxberg experiment (see Table 6). These equations are only applicable to chloride exposure times > 2.5 years, because the trend lines were obtained by excluding the 1.4 year data points. These equations can be used to calculate the apparent diffusion coefficient and surface concentration for any type of Naxberg concrete at any point in time. In this report we calculated the chloride profiles after 2.5, 4.4, 12 or 12.8 years using these equations and the error-function (eq. 2) and compare them to the measured profiles at these exposure times. The purpose of this exercise is to investigate how well all measured chloride profiles in Naxberg can be described by a basic set of empirical equations. If they can, this may show that the data sets follows a first-order Fickian-type behaviour, and that an error-function empirical model can be used to predict chloride ingress in road settings with a chloride exposure similar to Naxberg.

The calculated chloride profiles at 2.5, 4.4, 12, and 12.8 years are compared to the measured profiles given in Fig. 12 and 13. The apparent diffusion coefficient (D_{app}) and surface concentration (C_{s_app}) at the starting point time t_m is determined from either the profile at 2.5 or 4.4 years, and the predicted curves are, respectively black or red for these two cases (see Fig. 12 and 13). The predicted chloride profiles are finally corrected for the maximum expected chloride concentration as measured (and described by equation 17 in Table 6). That is, for predicted values of $C_p > C_{max\_p}$, the value of C_p will be given the value C_{max_p}. This is the reason for the initial plateau in the chloride profiles.

Overall, there seems to be a reasonable agreement between the predicted and measured chloride profiles in terms of profile shape and evolution in most cases. The corresponding black and red prediction lines are often in close proximity, and this is expected when the Naxberg data set follows a diffusion-controlled time-evolution (as defined by the ERFC). This trial exercise shows that the trends in the Naxberg data do not deviate much from the ones given by the ERFC solution of Fick's second law of diffusion. It therefore seems reasonable to use the ERFC solution as a basis for an empirical prediction model for the Naxberg case and similar settings.

***Tab.6**: Empirical equations describing the Naxberg data-set in combination with eq. 2.*

Cement type (concrete)	**Ageing equation (>2.5 years chloride ingress)**	**Equation nr.**
CEM I – 0.5 (B,C,H)	$D_p = 0.026 \cdot (t_p - t_m) + D_m$	**(11)**
CEM I – 0.35 (G)	$D_p = 0.012 \cdot (t_p - t_m) + D_m$	**(12)**
blastfurnace slag (D)	$D_p = D_m \cdot (t_p/t_m)^{-0.148}$	**(13)**
silica fume (F)	$D_p = D_m \cdot (t_p/t_m)^{-0.525}$	**(14)**
fly ash (E)	$D_p = D_m \cdot (t_p/t_m)^{-0.304}$	**(15)**
Equations for chloride concentrations (valid for all Naxberg concretes):		
extrapolated surface concentration (regression)	$C_p = C_m \cdot (t_p/t_m)^{0.410}$	**(16)**
maximum surface concentration (measured)	$C_{max\_p} = C_{max\_m} \cdot (t_p/t_m)^{0.241}$	**(17)**

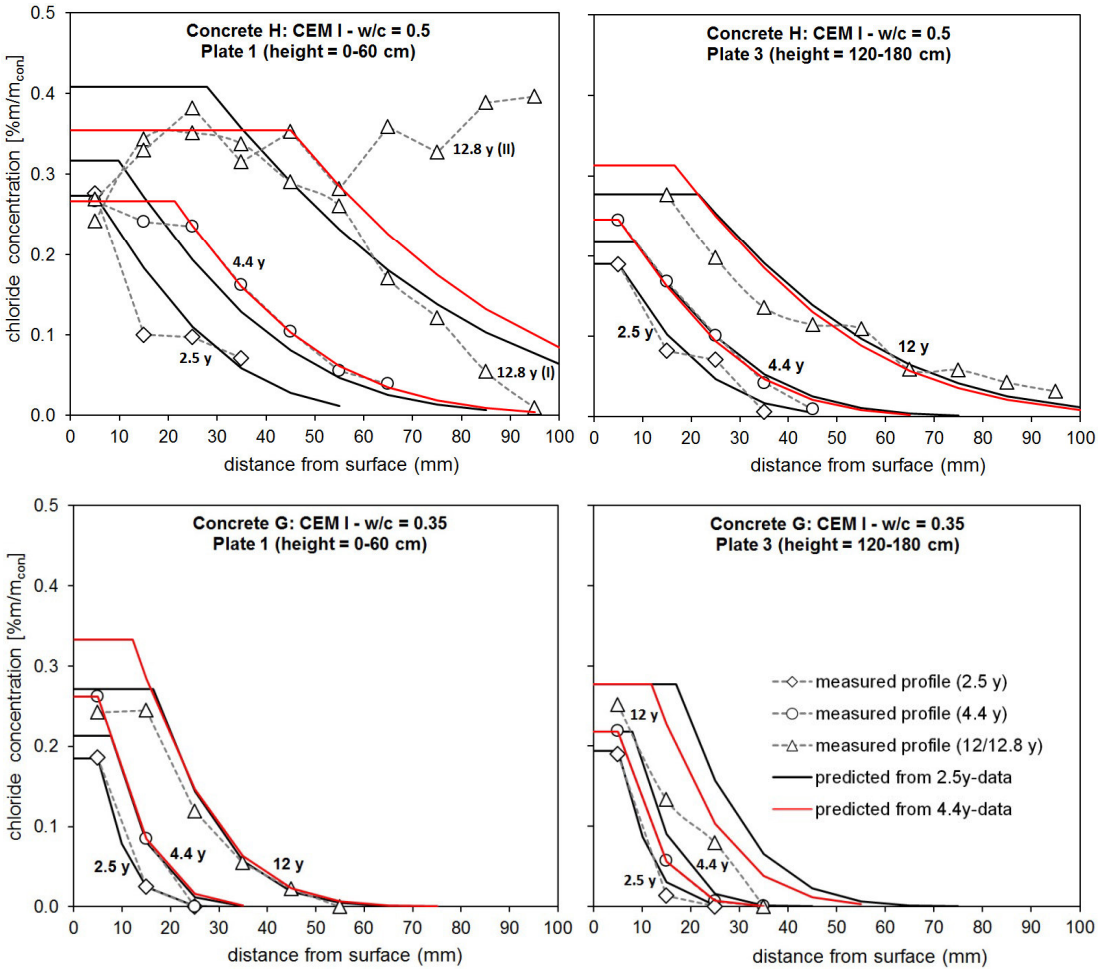

Fig.12: *Measured and predicted chloride profiles for concretes H and G using the equations in Table 6 in combination with the ERFC-equation (eq. 2).*

3.5 Migration coefficients and other properties (lab tests)

Migration coefficients and other properties were determined at ages of 28, 90, 365 and 1000 days from cubes that were prepared of the same concrete as the Naxberg plates [Ungricht 2004]. The cubes were stored in the laboratory under wet-curing conditions. The migration coefficient was determined using the Swiss standard test [SIA 262/1], and 3-6 measurements were performed on every concrete for every time step (see Table 7). The purpose of measuring M was to investigate if a relationship exists between the short-term chloride migration coefficient (as measured in the lab at early ages) and the long-term chloride ingress rate as observed in the field. Only one migration coefficient was determined at age of 12 years on a chloride-free core-part from a Naxberg G-plate (M_{12y} = $3 \cdot 10^{-12}$ m^2/s). The other Naxberg concrete plates were too much contaminated with chlorides for the measurement of M at an age of 12 years.

The average migration coefficients are plotted against time in Fig. 14. The trends are rather erratic, but an overall long-term decrease in M-values can be observed. Also plotted in Fig. 14 are the long-term evolution of D_{app} and the compressive strength. Hunkeler et al [2002] showed that there is a correlation between migration coefficient and compressive strength of concrete. Therefore the compressive strength is plotted as reciprocal compressive strength in order to identity a possible relationship between the development of strength and migration coefficient. It can be observed that the trend in

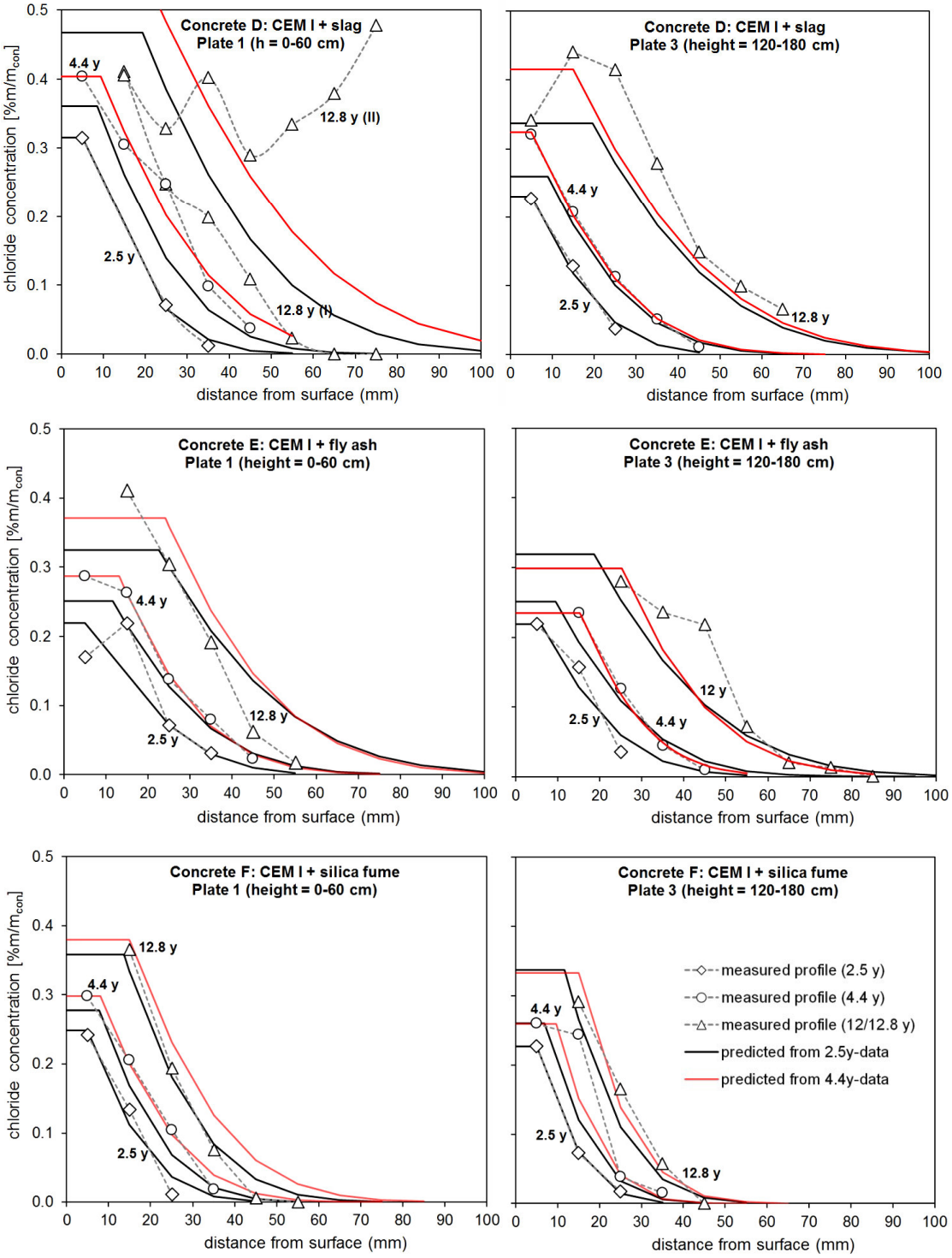

Fig.13: *Measured and predicted chloride profiles for concretes D, E, and F using the equations in Table 6 in combination with the ERFC-equation (eq. 2).*

strength development is continuous and not erratic. The early-age fluctuations in M are not believed to reflect real material behaviour, since a continuous decrease in transport properties with early age hydration degree, as for compressive strength, is to be expected.

Dalen et al [2006] showed that large numbers of M-measurements on Portland cement concrete produced a standard deviation of around 15%, and on slag cement concrete of about 25%. In this study the standard deviation ranged between 10 and 40% (see Table

7). Since the M-values at 90 days are higher than those at 28 days, we believe that this unexpected fluctuation is caused by variation among the concrete cubes and issues concerning the measurement technique. We assume that the average migration coefficient at 28 and 90 days represents the early age M-value, i.e., the M_{28d}-value required as input in the DuraCrete-model (see Chapter 5).

A comparison between the trends shown by the migration coefficient, compressive strength, and D_{app} versus time, also suggests that the initial 3 M-values measured for concrete F with silica fume are disproportionately small (at 28, 90, and 365 days). The continuous increase of M with time is unexpected. The reason for this behaviour is unknown. M measured for silica fume concrete may possibly be erroneous and needs to be confirmed by new measurements. Based on the expected correlation between various transport and density properties, M for silica fume concrete was determined in this study as explained in Table 8. The value of M_{28d} = 12.6 x 10^{-12} m^2/s for concrete F was obtained in this way.

Tab.7: *Migration coefficients measured using the method in [SIA 261/1]* (x10^{-12} m^2/s).

Concrete:	D	E	F	G	H
Age 28 days:	**+slag**	**+fly ash**	**+silica fume**	**CEMI-0.35**	**CEMI-0.5**
M1	14.5/10.7	15.6	2.6	7.8/5.8	13.2
M2	11.7/8.1	16.8	3.2	6.0/1.0	15.9
M3	12.7/9.4	14.7	3.8	8.1/7.7	13.1
M-average ± St.	11.2±1.4	15.7±1.1	3.2±0.6	7.6±2.2	14.1±1.6
Age 90 days:					
M1	12.0/10.1	11.1	3.9	10.3/7.8	14.5
M2	12.8/11.9	17.5	3.5	9.4/10.2	16.1
M3	10.5/11.8	15.2	5.2	9.5/8.1	15.7
M-average ± St.	11.6±1.2	14.6±3.2	4.2±0.9	9.2±1.3	15.4±0.8
Age 360 days:					
M1	13.8/7.53	12.4	5.2	8.2/4.3	10.9
M2	9.9/8.1	14.2	4.2	8.0/6.7	10.0
M3	13.5/-	17.2	5.0	7.6/7.6	-
M-average ± St.	10.1±2.2	14.6±2.4	4.8±0.6	7.1±3.2	10.4
Age 1000 days:					
M1	5.2	4.4	10.2	4.9	12.3
M2	8.8	4.6	5.2	3.9	11.5
M3	4.3	5.9	5.0	5.9	9.4
M-average ± St.	6.1±2.4	4.9±0.8	6.8±3.0	4.9±1.0	11.0±1.5

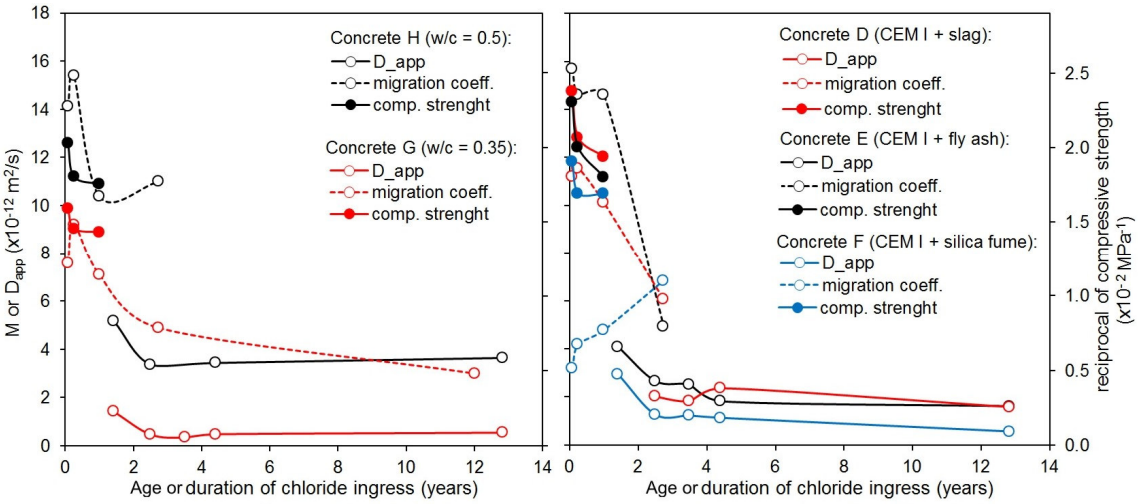

Fig.14: *Chloride migration coefficient (M), D_{app}, and compressive strength versus time. Note that for M and compressive strength time is concrete age; for D_{app} time is chloride exposure duration.*

Tab.8: *Determination of M_{28d} for silica fume concrete F: For all concretes (D, E, G, H) the M-value is plotted versus e.g., the compressive strength. The best-fit through the scatter diagram is then used to obtain M-value of concrete F by means of interpolation.*

	D +slag	**E +fly ash**	**F +SF**	**G CEMI-0.35**	**H CEMI-0.5**	**F M_correlation**
comp. strength (N/mm^2) 28d (average of 3-6 tests)	42.1	43.4	52.5	62.8	49.3	**11.7**
cap. porosity (Vol-%) 28d (average of 3-6 tests)	10.5	10	10.9	8.3	11.2	**14.3**
gas permeability (m^2) 28d (average of 3-6 tests)	5.5	2.6	2.2	1.1	5.5	**11.4**
water flux (g/m^2h) 28d (average of 3-6 tests)	3.5	2.9	3.5	1.9	4.4	**13.1**
M ((28 + 90)/2) 10^{-12} m^2/s	11.38	15.15	**?**	8.4	14.76	**Av = 12.6**

Despite the apparent inaccuracies in the M-measurements, it is clear that M is much larger than D_{app} by about a factor 2-3 at an age of ca. 2 years. As will be explained in Chapter 5, this is mainly caused by differences in temperature and moisture content between the laboratory and field experiments.

3.6 Discussion of results

3.6.1 Chloride transport mechanisms

What can be concluded with regard to chloride transport mechanisms in the Naxberg experiment from all available data? It has been shown that the Naxberg chloride profiles can be reasonably well predicted using the error-function derivation of Fick's second law of diffusion. The primary chloride transport mechanism therefore appears to be diffusion. However, there are several indications that suggest that capillary suction also played a role in the chloride transport process. The most import being that at 12 or 12.8 years age the lower plates (nr. 1 and 2) of the most porous concretes (H and D) show 'horizontal' chloride profiles, i.e., concretes 'saturated' with chloride over the entire 10 cm thickness of the plates. The high concentrations of chlorides at a depth of 70-100 cm was not predicted by the error-function (Fig. 12). The high ingress of chlorides was therefore probably caused by capillary suction ingress of chlorides.

From the in-situ measurements of water and chloride content in the early years of the Naxberg experiment, it was concluded that chloride ingress by capillary suction is important [Ungricht 2004]. However, the magnitude of the contribution of chloride ingress at larger depths in the concrete and at later ages is not clear. The height effect on the measured chloride profiles (C_{max}, C_{s_app}, and D_{app}) can possible be explained by capillary suction effects. At the lower plates there is a larger availability of (spray) water with dissolved chlorides, and this may result in faster chloride ingress due to increased capillary suction. Another explanation is that due to the larger availability of spray water at the lower plates, these concrete plates are wetter. As explained in section 2.2.2, the diffusion coefficient of concrete will increase with moisture content. Moreover, a wet concrete carbonates slower, which could be another contributing factor to the effect of height on D_{app}.

Another indication of the active transport mechanisms could come from the shape of the chloride profiles. It has been predicted and shown that capillary effects lead to chloride profiles with an 'S'-shape [Lay 2005, Kapteina 2011]. The 'S'-shape is however easily obscured by other processes, such as drying and carbonation leading to the development of a mountain-shaped profile, or larger aggregate particles or compaction pores causing a 'bump' in the profile. Apart from the 'horizontal' profiles observed in some porous concretes, there are no clear geometrical signs in the other chloride profiles that suggest strong effects of capillary suction at larger depths (>2 cm).

3.6.2 Ageing of D_{app}

The apparent diffusion coefficients of all Naxberg concrete show a clear ageing trend. All concretes have a strong initial ageing (<2.5 years exposure), and a weaker long term ageing (2.5 – 12.8 years exposure). The initial ageing is probably related to a densification of the material by cement hydration. In concretes with fly ash, slag, or silica fume additions, cement hydration is slow and may continue on a relatively long-term. Part of the long-term ageing of concrete D, E, and F may therefore still be hydration related. Another reasons for the ageing is a result of the interaction of the chlorides with the concrete. Part of the chloride diffusing into concrete get bound to the material, and this could possibly lead to a slow reduction of permeability and ingress rate.

For Portland cement concrete with a w/c-ratio of 0.35 (concrete G) no long-term ageing in D_{app} is observed after 2.5 years. It seems probable that this is simply related to a long-term stabilisation of the concrete density. In OPC-concrete with a w/c-ratio of 0.5 (concrete H), there also appears to be no long-term ageing. As explained in Section 3.3 this trend is biased, because the high chloride ingress observed in the cores with 'saturated' profiles is not included in this trend. If a D_{app} would have been estimated for these 'horizontal' profiles, the average D_{app} values at 12 years would have been much larger, and an increase of D_{app} with time would have been shown. Capillary suction effects will enter the apparent diffusion coefficient, and if there is a long-term change in the contribution of capillary suction effects, then the ageing factor may also be affected.

Surface effects, such as drying and carbonation that progress slowly in time, slow down the ingress of chlorides and thus are expected to affect the apparent diffusion coefficient. Mathematical effects may also cause apparent ageing of D_{app}: The D_{app} is the average D over the entire diffusion period resulting in the chloride profile. Thus even when the actual aging of the material has stopped and the instantaneous D is not changing anymore, the apparent ageing will continue to decrease because the contribution of high initial D will keep on affecting the average. Another possible 'mathematical' effect occurs when a mountain-shaped chloride profile is being developed. Regression of such profiles will lead to extrapolated surface concentration (C_{s_app}) that is much higher than the measured peak concentrations. The result is that D_{app} determined for a mountain-shaped profile has a somewhat different meaning, since it is determined in combination with a virtual driving force.

4 Critical chloride content for corrosion initiation

4.1 Method

The critical chloride content (C_{crit}) is the chloride concentration in concrete or concrete binder at which steel in concrete depassivates (i.e., starts to corrode). Service life is here considered to be the time required to reach C_{crit} at the depth of the first reinforcement layers. C_{crit} is one of the decisive parameters in lifetime modelling. In chapter 2.3.2 the experimental measurement of C_{crit} has been reviewed. Different methods have been proposed to obtain this parameter, but so far no consensus exists about how to measure C_{crit}. At TFB the following C_{crit} measurement method has been developed on basis of existing techniques as described in literature [Nygaard 2005, Angst 2009; SN EN 480-14] and on basis of our own experiences.

A steel bar with a diameter of ca. 10 mm and a length of ca. 10 cm is embedded in a mortar specimen with a diameter of 30 mm in order to obtain a cover thickness of 10 mm (Fig. 15). One steel end lies in the mortar specimen while the other end sticks out of the sample. Both ends of the steel in the mortar are covered with a thin layer of cement paste and epoxy resin to avoid corrosion initiation at these locations (Fig. 15). These so-called lollipop-samples are placed in a salt solution with a concentration of 5 M_{NaCl}/l, and the chloride enters the specimen by passive diffusion. Given an anticipated chloride diffusion coefficient and C_{crit} for the test mixtures, a suitable cover thickness (i.e., 10 mm) was calculated using the diffusion error-function (see Section 2.4.2) to obtain maximum test duration of ca. 2 months.

The mortars were standard mixtures prepared according to Swiss standard SN EN 196-1 [SN EN 196-1], but with adjusted w/c-ratio and maximum grain size. The mortars were prepared using a high water-cement ratio (of 0.6) to increase the chloride ingress rate (i.e., lower test duration). Standard CEN sand was sieved to obtain the fractions with a maximum grain size of 1 mm, in order to create uniform specimens with a cover/aggregate size ratio of ca. 10. All samples were precured in a saturated lime solution for 7, 22 or 98 days in order to passivate the steel bar.

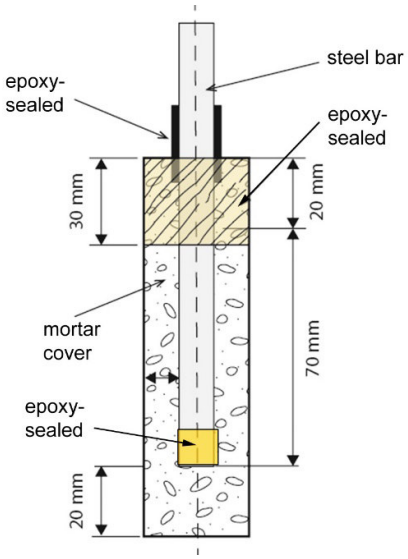

Fig.15: *'Lollipop' sample set-up.*

Fig.16: *Split sample showing steel bar (right) and the rib-imprints in the mortar specimen (left).*

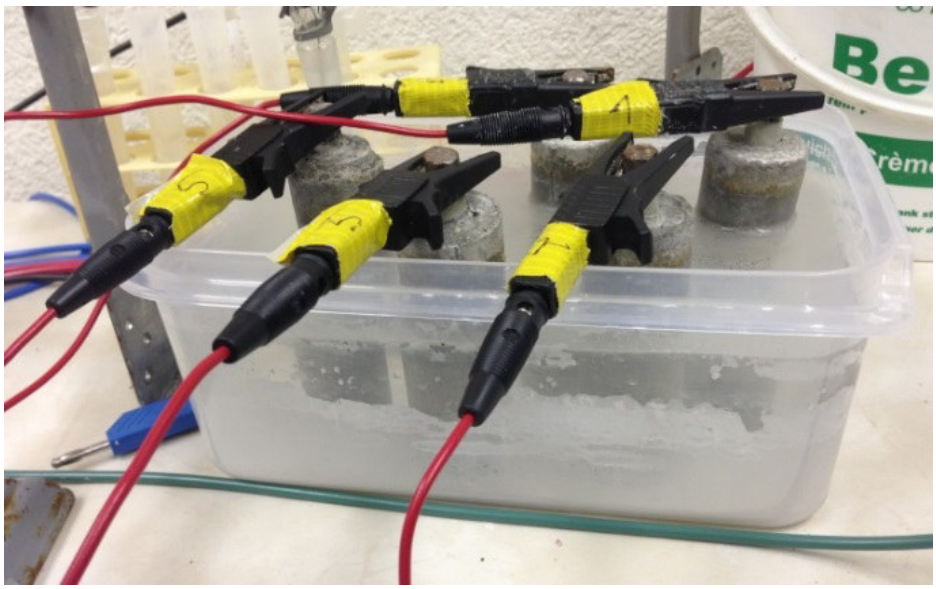

Fig.17: *Lollipop-samples connected to a potential meter in a salt solution.*

The corrosion (depassivation) state was monitored by continuously measuring the open circuit potential (Fig. 17). The reference electrode for the measurements of potential was a silver/silver-chloride electrode (SSE). The onset of corrosion (depassivation) is indicated by a large drop in potential (of several 100's of mV's), see Fig. 18.

At depassivation, the samples are taken out of the solution and dried at 50°C for ca. 1 hour. Test experiments showed that the drying time in range of 1 to 48 hours did not affect the C_{crit}-value. Subsequently, the steel was detached from the mortar by splitting the sample into several parts (Fig. 16). The chloride concentration surrounding the steel bars was measured from a powder sample that was collected by grinding off the rib-imprints in the mortar (Fig. 16). The ribs contain between 1-1.5 gram mortar, a sample amount that was sufficient for chloride content measurement using XRF in compliance with Swiss standard SN EN 14629 [SN EN 14629].

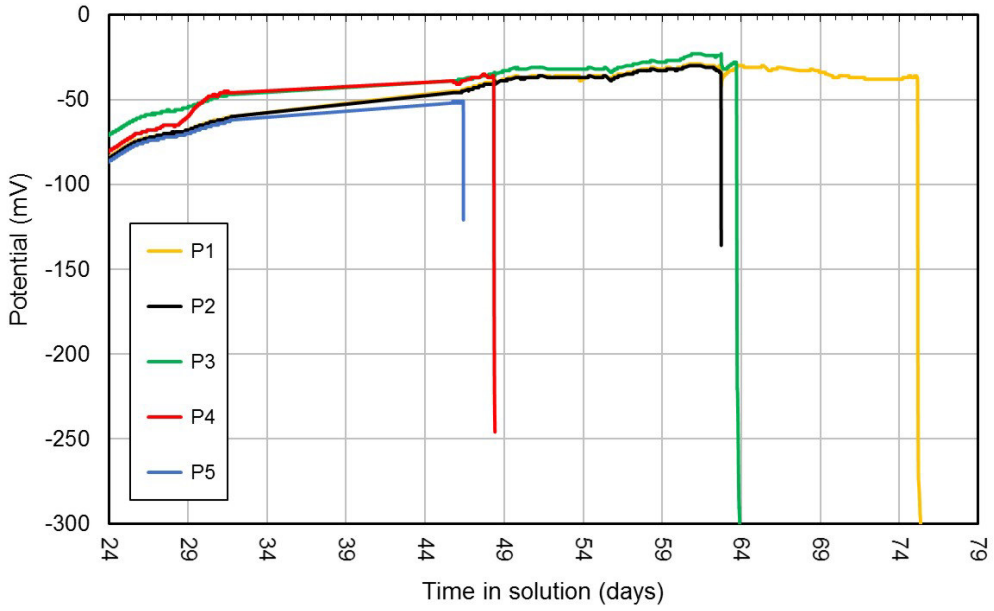

Fig.18: *Potential (mV) versus exposure time for the Top12-steel with rolled skin (see Table 9). In this example, depassivation of 5 samples occurred between 45 and 76 days.*

4.2 Results

Different types of rebars (either Top12 and ordinary rebar steel) with different types of surface treatments were tested using the TFB lollipop-method (see Table 9). In this first series of experiments, the mortars contained ordinary Portland cement (CEM I 52.5R). The experiments are being repeated in mortar containing CEM II/B-M (S-T) 42,5 R, a modern blended cement with slag and burned shale. These latter experiments should elucidate if C_{crit} in blended cements differs significantly from the one in ordinary Portland cement.

Table 9 shows the (diffusion) time to depassivation in days; the measured chloride content ($C_{measured}$) as a weight fraction of all the rib-material surrounding the steel bar; the calculated critical chloride content (C_{crit}) as a weight fraction of the binder in the mortar; and the expected critical chloride content (C_{crit}) calculated for a CEM I concrete with a density of 2400 kg/m^3 and a cement content of 300 kg/m^3. The calculation of the values in the last two columns in Table 9 requires knowing the sand content in the ribs. The rib sand content was measured by means of image analyses of Scanning Electron Microscopy (SEM) images (Fig. 19). The ribs contain an average 31.6 vol-% quartz sand and 68.4 vol-% cement paste, which correspond to 41.8 and 58.2 weight-%, respectively (for a mortar with quartz sand and a w/c-ratio of 0.6). It follows that the cement content of the mortar ribs was 36.4 weight-%. The measured chloride contents in the mortar therefore need to be multiplied by a factor 100/36.4 = 2.75 to obtain chloride content as a weight fraction of the binder content. $C_{crit,con}$ in last column is obtained by simply dividing the $C_{crit,cem}$-value by 8.

The results in Table 9 show clear systematic differences between the different types of steel tested. The standard deviation of 5 measurements per steel type is smaller than the difference in the mean for each steel type. The experimental duration (= diffusion time to reach C_{crit}) increased with C_{crit} as expected for 3 out of 4 series (see Table 9). The series Top12-steel with rolled skin did not follow the expected trend with an average C_{crit} = 0.75 and an average diffusion time of 59 days. The reason for this behaviour is probably that a thicker skin of carbonates or salt formed on the specimens in this series. A salt skin of the lollipop-specimen will slow down chloride ingress, but is not expected to affect the C_{crit}-value.

Tab.9: *Chloride contents measured by using the TFB lollipop method (with CEM I).*

Steel type	specimen	time (days)	$C_{measured}$ (%/m_{mortar})	C_{crit} (%/m_{cem})	C_{crit} (%/m_{con})
Standard rebar steel B500B (Ø = 10 cm) t_{cure} = 22 days	P1	9	0.28	0.78	0.10
	P2	13	0.33	0.91	0.11
	P3	13	0.48	1.32	0.17
	P4	2.5	0.41	1.13	0.14
	P5*	22.5 (ol)	0.78 (ol)	2.14 (ol)	0.27 (ol)
	ave	9	0.38 ± 0.09	1.04 ± 0.24	0.13 ± 0.03
Top12-steel (≈1.4003) rolled skin (Ø = 10 cm) t_{cure} = 7 days	P1	76	0.82	2.26	0.28
	P2	63	0.82	2.24	0.28
	P3	64	0.83	2.29	0.29
	P4	48.5	0.68	1.88	0.23
	P5	45	0.58	1.60	0.20
	ave	59	0.75 ± 0.11	2.06 ± 0.30	0.26 ± 0.04
Top12-steel (≈1.4003) pickled skin method I (Ø = 10 cm) t_{cure} = 98 days	P1	44	1.36	3.75	0.47
	P2	44	1.52	4.19	0.52
	P3	44	1.39	3.81	0.48
	P4	63	1.83	5.04	0.63
	P5	67	1.68	4.61	0.58
	ave	52	1.56 ± 0.20	4.28 ± 0.55	0.53 ± 0.07
Top12-steel (≈1.4003) pickled skin method II (Ø = 12 cm) t_{cure} = 98 days	P1	65	1.73	4.75	0.59
	P2	44	1.56	4.29	0.54
	P3	44	1.76	4.83	0.60
	P4	44	1.83	5.02	0.63
	P5	72	2.04	5.60	0.70
	ave	54	1.78 ± 0.17	4.90 ± 0.48	0.61 ± 0.06

** outlier not included in series average.*

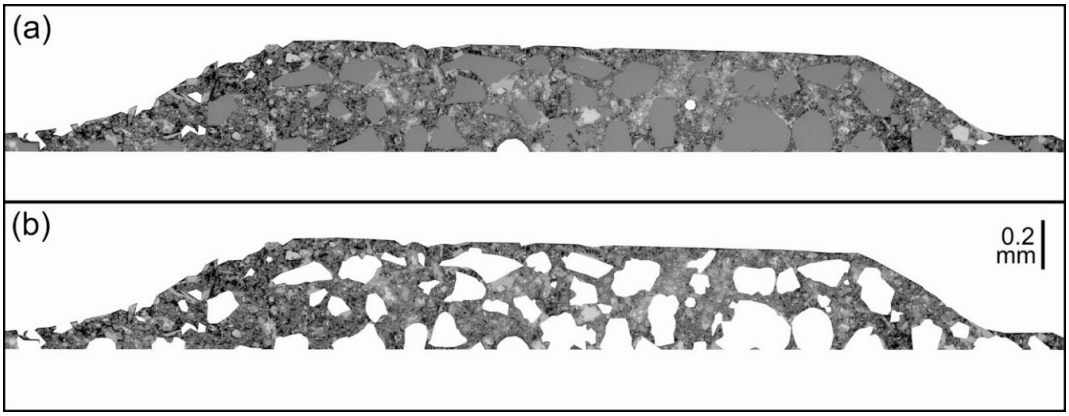

Fig.19: *(a) SEM-BSE image of a rib cross-section, sand is predominantly quartz. (b) Rib with sand grains highlighted in white, the remaining material being cement paste with hydration products, unhydrated cement and capillary porosity.*

The obtained C_{crit}-values for standard rebar steel are higher (roughly by a factor 2) than those generally reported in literature (conf. [Angst 2009] or in technical specifications (see Table 4). However, the measured C_{crit}-values do compare to those reported by Angst et al [2011c]. It has been suggested that C_{crit}-values measured in the laboratory on well compacted concretes and mortars are higher than actual C_{crit}-values in practical field concretes (see [Angst 2011c]). Further research is needed to determine the relationship between C_{crit}-values determined in the laboratory and in the field.

All steel rods were checked for corrosion signs after the experiments under a microscope. A total of 6 (out of the 20 rods) showed clear corrosion-pitting that was linked to the depassivation in these experiments (example in Fig. 20). Other samples showed no signs of corrosion, or small superficial corrosion patches that may or may not have been present on the rods already before the experiments. It is unclear if depassivation in these experiments can occur without corrosion-pitting. Perhaps, the corrosion pits were present but undetectable due to their small size or due to pre-existing roughness of the steel surface.

In Section 5.6.3 it will be shown how the C_{crit} determined for these different steel types and surfaces will affect the service life of concrete.

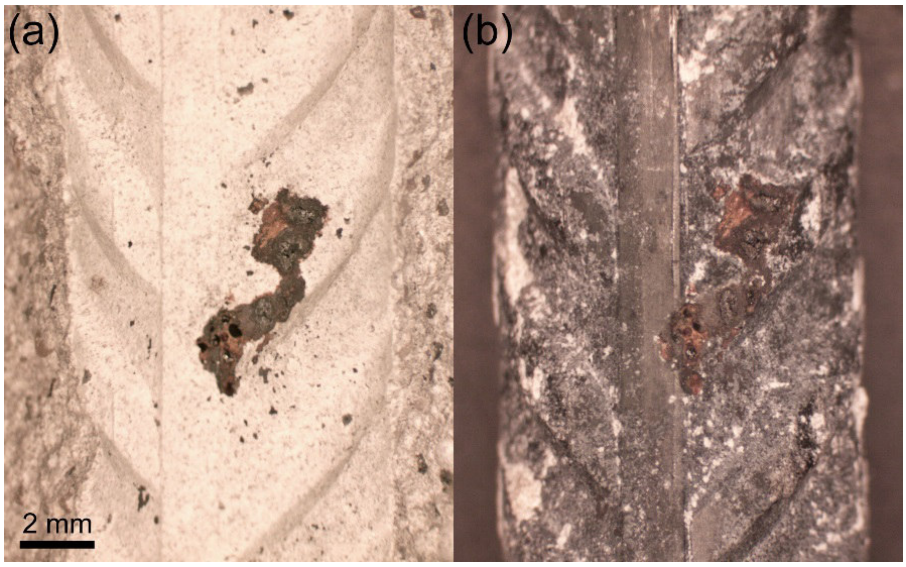

Fig.20: *Corrosion-pitting in Top12-steel with rolled skin (sample S1) at the moment of depassivation. (a) Corrosion products on mortar surface (black/red rust); (b) Corrosion pits and corrosion products on steel surface.*

5 ERFC prediction model for chloride transport

5.1 Introduction

The prime objective of this study is to propose an user-friendly and accessible prediction model for the reinforcement corrosion initiation in concrete in road environments with deicing salts such as they occur in Switzerland. Under the assumption that the onset of corrosion occurs when the critical chloride content is reached, only chloride transport needs to be considered, i.e., the time required to reach the critical chloride content is to be predicted. The critical chloride content of concrete is a property that can be experimentally determined (see Chapter 4), or taken from literature or prescriptions in national standards (Table 4).

The first requirement for the prediction model concerns its accessibility. Some mechanistic models that have been described in literature may be suitable for making real-life predictions, but are not available to construction engineers because they lack a user-friendly interface or are otherwise difficult to use. An exception is perhaps STADIUM, a mechanistic service life prediction tool provided by Simco Technology. Along with the availability of the model itself, comes the availability of the required model input parameters. Preferably, a prediction model requires a minimum of input parameters that can be easily determined, e.g., measured in a rapid experiment. The second main requirement is that the model has a proven functionality, i.e., has been validated against the results of long-term field experiments.

Here an 'error-function' (ERFC) prediction model is proposed that fulfils the above requirements. It is largely similar to existing empirical models such as DuraCrete [DuraCrete 2000], and differs only in detail from those models. The error-function is easily implementable in spreadsheet software such as Excel, and is easy to operate and therefore available to everyone. All required input parameters can be found in this report or other literature. For higher prediction reliability, it may be necessary to measure certain input parameters on the actual concrete that is to be used, as will be shown in this chapter. This error-function approach is widely used in Europe and elsewhere and has already been proposed before as a durability prediction model for road systems in Switzerland [Vogel 2005]. Moreover, the M_{28d}-parameter used in the DuraCrete model is used as a durability measure in Swiss standards.

In this chapter the proposed prediction models will be tested against the results of the Naxberg field experiment, and other long-term field experiments in Switzerland and Sweden. Some Naxberg chloride profiles were simulated using a mechanistic chloride ingress model (TransChlor). These simulation results show the advantages and disadvantages of using a comprehensive mechanistic prediction model. In the final sections some example lifetime calculations are given, and the topic of chloride redistribution after concrete sealing is addressed. Note that in cases of a slow development of corrosion-induced damage, the practical service-life of concrete structures may be much longer than the ERFC-predicted service-life.

5.2 Error-function model description

The basis of the proposed model is the solution of Fick's second law under the assumption of constant diffusion coefficient (D) and chloride surface concentration (C_s), i.e., the error-function solution:

$$C(x,t) = C_{s,app} \cdot erfc\left(\frac{x}{2\sqrt{D_{app} \cdot t}}\right) \qquad (18)$$

For the Naxberg case and many other cases it has been shown that the parameters D and C_s are not constants, but change with time. The error-function may thus be a mathematically incorrect solution for those cases. However, instead of making D and C_s time-dependent in the prediction model, they can be considered as being constants, i.e., as the constant average D and C_s that led to the formation of chloride profiles at exposure duration *t*. As explained in section 2.4.2 this is one of the reasons why D and C_s are referred to as apparent diffusions coefficient (D_{app}) and apparent surface concentration (C_{s_app}) in the ERFC-prediction models. Thus, the time-dependence is dealt with by giving D_{app} and C_{s_app} an appropriate value that represents the average behaviour in the period in which a certain chloride profile formed. D_{app} and C_{s_app} change with exposure time and need to be calculated for each exposure duration.

In the DuraCrete-approach, D_{app} is calculated for a given exposure duration using the following expression:

$$D_{app} = K \cdot M_{28d} \cdot \left(\frac{t_0}{t} \right)^n \tag{19}$$

with M_{28d} being the chloride migration coefficient at a concrete age of 28 days. The time t_0 is the reference time (in years) at which M is measured (t_0 = 28 days) or the age of first chloride exposure. The time *t* is the exposure period in years. The correlation factor K is a constant that links the experimentally measured M to field performance (D_{app}). The factor n is the ageing factor, describing how the apparent diffusion coefficient of the concrete changes with time.

The factor K is supposed to correct for all the differences between the chloride migration in the laboratory experiment and the actual field performance (chloride ingress by diffusion and capillary suction). Apart from the difference in transport mechanism, there may also exist differences in temperature (20 vs. e.g., 8^0C), moisture content (saturated vs. e.g., 70-90% RH), and age of first chloride exposure (28 days vs. e.g., 6 months). Thus, correlation factor K is composed of a number of subcorrelation factors k1, k2, k3, and K = k1·k2·k3. In the DuraCrete model some of this subcorrelation factors are defined as specific transition factors such as k_e, k_c, k_t with specific values (see [Tang 2005; STRUREL 2012]. In the model proposed here, no subcorrelation factors are defined, and a single value for K is assumed for all studied concretes at a given temperature.

The factor K is probably best used as a fitting constant, and therefore should be determined by means of a fitting procedure. Preferably, the correlation factor K and the ageing factor n should be determined together empirically by tuning equation 19 against the results of long-term field experiments. Great care is needed when the K or n-values are calculated from theoretical considerations or taken from literature. The ageing factor should represent the ageing in the field, and not the ageing factor determined in laboratory experiments (see Section 2.2.6). If K is given a specific theoretical value that does not completely capture the correlation between M_{28d} and D_{app}, then the ageing factor *n* will also partly function as a correlation factor if a fitting procedure is used to obtain n. The values of K and n are also affected by the choice of t_0 being the time of the M-measurement or the age of first chloride exposure. In this study K and n are determined by setting t_0 = 28 days (= 0.074 year).

The chloride surface concentration (C_{s_app}) is made time-dependent by using the following empirical equation that followed from the Naxberg measurements (see Chapter 3):

$$C_{s\_app} = 0.2288 \cdot t^{0.410} \tag{20}$$

This is the virtual, extrapolated surface concentration obtained by regression of a chloride profile (*t* is in years). The actual maximum chloride concentrations that were reached in the Naxberg concretes is described by the following equation:

$$C_{max} = 0.1926 \cdot t^{0.241} \tag{21}$$

The predicted chloride profile is (optionally) corrected by using eq. 21: When $C_{s\_app} > C_{max}$ then $C_{s\_app} = C_{max}$.

The mathematical correctness of DuraCrete and the model proposed here is certainly an issue (see e.g., [Tang 2005]. The model is just an empirical model that captures the first-order diffusion kinetics. The fitting parameters K and n will change with average yearly temperature and moisture content, and the model may not be practical when chloride ingress is non-diffusional, i.e., has a large or fluctuating component of transport due to capillary suction.

5.3 Tuning the ERFC model with Naxberg data

The error-function model was tuned against the Naxberg experiment by choosing K and n in a way to obtain chloride profiles that are in agreement with the measured Naxberg chloride profiles after 2.5, 4.4 and 12/12.8 years chloride exposure. The migration coefficients (M_{28d}) were determined for the various mixtures as explained in section 3.5. In a first fitting step it was found that K = 0.5 produced reasonable results for all concretes. It was then decided to keep K = 0.5 constant for all these mixtures and tune the ageing factor (n) to obtain the best fit. In other studies, a K-value of 0.45 [Kapteina 2011] and 0.53 [Tang 2005] have been used for the DuraCrete-model. The STRUREL-software uses K ($k_e \cdot k_t$) = 0.5 as default value for T = 8°C. It thus seems that K = 0.5 is a rather universal value for road-environments with deicing salts and similar yearly average temperature.

As an illustration that both K and n can function as merely fitting constants with little physical meaning, it is shown in Fig. 21 that for different combinations of K and n roughly similar predictions are obtained.

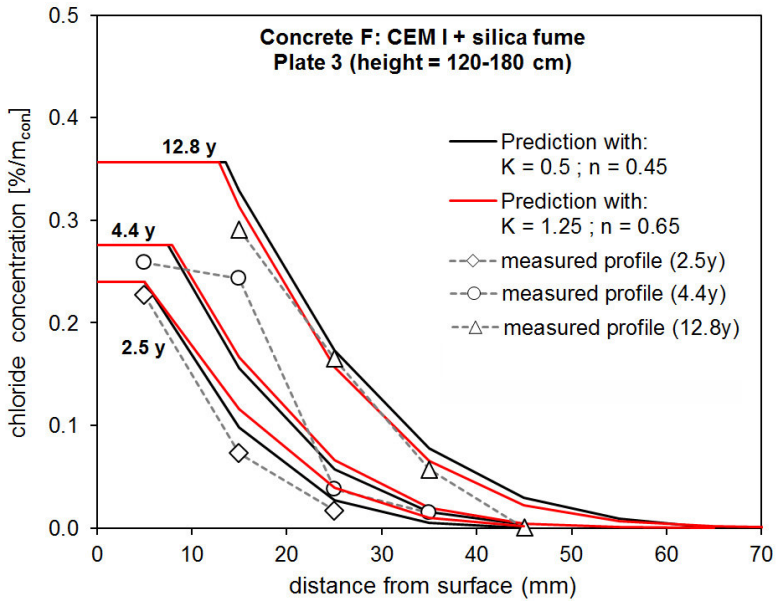

Fig. 21: *Different combinations of correlation factor (K) and ageing factor (n) lead to similar predictions.*

In this study only one general equation for the development of apparent chloride surface concentration of all concrete types was used in order to keep the model as general as possible. The development of C_{s_app} of all concretes was similar in the first 5 years. After 5 years exposure, concrete G started to significantly deviate from the other concretes (Fig. 10), probably because of its lower w/c-ratio.

The obtained parameters K and n are given in Table 10, and the predicted chloride profiles are compared to the measured ones in Figures 23 and 24. Since the input-parameters K and n were obtained by fitting against the Naxberg profiles, the agreement between predictions and measurements is a chosen agreement in this case. The main reason for disagreement between prediction and measurements is caused by the height-effect that is not considered in the model. In the Naxberg experiment a significant effect of height from road on D_{app} and C_{s_app} was measured. This effect is ignored here in

Tab.10: *Input and fitting ERFC model parameters obtained for Naxberg.*

Input Parameter	D +slag	E +fly ash	F +silica fume	G CEMI-0.35	H CEMI-0.5
M_{28d} ($\cdot 10^{-12}$ m^2/s)	11.5	15	12.5	8.5	15
K	0.5	0.5	0.5	0.5	0.5
Aging factor *n*	0.20	0.30	0.45	0.55	0.1 (1) / 0.45 (3)
C_{s_app}	Eq. 20	Eq. 20	Eq. 20	Eq. 20	Eq. 20
C_{max}	Eq. 21	Eq. 21	Eq. 21	Eq. 21	Eq. 21

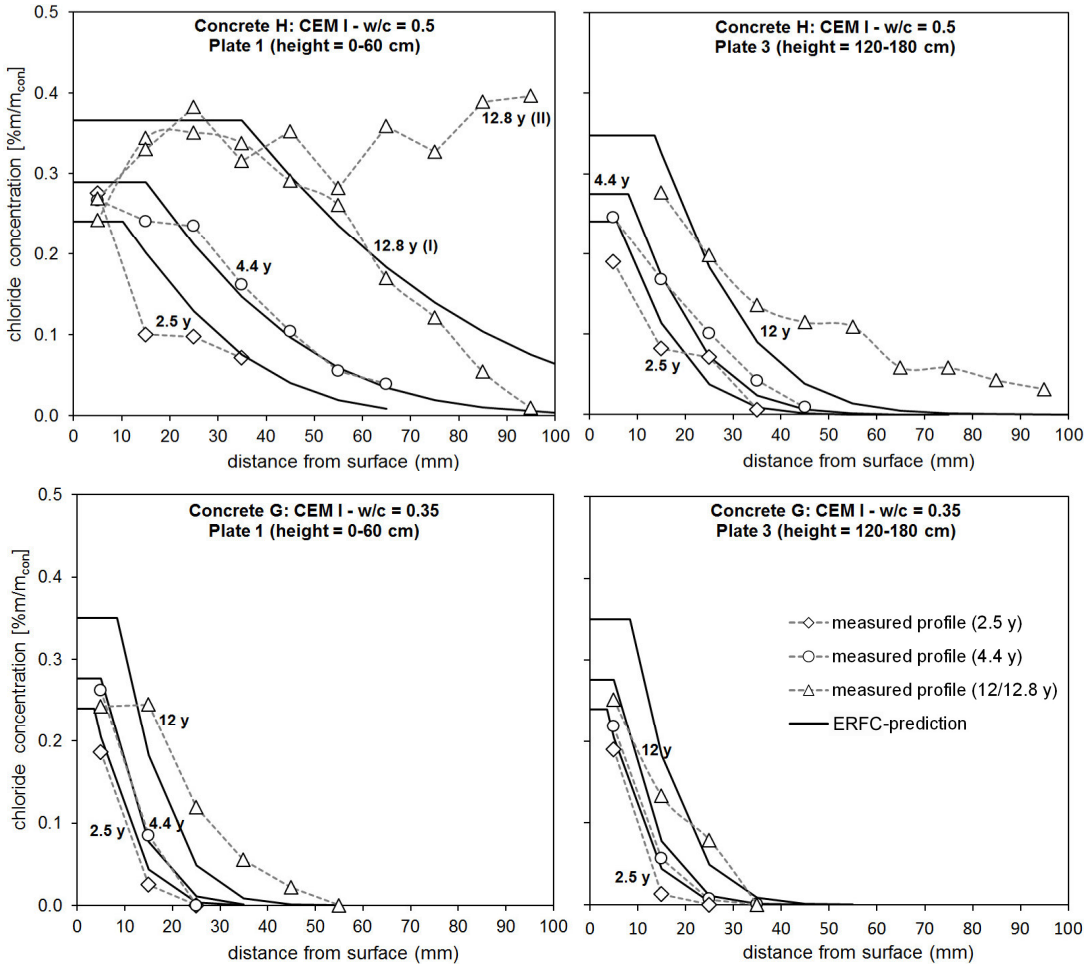

Fig.22: *Measured and predicted chloride profiles for concretes H and G. The profiles are predicted with the error-function model described in Section 5.2 using ageing factors of 0.1 (Plate 1) and 0.45 (Plate 3) for concrete H and 0.55 for concrete G.*

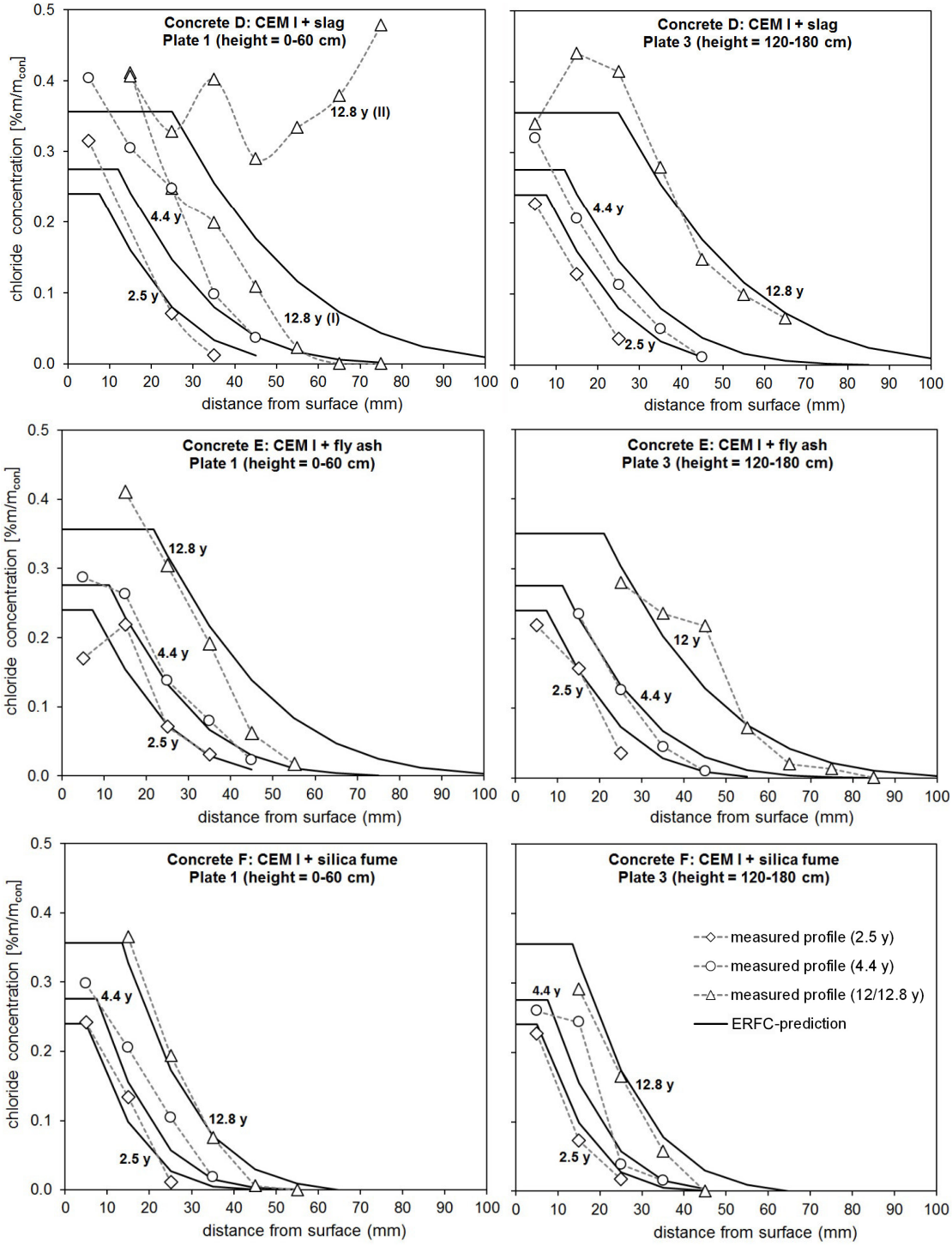

Fig.23: *Measured and predicted chloride profiles for concretes D, E, F. The profiles are predicted with the error-function model described in Section 5.2 using ageing factors of 0.2 (concrete D), 0.3 (concrete E), and 0.45 (concrete F).*

order to keep the prediction model as general as possible. However, it would be possible to apply an empirical height correction factor to the parameters K or n. Also, equations 20 and 21 could be made height-dependent using the Naxberg data. However, it is unclear if such height-dependent parameters can be applied to other settings since the chloride ingress is expected to also depend on the horizontal distance from road, traffic intensity, etc. Note that for concrete H the height effect was so large that reasonable fits could only be obtained by specifying different ageing factors for plate 1 and plate 3.

Note that for the upper plates of CEM I concretes (G and H) an aging factor n = 0.55 and 0.45 were used, respectively. These concretes do show an initial strong ageing up to an age of ca. 2.5 years (Fig. 14). After 2.5 years, the D_{app} does not change much with time, or even increases for plate 3 of concrete H (Fig. 9). Setting the ageing factor to a value of 0.45-0.55 is a solution to capture the initial ageing. The ageing will continue forever in the proposed model using this ageing factor. However, in reality there is not much ageing, and we can therefore expect that the model results will increasingly start to deviate from the measurements at later ages. The reason for the lack of ageing of concrete G is likely the end of material densification/hydration. In concrete H the end of cement hydration and/or capillary suction effects are likely reasons for the stable or slightly increasing D_{app}. An alternative for concretes with no long-term ageing is to set the ageing factor to zero. This may produce better long-term predictions, but would require adjusting the K-value to compensate for the initial early-age ageing.

5.4 Evaluation of the Naxberg prediction parameters

5.4.1 Application to the Bonaduz field experiment

Can the ERFC input parameters K and n obtained from the Naxberg experiment be used for making predictions in other settings with deicing salts? This will be assessed here for two other long-term field experiments: (1) Bonaduz in Switzerland [Angst 2013; Angst 2015] and (2) Borås in Sweden [Tang 2007]. These experiments were selected because they produced at least 2 chloride profiles at different exposure times, and the concrete compositions are similar to ones used in Naxberg. Information about concrete composition and setting for these two experiments is given in Table 11.

The field experiment Bonaduz is a long term experiment of the highway department (Tiefbauamt) of the canton Graubünden and Sika, monitored by the SGK. It is located along the highway E43 near the village of Bonaduz in eastern Switzerland at an altitude of 660 m (Fig. 24). It is a 2 meter high wall with a thickness of 20 cm and a width of 3 x 1.7 m exposed to spray water from the adjacent highway. The migration coefficients of the concretes were estimated on basis of the Naxberg results (see Section 3.5) with proportionality corrections for the lower w/c-ratio.

Fig.24: *The Bonaduz field experiment (red arrow) in the canton of Graubunden (altitude 660 m).*

Tab.11: *Concrete compositions, properties, climate information and modelling parameters for the Bonaduz (CH) and Borås (S) field experiments.*

Input Parameter	E1 Bonaduz (CH)	E3 Bonaduz (CH)	SRPC Borås (S)	SRPC-SF Borås (S)
cement	CEM I	CEM I + 6%SF	CEM I	CEM I + 5%SF
cement content (kg/m^3)	325	345	420	420
w/b	0.46	0.48	0.4	0.4
concrete density (kg/m^3)	2526	2562	2327	2309
chloride profile ages	8.5 / 18y	8.5 / 18y	1.5 / 4.5 / 9.8y	1.5 / 4.5 / 9.8y
exposure class	XD3 (+XD1?)		XD3 / snow covered in winter	
average annual T (°C)	ca. 8°C		ca. 8 °C	
height from road	ca. 1 m		0.5 m	
M_{28d} ($\cdot 10^{-12}$ m^2/s)	13.3	12	13	8
K	0.5	0.5	0.5	0.5
aging factor	0.1 / 0.45	0.45	0.1 / 0.45	0.45
C_{s_app}	eq. 20 / fitted	eq. 20 / fitted	eq. 20 / fitted	eq. 20 / fitted
C_{max}	equation 21	equation 21	equation 21	Equation 21

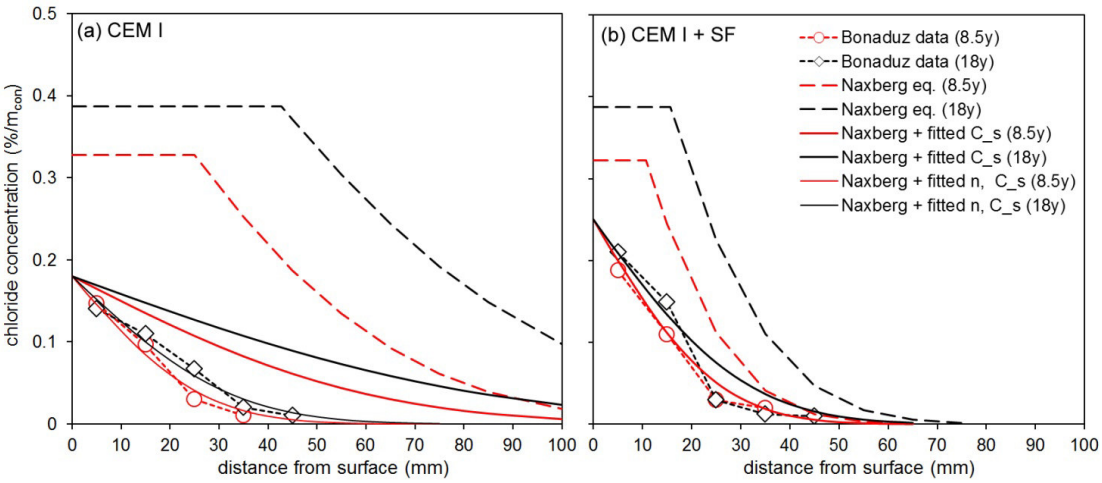

Fig.25: *Chloride profiles and error-function model prediction results for the Bonaduz field experiment for (a) concrete E1 with CEM I, and (b) concrete E3 with CEM I and 6% silica fume.*

The following sequence of predictions was carried out: first all Naxberg-input parameters and equations were used to predict the chloride profiles. Secondly, the calculations were repeated with adjusted surface concentration, that is, the surface concentration was reduced to a value close to the actual near-surface measurement in the Bonaduz and Borås field experiments. Finally, for the CEM I concretes, the ageing factor (n) was empirically adjusted from 0.1 to 0.45 for CEM I. The correlation factor (K) was held constant at a value of 0.5 in all calculations.

The Naxberg-tuned ERFC-model significantly overestimates the depth of chloride penetration in the Bonaduz concretes (Fig. 25). This clearly is a result of the much higher driving force (surface chloride concentration) that occurs in the Naxberg experiment. If the driving force is adjusted to the one that was actually measured in Bonaduz, then the ERFC-model produces a good prediction for the concrete E3 with silica fume. The model predicts relatively little progress in the chloride penetration from 8.5 to 18 years, and this is how it was observed in concrete E3 (Fig. 25b).

For concrete E1, the initial poor prediction of the Naxberg-tuned ERFC-model is not only a result of a much higher driving force in Naxberg, but also of a overestimated diffusion coefficient after 8.5 and 18 years. If the driving force is adjusted to the one that was

actually measured in Bonaduz then the ERFC-model with an ageing factor of 0.1 still produces chloride profiles with a too large penetration depth. By empirically increasing the ageing factor from 0.1 to 0.45 for CEM I concrete the results of the ERFC model become satisfactory in combination with the fitted surface concentration (Fig. 25a). Again we see that the model predicts relatively little progress in the chloride penetration from 8.5 to 18 years as was observed (Fig. 25a).

Possible reasons for the observed difference in the chloride surface concentration between Naxberg and Bonaduz are: (i) use of more deicing salts in Naxberg; (ii) more and faster traffic in Naxberg tunnel; (iii) less drainage potential of water + salts in Naxberg tunnel; (iv) larger mean humidity of Naxberg concrete; (v) lower concrete density of Naxberg concretes; (vi) larger distance from road in Bonaduz; (vii) obstruction of spray water by the crash barrier in Bonaduz.

5.4.2 Application to the Borås field experiment

The field experiment Borås is located along the highway 40 between Borås and Gothenburg in Sweden. The test concretes are cubic specimens with a height of ca. 50 cm that were placed directly adjacent the road. Deicing salts are intensively used on this road during winter time. However, the test specimens are often covered with snow in winter time, and this may affect the exposure class and chloride ingress rate [Tang 2007]. Table 11 gives information about concrete composition and setting in this experiment. The migration coefficients of the concretes were estimated from the migrations coefficient measured after 6 months for these concretes, 12.2 and $4.43 \cdot 10^{-12}$ m^2/s for SRPC and SRPC-SF, respectively [Tang, 2010], and the M-values measured on the similar concretes in the Naxberg project. The chloride profiles in Fig. 26 were selected from [Tang, 2007] and expressed in concentration as fraction of concrete weight using the given cement content.

The following predictions were carried out: first all Naxberg-input parameters and equations were used to predict the chloride profiles. Secondly, the calculations were repeated with adjusted surface concentration: the surface concentration was reduced to a value close to the near-surface measurement for each individual profile. Finally, for the CEM I concretes, the ageing factor (n) was empirically adjusted from 0.1 to 0.45 for CEM I. The correlation factor (K) was held constant at a value of 0.5 in all calculations. The results are depicted in Fig. 26.

The results are the same as for the Bonaduz experiment: the Naxberg ERFC model (with n = 0.45; K = 0.5) predicts all measured curves for the concrete with silica fume well if we adjust the driving force (C_{s_app}) to the measured value (Fig. 26d). If we use the strong driving force of Naxberg the chloride ingress is overestimated (Fig 27b). For the CEM I concrete, the model only produces a good prediction if the both the surface concentration is fitted, and the ageing factor n changed from 0.1 to 0.45 (Fig. 26c).

The measured chloride profiles in the concrete with silica fume shows an unexpected progress: the profile after 9.8 years lies below the profile measured after 4.5 years. A possible explanation for this behaviour is that in summer time chlorides may be leached-out from the concrete surface layers by rain water followed by drying [Poulsen 2006]. If subsequent chloride profiles are not systematically measured in the same month, seasonal fluctuations may contribute in the scatter of profiles. Also changes in climate or deicing techniques may be the source of a measured chloride front retraction. Nevertheless, the ERFC-model can predict chloride profiles correctly in this case, if the surface concentration is fitted to the observed value.

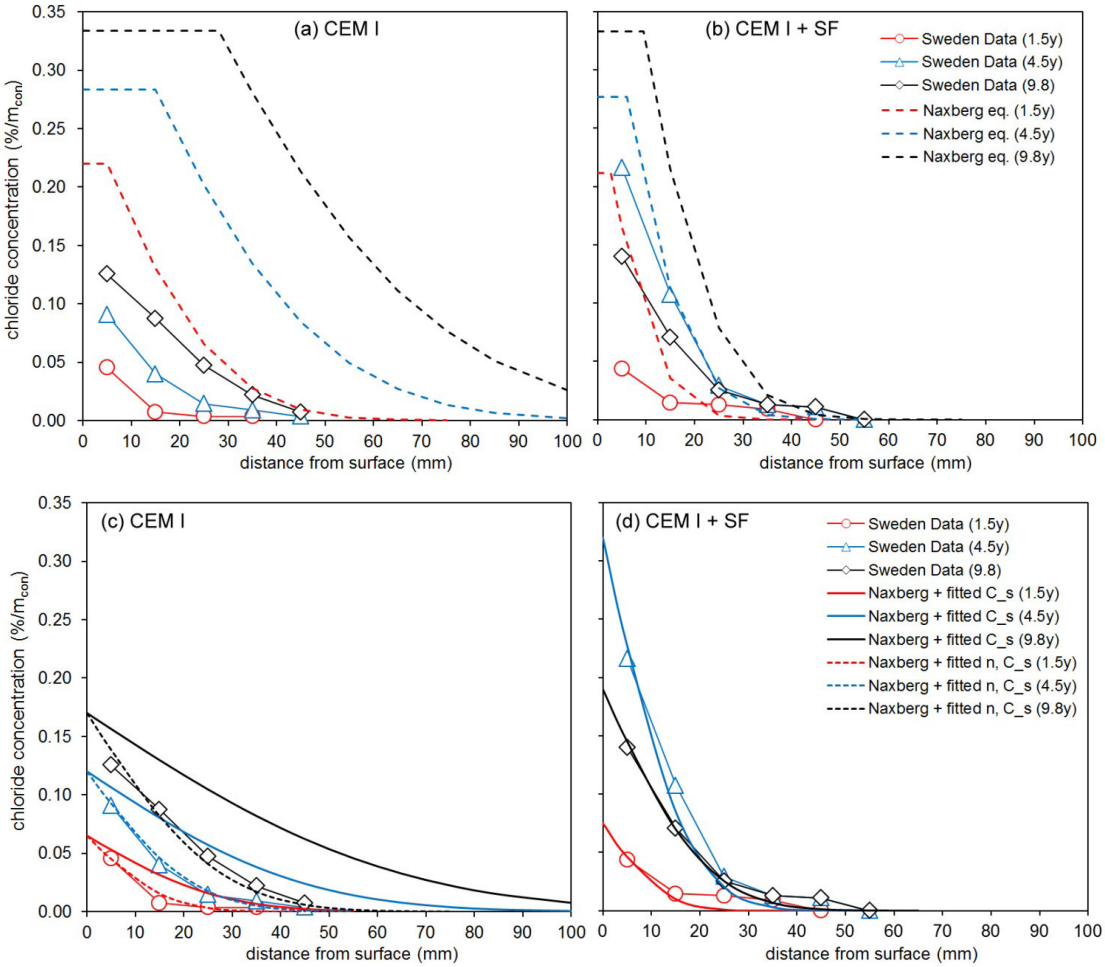

Fig.26: *Chloride profiles and error-function model prediction results for the Borås field experiment for (a, c) concrete E1 with CEM I, and (b, d) concrete E3 with CEM I and 5% silica fume. Chloride profiles from the horizontal surfaces of the cubes.*

5.4.3 The ageing factor of 0.45 applied to Naxberg

From the validation exercise in previous sections it has become clear that Naxberg chloride surface concentrations are high compared to two other field experiments (Bondaduz, Borås). When surface concentrations are fitted, then the use of an ageing factor of 0.45 (instead of 0.1 or 0.55) in the ERFC-model produced chloride profiles in good agreement with the observations in these other field experiments. What happens if we try to do the same for the profiles in the Naxberg experiment? Instead of using the average development of $C_{s\_app,}$ we vary the surface concentration in order to get an as good as possible 'fit' using an ageing factor of 0.45. The idea behind this procedure is to test if surface concentration is perhaps an unknown that increases in a fluctuating manner. Thus, the question is if the shape and position of each individual chloride profile can be predicted if we set the ageing factor to 0.45 and adjust the surface concentration?

For Naxberg concrete H with a w/c-ratio of 0.5 it is not possible to obtain any reasonable prediction using an ageing factor of 0.45 and adjusted surface concentration. On the contrary, we see for concrete G, that a slightly better fit can be obtained using an ageing factor of 0.45 (instead of 0.55) if the surface concentration is fitted for each individual profile (Fig. 27a). This is probably a result of the fact that after 12 years chloride exposure, the surface concentration of the concrete G is much lower than the average surface concentration of all concretes. Thus, in the original predictions a too large driving force for the concrete G was used, and this needs to be compensated by an increase in ageing factor to achieve a match with the observation.

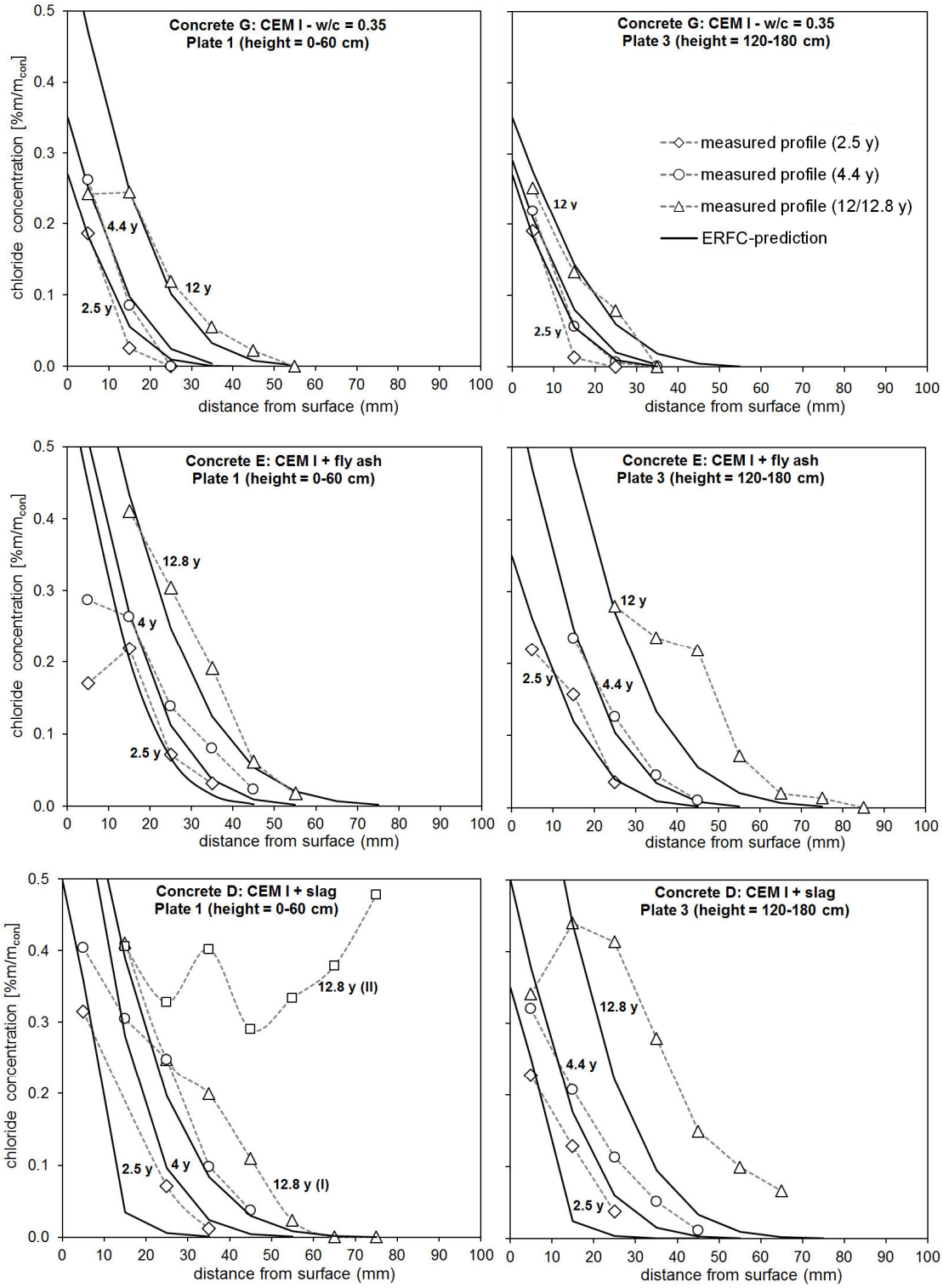

Fig.27: *Naxberg chloride profiles and error-function model prediction results using an ageing factor of 0.45 and a profile-confined adjustment of surface concentration for concrete G, D and E.*

For concrete E (with fly ash) the predictions of the ERFC model do not decrease much in quality if an ageing factor of 0.45 (instead of 0.3) is used in combination with an adjusted surface concentration (Fig. 27b). At an exposure duration of 12 years, an ageing factor of 0.45 seems no longer to be functioning. However, at this exposure age, the chloride profiles do not have a shape compatible with a diffusion-controlled process, and other combinations of n and C_{s_app} do also not produce a good agreement using an ERFC model (e.g., see Fig. 23). Finally, for concrete D (with slag) it is not possible to make

reasonable predictions using n = 0.45 (instead of n = 0.2) and adjusted surface concentration (conf. Fig. 27c with Fig. 23).

The differences in ageing factors between Naxberg concretes can partly be explained by the individual surface concentrations deviating from the averaged behaviour. For concretes H and D it is clear that the shape and evolution of the chloride profiles cannot be described by using an ageing factor of 0.45. Other factors must have contributed to the relative fast chloride ingress rate of concretes H and D and caused the decrease of the ageing factors for these concretes.

5.5 TransChlor simulations

A number of TransChlor-simulations were carried out to predict the chloride profiles in the Portland cement concrete (H) in the Naxberg tunnel. A description of the TransChlor model is given in Section 2.4.4 and the mentioned references. The simulations were carried out by one of the developers of the TransChlor chloride transport model, Dr. David Conciatori. Dr. Conciatori was provided with all necessary input-parameters (microclimate data, material composition, transport/mechanical properties at early ages), but initially not with the measured chloride profiles. Spray water conditions were assumed for the exposure class of the concrete in the tunnel.

With the meteorological data from the nearest meteorological station (Guetsch) and a yearly regional deicing salt consumption of 3000 g/m^2.year, the number and timing of passing salt trucks in the Naxberg region was determined. A salt truck expands between 5 to 40 g/m^2 in each passage. If an average expansion of 10 g/m^2 is assumed, the number of truck passages is 300 times. A truck will expand deicing salt if one of these three events occurs: snow precipitation, rain precipitation, or high relative humidity with a certain low threshold temperature (1.8°C as calculated by TransChlor). After salt spreading three different chloride concentrations can be appear on the road: (i) if the road is wet, TransChlor calculates the chloride surface concentration (C_s) from the average salt application (= 10 g/m^2) divided by the water density and water film thickness. If the road is dry, C_s = 36% salt concentration in water, which is the saturation concentration. After the passage of trucks, C_s decrease in time with the amount of precipitation.

By using the calculated surface salt concentrations and the microclimatic conditions that follow from the regional meteorological history, a first set of chloride profiles were calculated for chloride exposure durations of 2.5, 4.4 and 13 years. The calculated maximum chloride concentrations in the concrete turned out to be around 3 times higher than the actual measured values. It was therefore decided to reduce the chloride surface concentration used in TransChlor (from 36% to 12%) in order to produce maximum chloride concentrations that more or less matched the measured values

The results of the TransChlor simulations with adjusted (fitted) surface concentration and the measured chloride profiles are shown in Fig. 28. It is clear that the simulated chloride ingress after 2.5 and 4.4 years is much larger than the actual chloride ingress. This strong initial chloride ingress in the simulations is due to the large predicted ingress by capillary suction under the assumption of spray water conditions. After 13 years the simulated chloride ingress is within the range of measured values. For the lowest panels of H-concretes, there are strong indications that capillary suction played an important role for the chloride ingress after 12 years chloride exposure (see Section 3.6.1). Thus, the simulations (with adjusted C_s) seem to be in agreement with measured chloride ingress at later ages (>12 years). Also the overall mountain-shaped chloride profile predicted by TransChlor is in agreement with the chloride profiles often observed at later ages.

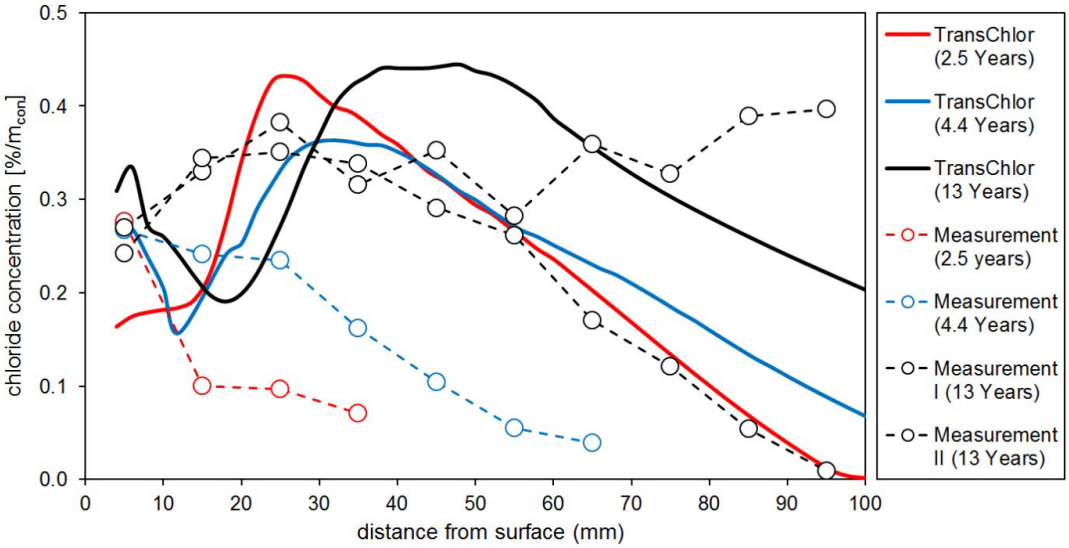

Fig.28: *Result of TransChlor simulations for CEM I concrete (H) under Naxberg microclimatic conditions. Also shown are the measured chloride profiles for concrete H at height of 0-60 cm with the highest expected contribution of spray water. The simulated and measured chloride concentrations are the total chloride concentrations in concrete.*

The various disagreements between the simulations and measurements indicate the challenges of making mechanistic chloride ingress predictions under spray water exposure. The measured chloride profiles progress according to Fick's law at early ages, while the simulations predict a much stronger effect of capillary ingress. These discrepancies may have originated from unstable and unpredictable actual microclimate conditions in the tunnel, i.e., from simplifying assumptions made in the TransChlor model regarding boundary conditions. For example, the traffic intensity will affect the degree and distance of salt spraying, but this effect is not considered in the model. More scientific research is needed to come to better understanding of which factors affect the surface concentration under spray water exposure and how these factors may fluctuate in time as a function of climate conditions and intensity of deicing salt application and traffic.

5.6 Example lifetime calculations

5.6.1 Effect of ageing factor and cover thickness on lifetime

The impact of the ERFC input parameters on the calculated lifetime of the Naxberg reinforced concrete plates are illustrated with a number of examples. Mathematical sensitivity analyses of the ERFC-type or other chloride models can be found in literature [Tang 2010; Kapteina 2011; Conciatori 2015]. Lifetime is defined here as the corrosion-free lifetime, i.e., the time required to reach the critical chloride content at the 'uppermost' layer of reinforcement bars. In this section the effect of the ageing factor and w/c-ratio (or migration coefficient) on the calculated lifetime of Naxberg concrete plates with CEM I is shown. The lifetime is plotted as a function of cover depth in the range of 0-80 mm (see Fig. 29). Note that these are example calculations for specific concretes in specific settings, and they therefore have limited application. The issue of expected lifetime for reinforced concrete in XD3 as prescribed by Swiss standards is addressed in Chapter 6.

In the calculations we use the migration coefficient as measured in our study: M_{28d} = 8.5·10^{-12} m^2/s for concrete G with w/c = 0.35 and 15·10^{-12} m^2/s for concrete H with w/c = 0.5, and a 'moderate' constant C_{s_app} of 0.3%/m_{con} (see Section 5.6.2). The ageing factor (n) was changed in the range of 0.45 to 0.65 for w/c = 0.35 and from 0 to 0.65 for the w/c = 0.5 concrete. The upper bound value of n = 0.65 is the value often used in the DuraCrete model under mist (and spray) water conditions (see Table 3). Furthermore for concrete G

the value of n = 0.55 was used as was found by the fitting procedure for this concrete using the average Naxberg development of C_{s_app}. The value of n = 0.45 was also tested, since this seems to be the better ageing factor for CEM I concretes if C_{s_app} is adjusted to the measured chloride profile. For the concrete H, n = 0.45 and 0.65 were tested for the same reasons as for concrete G. Moreover, n = 0 and 0.2 were tested as lower bound values for the case of strong suspected capillary suction effects as was found for lower plates in the Naxberg experiment (n = 0.1). Note that the use of a low ageing factor (n = 0 to 0.2) in combination with the 'moderate' C_{s_app} of 0.3%/m_{con} is hypothetical since in Naxberg this n-value occurs in combination with much larger C_{s_app}.

The ERFC model results show a strong effect of w/c-ratio (M_{28d}-value), ageing factor and cover thickness on lifetime. Reducing w/c-ratio and increasing cover thickness are effective measures to increase serivce life. The predicted lifetime of Naxberg concrete H (lower plates with suspected strong capillary chloride ingress) is 2-5 years for a cover thickness 30-40 mm, and this is in agreement with the observations [Schiegg 2014].

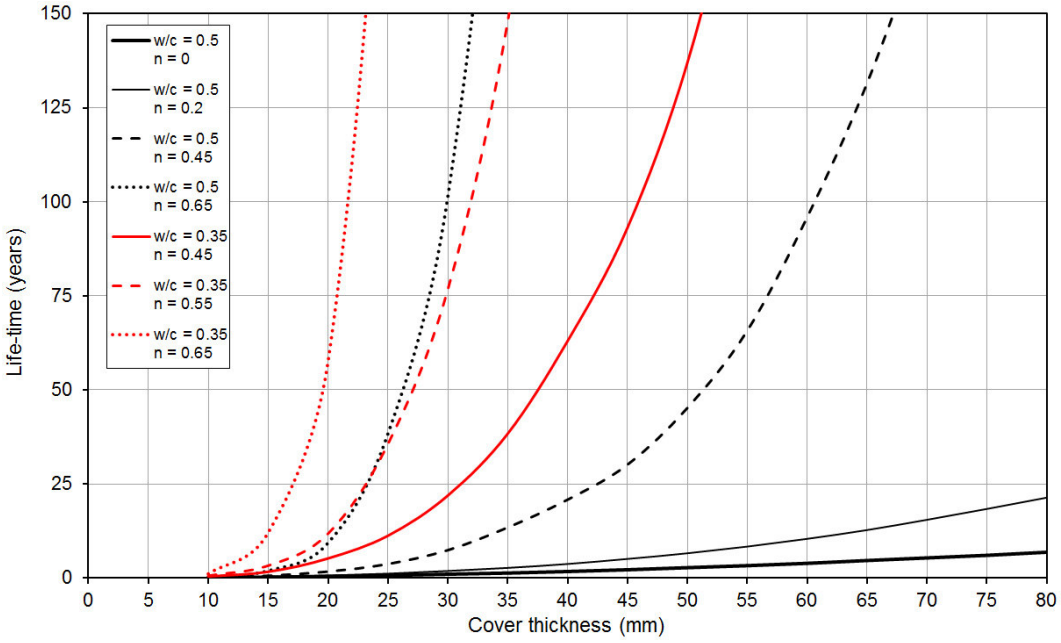

Fig.29: *Effect of cover thickness, ageing factor (n) and w/c-ratio on the ERFC-lifetime of CEM I concrete. Assumed C_{crit} = 0.05 %/m_{con} (≈ 0.4 %/m_{cem} for concrete with 300 kg/m³ cement); K = 0.5; C_{s_app} = 0.3 %/m_{con}.*

5.6.2 Effect cement type and surface concentration on lifetime

The effect of Naxberg cement type on the corrosion-free lifetime as calculated with the ERFC-model is shown in Fig. 30-32. Note that these are example calculations for specific concretes in specific settings and therefore have with limited application. The issue of expected lifetime for reinforced concrete in XD3 as prescribed by Swiss standards is addressed in Chapter 6.

In the calculations we use the migration coefficient as measured in our study (see Table 10). The effect of chloride surface concentration (C_{s_app}) was studied for 3 cases which are defined as follows:

I. A constant value of C_{s_app} = 0.3 %/m_{con} representing 'moderate' chloride surface ingress as occurred in Bonaduz and Borås experiments (up to 18 years) for concretes with w/c = 0.4-0.46 (see Table 11). Note that 0.3 %/m_{con} corresponds to 2.4 %/m_{cem} for concrete with 300 kg/m³ cement.

II. A constant value of C_{s_app} = 0.4 %/m_{con} representing 'strong' chloride surface ingress as occurred in Naxberg for concrete G with w/c-ratio of 0.35 (up to 13 years). Note that 0.4 %/m_{con} corresponds to 3.2 %/m_{cem} for concrete with 300 kg/m^3 cement.

III. Time-dependent C_{s_app} given by equation 20 (see Section 5.2), which represents the average extreme chloride surface ingress in the Naxberg experiments for relatively porous concrete with a w/c-ratio of mostly 0.5. Note that C_{s_app} = 0.5-08 %/m_{con} are regularly observed for parking floors in Switzerland, and these extreme chloride concentrations may also be associated with relatively porous concretes.

The designations 'moderate', 'strong' and 'extreme' for chloride surface concentrations are preliminary. Further field studies are needed to get to a better categorization of chloride surface concentrations as they occur in road environments.

The ageing factor (n) for concrete F (silica fume) was kept at 0.45 in all calculations, since this is the common n-value found for Naxberg and the other studied field experiments. For concretes D and E, the Naxberg ageing factors of, respectively, 0.2 and 0.3 as lower bound and the often-used DuraCrete value of 0.65 (see Table 3) as upper bound, were used. The DuraCrete value of 0.65 or higher is used in conjunction with higher amounts of slag or fly ash than was used in Naxberg (see Table 3).

Again we observe a strong effect of ageing factor and cover thickness on the corrosion-free lifetime (Fig. 30-32). The effect of C_{s_app} in the range of 0.3 to 0.4 %/m_{con} is also significant. For example, for concrete F the difference in predicted lifetime between these two degrees of chloride surface ingress, is 25 years for a cover thickness of 50 mm. The lifetime predictions and the effect of C_{s_app} for Concrete D and E are quite similar (Fig. 31 and 32). This differences are caused by the difference in M_{28d}-value (11.5 vs. $15 \cdot 1010^{-12}$ m^2/s, resp.) and the ageing factor (0.2 vs. 0.3, resp.). With the Naxberg ageing factors of 0.2 and 0.3 the effect of C_{s_app} is small for normal cover thicknesses (40-55 mm). The predicted lifetime of concretes D and E in the Naxberg experiment is in the order of 5-10 years for a cover thickness in the range of 40-55 mm.

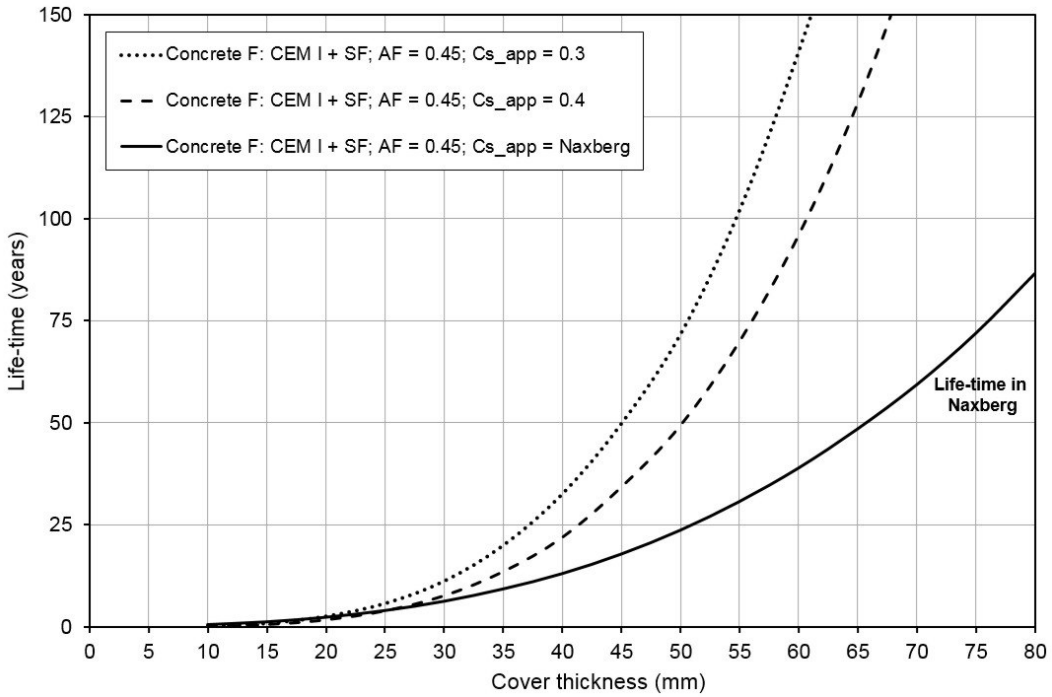

Fig.30: *Effect of cover thickness and surface concentration (C_{s_app}) on the ERFC-lifetime of concrete with 7% silica fume. The C_{s_app} is 0.3 or 0.4 %/$m_{con,}$ or Naxberg equation 20; the ageing factors (AF) is 0.45; K = 0.5; and assumed C_{crit} = 0.05%/m_{con}.*

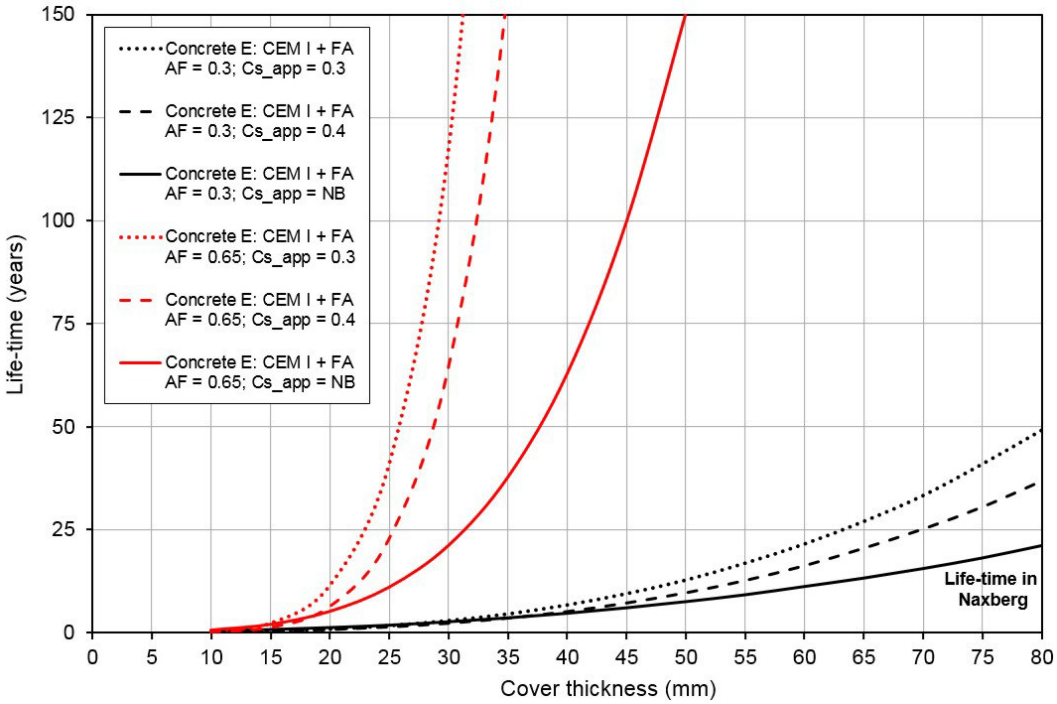

Fig. 31: *Effect of cover thickness, surface concentration (C_{s_app}), and ageing factor on the ERFC-lifetime of concrete with fly ash. The C_{s_app} is 0.3 or 0.4 %/$m_{con,}$ or Naxberg equation 20 (= NB); the ageing factors (AF) is 0.3 or 0.65; K = 0.5; and assumed C_{crit} = 0.05%/m_{con}.*

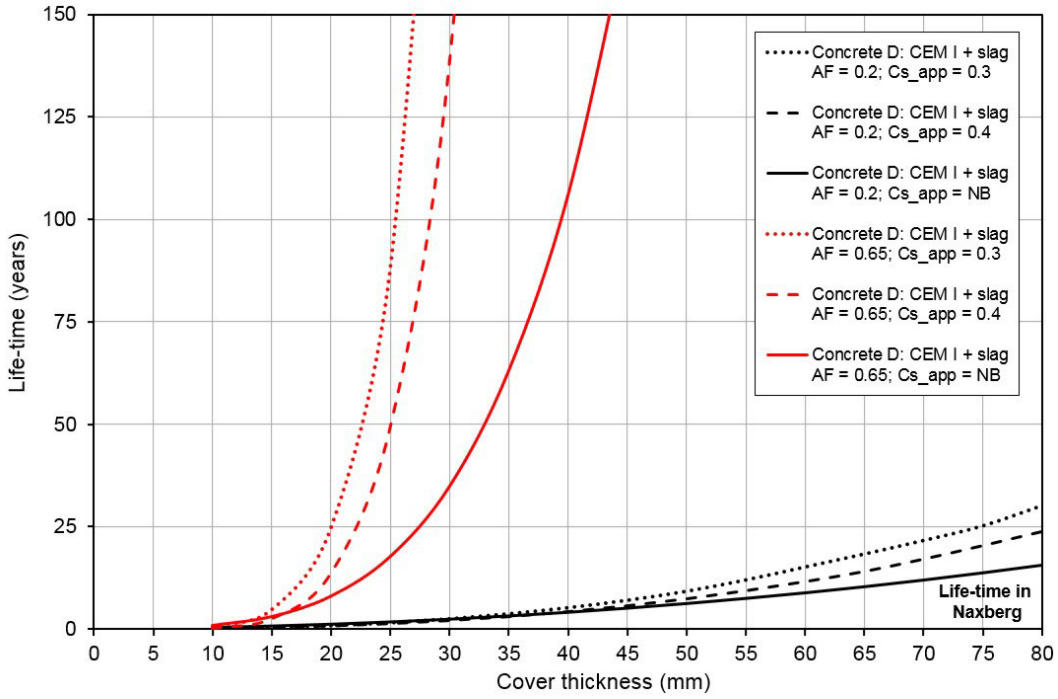

Fig. 32: *Effect of cover thickness, surface concentration (C_{s_app}), and ageing factor on the lifetime of concrete with slag. The C_{s_app} is 0.3 or 0.4 %/$m_{con,}$ or Naxberg equation 20 (= NB); the ageing factors (AF) is 0.2 or 0.65; K = 0.5; and assumed C_{crit} = 0.05%/m_{con}.*

5.6.3 Effect of reinforcement steel type (C_{crit}) on lifetime

An important effect of reinforcement steel type and surface processing on the critical chloride content (C_{crit}) in CEM I concrete was observed in this study (see Chapter 4, Table 9). The critical chloride content of Top12-steel was almost twice as large as the one of normal rebar steel in case of a rolled skin. For a Top12-steel with a pickled skin, C_{crit} was about 4 times larger than for standard rebar steel with an ordinary skin (see Table 9).

The effect of C_{crit} on the calculated ERFC lifetime is shown in Table 12. For these calculations a maximum migration coefficient of $10 \cdot 10^{-12}$ m²/s as defined by Swiss standard SN EN 206-1 is used, and the degree of surface chloride ingress is set to 0.4 %/m_{con} (= strong). In the hypothetical case of no concrete ageing (n = 0), the lifetime increases linearly with C_{crit}. In case of an ageing factor n = 0.45 for CEM I concrete, we see and exponential increase of lifetime with C_{crit}: Doubling of C_{crit} leads to a three times larger lifetime, while a three times larger C_{crit} leads to a 7 times larger lifetime.

Tab.12: *Effect of C_{crit} on predicted ERFC lifetime for CEM I concrete.*

Parameter	CEM I no ageing		CEM I strong ageing	
	cover 3 cm	cover 5 cm	cover 3 cm	cover 5 cm
M_{28d} ($\cdot 10^{-12}$ m²/s)	10	10	10	10
K	0.5	0.5	0.5	0.5
ageing factor	0	0	0.45	0.45
C_{s_app} (%/m_{con})	0.4	0.4	0.4	0.4
time to reach C_{crit} = 0.05 %/m_{con}	1.2 years	3.4 years	11.6 years	74.3 years
time to reach C_{crit} = 0.10 %/m_{con}	2.2 years	6.0 years	33.2 years	212 years
time to reach C_{crit} = 0.15 %/m_{con}	3.6 years	10.1 years	85 years	548 years
Lifetime increase by doubling of C_{crit}	x 1.8	x 1.8	x 2.9	x 2.9
Lifetime increase by tripling of C_{crit}	x 3	x 3	x 7.3	x 7.3

5.7 Redistribution of chlorides after concrete sealing

A possible measure against the ingress of chloride is to seal the concrete, make it water-repellent (i.e., hydrophobic impregnation), and/or replace (part of) the cover with a layer of new concrete or mortar. Even after many years of chloride ingress such measures could significantly increase the lifetime of a reinforced concrete structure. However, the redistribution of remaining chlorides in the concrete after sealing/repair should be considered. Chloride profiles are not stable after the chloride supply has been cut-off, i.e., they tend to flatten in order to achieve concentration equilibrium in the concrete.

Depending on the restoration method various situations may arise (see Fig. 33). If the chloride contaminated concrete is only partly removed and replaced by a repair layer of mortar or concrete, then the chloride permeability of the repair material determines the redistribution of the chloride [Skoglund 2007; Ungricht 2007; Rahini 2014]. Relatively porous repair materials, may uptake chlorides form the old substrate concrete, and thereby reduce the risk of rebar-corrosion in the old concrete (Fig. 33c). In this case the lifetime of the restored concrete will depend on the chloride concentration of the remaining concrete, the thickness of the repair layer, and the degree of renewed chloride ingress. In the case of a dense repair material, absorption of chlorides from the old concrete may be negligible, and a long-term redistribution of the chlorides will result in a raise of chloride concentration at the depth of the rebar (Fig. 33d). The situation may exist that after restoration of a chloride-contaminated concrete, the critical chloride content is exceeded at rebar-depth due to chloride distribution, and corrosion can start.

The area under the current chloride profile (after repair or sealing) and the depth of reinforcement from the repair or sealed surface, will determine, if there is a potential to exceed the critical chloride content. If yes, further prediction modelling is needed to estimate the remaining lifetime. The chloride redistribution rate can in principle be estimated with Fick's second law of diffusion, if the chloride profile at the time of concrete sealing is known (measured). In this case there is, however, no error-function solution for Fick's second law, as in the case of constant chloride ingress. The chloride profile is flattening and this means that the concentration gradient across the concrete is changing in time. Moreover, the initial/actual shape of the chloride profile (as measured at time of concrete sealing), may deviate from a typical diffusion profile if ingress also occurred by capillary suction. This means that the redistribution process needs to be predicted by means of numerical modelling.

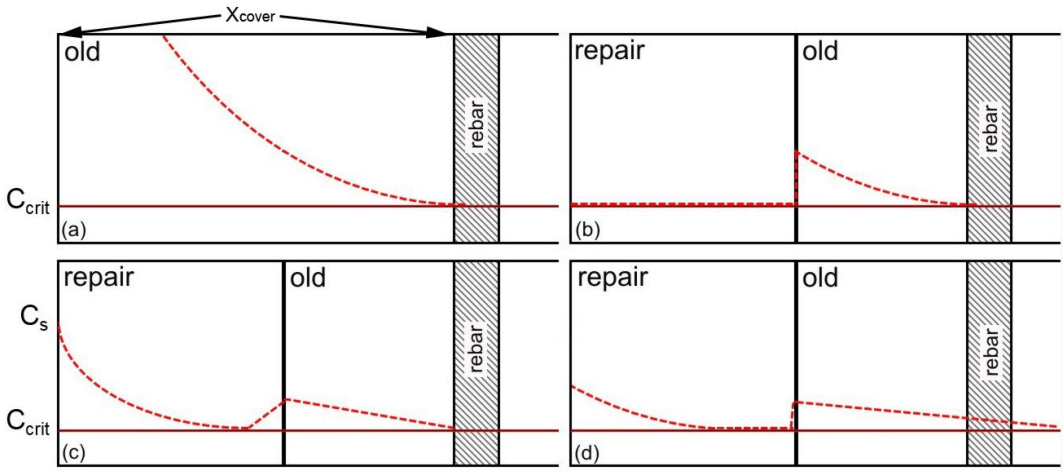

Fig.33: *Schematic illustration of chloride redistribution after concrete cover repair. (a) concrete with chloride profile prior to restoration; (b) Partial replacement of contaminated concrete by a repair layer, situation immediately after restoration; (c) chloride distribution in repaired cover after many years of renewed chloride ingress: repair layer with high permeability; (d) chloride distribution in repaired cover after many years of renewed chloride ingress: repair layer with low permeability and low/negligible uptake of chlorides from old concrete [after Skoglund 2007; Rahini 2014].*

The question remains what the value of the diffusion coefficient during redistribution is. The apparent diffusion coefficient (D_{app}) can be obtained by regression of the chloride profile at the time of concrete sealing, and this diffusion coefficient could possibly be used for conservative remaining lifetime calculations. In reality, the diffusion coefficient during redistribution may be significantly lower than for the case of ongoing chloride ingress: Part of the total chloride content in concrete concerns chemically or physically bound chlorides. During ongoing chloride ingress, more and more chlorides will be get bound, but the reverse process, unbinding of chlorides, may not be significant. However, during redistribution, chloride-unbinding may take place as a consequence of redistribution. To our knowledge, not much is known about the kinetics of chloride unbinding (dissolution and desorption) and whether this may limit the overall rate of chloride redistribution, and lower the diffusion coefficient significantly. Further research is needed to determine how remaining lifetime due to chloride redistribution is to be calculated.

6 Conclusions and recommendations

6.1 Summary of observations and model results

6.1.1 Effect of concrete composition on chloride ingress

The Naxberg long-term field experiment has provided a large database of chloride profiles for concretes with different compositions. The CEM I concrete (H) with a w/c-ratio of 0.5 showed the highest and the CEM I concrete (G) with a w/c-ratio of 0.35 the lowest chloride ingress rate. In between are the concretes blended with supplementary materials and a w/b-ratio of 0.5. The difference in chloride ingress rate for the blended concretes (with either 20% slag, 15% FA or 7% SF) was relatively small (see Fig. 8). The difference in chloride resistance at early ages was also relatively small for these blended concretes (see Table 8). The Naxberg experiment showed that the supplementary materials (slag, FA, SF) reduced long-term chloride ingress rate for a given w/b-ratio, but the mechanisms behind this behaviour have not been clarified in this study. It is also unclear from the Naxberg experiment what degree of replacement of CEM I by slag, FA, or SF would produce the most durable concrete in road environments with deicing salts. From the single replacement levels studied in this project, it appears that silica fume is most effective in reducing the long-term chloride ingress. Reduction in w/c-ratio and hydrophobic impregnation were also effective in reducing the long-term chloride ingress.

6.1.2 Effect of height on chloride ingress

The chloride ingress rate decreased with increasing height from road: The plates 1 at height of 0-60 cm showed higher chloride concentrations (Fig. 11) and larger apparent diffusion coefficients (Fig. 9) as plates 3 at a height of 120-180 cm. The probable reason is that the exposure conditions gradually change from bottom to top in the Naxberg experiment. The amount of salty spray water reaching the concrete surface probably reduced with height, and this resulted in a higher salt supply and a wetter concrete at lower heights. Both effects increased the diffusive ingress of chlorides at lower heights. Moreover, the ingress of chlorides by capillary suction can increase with more spray water, if the wetting is interrupted by spells of dryness. It is not clear if a transition from exposure classes XD3 to XD1 occurs within the height levels of the Naxberg experiment; the highest plates possibly also experience XD3 conditions.

The height effect observed in the Naxberg could in principle be accounted for in the proposed prediction model by means of an empirical height correction factor. However, it remains unclear if the Naxberg height effect is generally applicable to XD1/XD3 settings. The amount of salts that will reach concrete surfaces adjacent to roads also depends on other factors, such as horizontal distance from road, traffic intensity (speed limit), road sloping direction and magnitude (i.e., drainage conditions), and obstruction issues (crash barriers, shovelled snow, etc.). The effect of height is systematic in Naxberg, but for most concrete types the effect (up to 180 cm height) was not that large that it required an urgent consideration in the proposed prediction model. Only for the concrete H the height effect was so large that the height-independent ERFC-prediction model was unable to make an (approximate) prediction for all chloride profiles. Large height-effects (in range of 0 - 2 meter) are possibly restricted to concretes with relative high porosity/permeability, outside of the range of dense concretes that should be used for exposure classes XD1 and XD3.

6.1.3 Time-dependence of D_{app}, C_{max}, and C_{s_app}

A strong time-dependence of D_{app}, C_{max}, C_{s_app}, is observed in the Naxberg experiment (Fig. 9-11). The initial decrease of D_{app} (<2.5 years) may primarily be related to cement hydration densification. However, for the long-term change in D_{app} cement hydration is not expected to play a significant role anymore. As discussed in Section 2.2.6 other long-term

factors such as chloride binding, drying and carbonation of concrete may cause a decrease in D_{app}. For concrete H a long-term increase in D_{app} can be observed after the early age drop in D_{app}. As discussed in Section 3.3 this increase was even stronger in reality, since D_{app} of samples with the strongest chloride ingress after 12 years could not be measured, and were thus not included in the average D_{app}. In the particular case of concrete H, the long-term increase in D_{app} is a likely result of the (increasing) contribution of chloride ingress by capillary suction (Section 3.6.1).

The chloride concentrations C_{max} and C_{s_app} show a long-term increase that can be described by exponential time-relationships. The increase in surface and peak concentrations is likely to be a result of cumulative chloride binding, and due to the formation of a mountain-shaped profile. The C_{s_app} grew more or less linearly with C_{max} as long as C_{max} occured in the concrete surface slice. When C_{max} moved into the concrete (due to drying and carbonation of the concrete surface layer), C_{s_app} grew faster than C_{max}.

6.1.4 Results of prediction modelling

The main objective of this study was to propose a (user-friendly) model for predicting corrosion-free service lifetime of reinforced concrete. Since ERFC-type prediction models are relatively simple to use (e.g., do not require numerical modelling), are already widely being used in Europe (e.g., DuraCrete), we have tested and tuned this type of empirical model. In addition, we have applied an elaborate mechanistic model (TransChlor) to the Naxberg results.

Judging from the results for 3 different field experiments (see Section 5.4), it appears that the DuraCrete-type ERFC prediction model proposed in this report has the capability of making predictions with reasonable accuracy. The model works for chloride ingress that follows Fick's law of diffusion or chloride ingress due to a combination of diffusion and capillary suction, such that the overall process still can be approximated by the error function solution (ERFC). Recent experimental results showed that chloride profiles due to combined diffusion and capillary suction are roughly similar to those developing by pure diffusion under a wide range of drying-wetting conditions [Gang 2015]. Thus, in settings with expected effects of capillary suction, simple ERFC-models could also be applicable under a wide range of conditions.

The use of the early-age migration coefficient (M_{28d}) as input parameter makes the DuraCrete-type model useful for designing new concrete structures. However, the use of M_{28d} and the formulation of linking M_{28d} to D_{app} requires the use of a particular set of input parameters. Care should be taken to use the right combination of input parameters. The correlation factor (K) and ageing factor (n) should preferable be obtained by tuning / fitting against long-term field experiment, and used together in combination with a specifically assumed or determined C_{s_app}. Great care is needed when the K or n-values are calculated from theoretical considerations or taken from literature. The used ageing factor should represent the ageing in the field (with specific carbonation and drying conditions). Ageing factors determined in laboratory experiments (e.g., [Nokken 2006]) may only capture hydration-related and chloride binding ageing.

6.2 Lifetime under standard XD-conditions

6.2.1 Deterministic results

In this section the lifetime of concretes as defined by Swiss standard SN EN 206-1 will be calculated. According to this standard, shall for the concretes of type F and G (see Table NA.2) used in exposure classes XD2b or XD3 the migration coefficients at 28 days age (M_{28days}) not exceed a mean value of $10 \cdot 10^{-12}$ m^2/s. According to Swiss standard SIA 262 the mean cover thickness for these exposure classes shall be not less than 55 mm, and the minimum not lower than 45 mm [SIA 262]. For exposure classes XD1 and XD2a, the

mean cover thickness should be at least 40 mm, but no further requirements for chloride resistance are defined for these exposure classes. By using these standard prescriptions and the results of this study, the minimum expected lifetimes that are suggested by Swiss standards can be calculated.

In this study, we have determined different ageing factors for different concrete types and even different heights. However, these were determined by using migration coefficient in the range of $11.5\text{-}15 \cdot 10^{-12}$ m^2/s, i.e., these concretes (w/c = 0.5) do not comply with the standard prescription. To achieve $M = 10 \cdot 10^{-12}$ m^2/s, the w/c-ratio of the Naxberg concretes should be lowered. Only concrete G with w/c-ratio of 0.35 had $M = 8.5 \cdot 10^{-12}$ m^2/s and was conform the Swiss standard. The chloride profiles for concrete G were best predicted with an ageing factor of 0.55 in case of using eq. 20 for C_{s_app}. When C_{s_app} was adjusted for each individual profile, then an ageing factor of 0.45 led to reasonable predictions as well (see Section 5.4.3). The ageing factor of 0.45 was also one obtained from the validation study for CEM I (Section 5.4). For the concrete E (with 5-7% silica fume) an ageing factor of 0.45 was found in the Naxberg and other experiments. It may perhaps not be surprising that the field ageing behaviour of a CEM I concrete is similar to a CEM I concrete with only 5-7% mineral addition.

For the concretes, D and F the cement replacement levels are higher, 20% and 15%, respectively and this could perhaps lead to an ageing factor that differs from the one of plain CEM I concrete. For example, in experiments it has been observed that the ageing factors of slag and FA increase with replacement level (see Table 3: [Stanish 2003]). The ageing factors of 0.2 and 0.3 obtained in this study were obtained in combination with the general eq. 20 for C_{s_app} averaged over all mixtures. If we set n = 0.45 for concrete F and adjust the surface concentration for each individual profile, then reasonable predictions can also be obtained (see Section 5.4.3). For concrete D (with slag) we were unable to get a good prediction using n = 0.45 (see Fig. 27), however, like for concrete H, it might be that capillary effects reduced the n-value in this case. The obtained n-value may not be representative for concrete D with reduced w/c-ratio such that M_{28d} would be smaller than $10 \cdot 10^{-12}$ m^2/s. In literature, the n-value of 0.45 is commonly found and used for slag concretes in sea water [Wegen 2012].

For the moment we assume that for concretes with relative small amounts of mineral additions (<20%), the ageing of D_{app} can be described with n = 0.45 if the w/c-ratio is such that $M < 10 \cdot 10^{-12}$ m^2/s. If ageing factors increase with the amount of mineral addition, than that the use of n = 0.45 would be a conservative choice for concrete with high amounts (>20%) of mineral additions. Next, we thus calculate the lifetime for concretes with $M < 10.10^{-12}$ m^2/s and an 'universal' ageing factor of n= 0.45. We also calculate the case for $M = 8 \cdot 10^{-12}$ m^2/s, which is more practical value that needs to be achieved in order to ascertain that the mean M is lower than 10.10^{-12} m^2/s. For the critical chloride content, a conservative value of 0.05%/m_{con} was assumed as prescribed by various standards/specifications. For the chloride surface concentration, we use three possible cases as described in Section 5.6.2:

I. A constant value of C_{s_app} = 0.3 %/m_{con} representing 'moderate' chloride surface ingress as occurred in Bonaduz and Borås experiments (up to 18 years) for concretes with w/c = 0.4-0.46 (see Table 11);

II. A constant value of C_{s_app} = 0.4 %/m_{con} representing 'strong' chloride surface ingress as occurred in Naxberg for concrete G with w/c-ratio of 0.35 (up to 13 years);

III. A time-dependent C_{s_app} given by equation 20 (see Section 5.2), which represents the average extreme chloride surface ingress in the Naxberg experiments for relatively porous concrete with a w/c-ratio of mostly 0.5. Note that this case is hypothetical case that may not occur for porous concrete with $M_{28d} > 10.10^{-12}$ m^2/s. For standardized concretes this type of ageing may not occur. Still it can be regarded as extreme upper bound. As an example the effect of limited vs. ongoing ageing of C_{s_app} is also shown.

The results of the lifetime predictions for reinforced concretes that complied with Swiss standards is given in Fig. 34. The lowest lifetime (ca. 25 years) is achieved for the (hypothetical) case of extreme supply of chloride such as observed for porous concretes in the Naxberg experiment. It is unclear if such conditions actually exist, since concrete G with M = $8 \cdot 10^{-12}$ m^2/s showed a C_{s_app} of 0.4 %/m_{con} (plateau) after 12 years. C_{s_app} = 0.4 %/m_{con} could perhaps represents the maximum practical C_{s_app} for standard-compliant concrete in road environments. In the case of 0.4%/m_{con} the lifetime guaranteed is at least 50 years for a cover thickness of 45 mm. For the more practical case with the mean M_{28d} = $8 \cdot 10^{-12}$ m^2/s we get a corrosion-free lifetime of 75 years for a minimum cover thickness of 45 mm as required for XD1 and XD3.

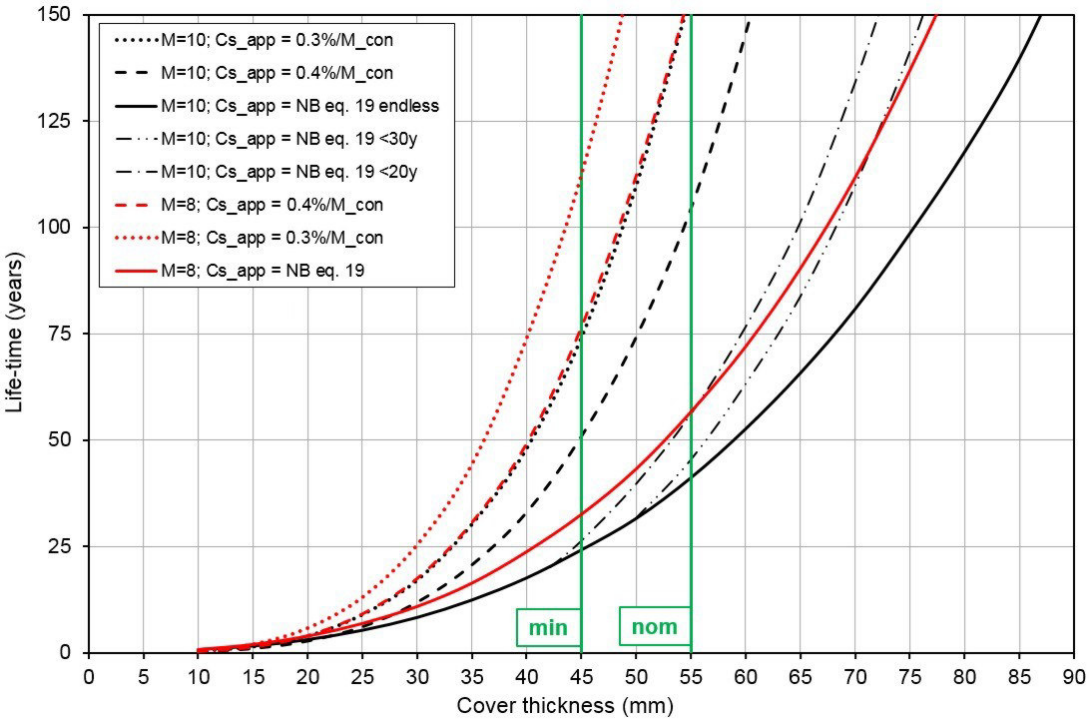

Fig.34: *Chloride-induced lifetimes as prescribed by Swiss standard SN EN 206-1 for exposure class XD3 for CEM I concrete and blended concretes with low amounts of slag, FA or SF. An ageing factor n = 0.45 was used in all cases.*

These lifetime calculations seem to indicate that Swiss standards only marginally guarantee sufficient durability (i.e., a service life of 50, 75 or 100 years) under XD3-exposure with (very) high chloride surface concentrations. A relatively small change in concrete density (i.e., M_{28d}) or cover thickness can have a relatively large beneficial effect on corrosion-free lifetime. A change of the standard XD3 limit values, e.g., M_{28d} = 8 instead of $10 \cdot 10^{-12}$ m^2/s, or a minimum cover thickness of 50 instead of 45 mm, can increase the corrosion-free lifetime of reinforced concrete under XD3 exposure by 25 years.

6.2.2 Probabilistic results

The DuraCrete model exists as an probabilistic version, which is, for example, commercially available as the STRUREL software package [STRUREL 2012]. A description of the DuraCrete probabilistic model approach can be found in literature [DuraCrete 2000; Gehlen 2000; STRUREL 2012]. The principle rests on quantifying the failure probability or reliability index on basis on the chloride impact and concrete resistance. According to the Eurocode Standard EN1990:2002 [Eurocode 2002], the reliability index (β) shall not drop below a value of β = 1.5 after a given chloride exposure duration of e.g., 50 or 100 years.

Here we present probabilistic DuraCrete calculations of the so-called reliability index using the STRUREL software under Swiss standard conditions for XD-exposure (Fig. 35). The used input parameters are given in Table 13. Different scenarios have been studied using Duracrete 'default' parameters or others. In all calculations we use a K-value of 0.5 which more or less is also the value obtained for k_e for a temperature of 8°C. The migration coefficient is set to 8.10^{-12} m^2/s, which is the practical value that should be achieved in order to certainly fulfill the Swiss standard requirement of $<10 \cdot 10^{-12}$ m^2/s. For C_{crit} we use the value of 0.35%/m_{cem} as prescribed by a number of national standards (see Table 4). The probabilistic distributions and standard deviations from STRUREL were used.

For the ageing factor we either used the value 0.3, 0.45, und 0.65 (Table 13): For chloride ingress under mist water exposure (XD1) STRUREL recommends to use the ageing factor of 0.65 in combination with a chloride surface concentration of 1 %/m_{cem}. For chloride ingress under spray water exposure (XD3) STRUREL recommends to use the ageing factor of 0.3 in combination with a 'maximum' chloride surface concentration of 2 %/m_{cem} (= 0.3 %/m_{con} for concrete with 350 kg/m^3 cement). In this study we propose to use an ageing factor of 0.45 for XD3 in combination with a C_{s_app} of 0.3 or 0.4 %/m_{con}. It is not clear if the uppermost plates in the Naxberg experiment reaches XD1 conditions or not. If so then the use of XD3-parameters for XD1-exposure is recommended. We use a 'moderate' chloride C_{s_app} of 0.3 %/m_{con} in all calculations, also in combination with the STRUREL ageing factor of 0.65.

The calculated reliability index versus cover thickness for chloride exposure times of 25 (dotted line) and 50 (solid line) years is shown in Fig. 35: The black lines show the predictions for the DuraCrete XD1 ageing factor of 0.65 but with a 'moderate' XD3 surface concentration of 0.3 %/m_{con}. If a DuraCrete XD1 surface concentration of ~0.15 %/m_{con} would have been used instead the calculated reliability index would have been higher. It is thus predicted that for a the standard-required minimum or mean cover thickness of 45 mm (green vertical lines), a life-time of 50 years in XD1 is achieved, but only if the value of $M_{28d} \leq 8 \cdot 10^{-12}$ m^2/s.

Tab.13: *Input parameters and values for the probabilistic predictions using STRUREL for a concrete with a cement content of 350 kg/m³.*

Parameter	Unit	Distribution	Mean value	Standard deviation
$C_s = C_{s\_app}$	%/m_{cem} (%/m_{con})	Log normal	2 (0.3)	1
C_{crit}	%/m_{cem} (%/m_{con})	Beta	0.35 (0.05)	s = 0.15 (a = 0.2, b = 2)
M_{28d}	mm^2/year ($\cdot 10^{-12}$ m^2/s)	Gaussian	250 (8)	50
n	-	Beta	0.3; 0.45; 0.65	s = 0.12; 0.15; 0.15 (a = 0, b = 1)
T	K	Gaussian	281	7
K	-	Constant	0.5	-
t	years	Constant	25, 50	-
d (cover)	mm	Gaussian	10-90	6
∧x	mm	Constant	0	-

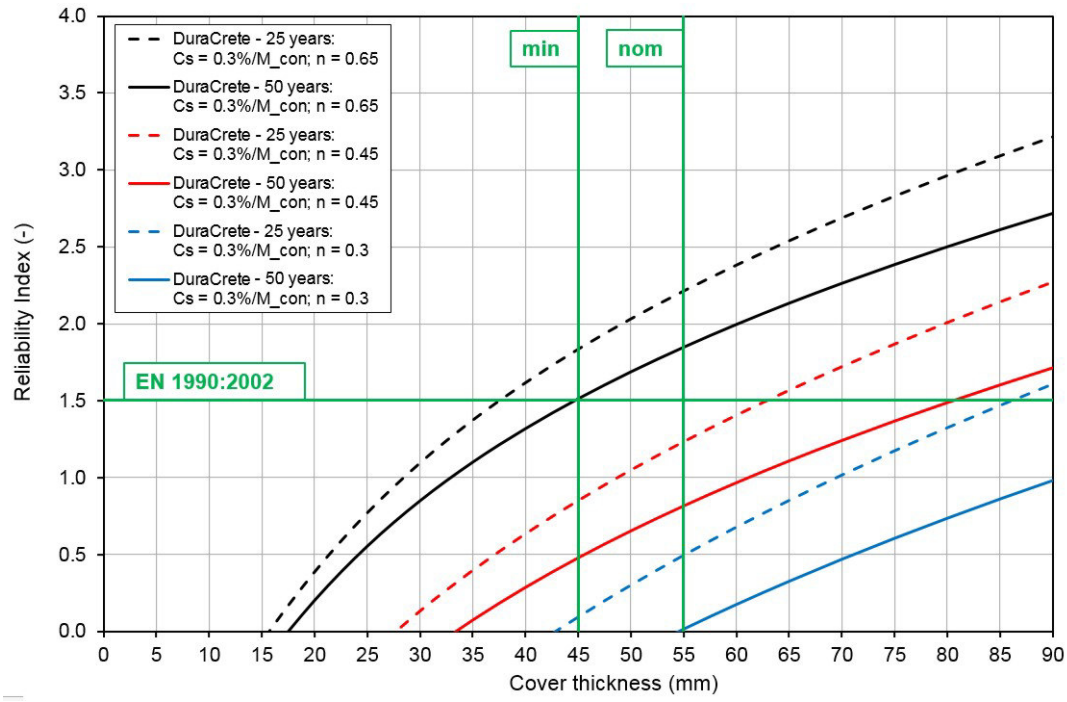

Fig. 35: *DuraCrete probabilistic durability calculations with STRUREL using input parameters as prescribed by Swiss Standard SN EN 206-1 for OPC with migration coefficient of M_{28d} = 8·10^{-12} m^2/s and cement content of 350 kg/m^3 (other parameters as given in Table 13).*

The blue lines show the reliability index (β) vs. cover thickness for the DuraCrete default ageing factor of 0.3 for XD3 (and XS-) exposure. Note that Van der Wegen et al [Wegen 2012] and Kapteina [2011] propose to use the ageing factor of 0.6 for probabilistic DuraCrete modelling under XD3-exposure. It is clear that with an ageing factor of 0.3 the Swiss standard required M_{28d}-value ≤ 10·10^{-12} m^2/s (at least down to a value of 8·10^{-12} m^2/s) would not guarantee a service life of 25 years (with β≥1.5 [Eurocode 2002]).

The red lines show the reliability index vs. cover thickness for the ageing factor of n = 0.45 as proposed in this study. For the given surface concentration of C_{s_app} = 0.3%/m$_{con}$ we also do not maintain Eurocode durability after 25 or 50 years for cover thicknesses <60 mm.

Interestingly, the deterministic output of the DuraCrete model seems to suggest that the Swiss standards guarantee a corrosion-free lifetime of at least 25 years under apparantly the most extreme chloride exposure. The probabilistic version of Duracrete suggests that this is not the case if the Eurocode definition of durability is used. Part of this discrepancy is the result of the probabilistic parameters in the latter model. The Eurocode limit value of β = 1.5 may also be too conservative for chloride-induced corrosion.

6.3 Proposed procedures for making lifetime predictions

6.3.1 Existing concrete structures

Based on the results of this study we propose the following approach for making (remaining) lifetime prediction for existing concrete structures. If the remaining lifetime is lower than the required lifetime of the concrete structure, than these calculations are the basis for a structure monitoring and rehabilitation plan. The more information about the

concrete composition, the current chloride ingress depth, and the cover thickness can be obtained, the more reliable the lifetime prediction potentially can be.

The measurement of preferably more than one chloride profile will be required for obtaining representative D_{app} and C_{s_app}. It should be established as well if there is any spatial variation in the chloride distribution, for example, between vertical and horizontal surfaces or as a function of distance/height from road. Alternatively, a chloride profile from the concrete structure with the highest expected chloride ingress should be collected. Concrete samples can be obtained by powder drilling or by coring and subsequent slicing. The depth intervals should be between 5 and 10 mm, and the total chloride content should be measured, and expressed as a weight fraction of the concrete. When the chloride content is expressed as a weight fraction of the binder, then the relevant model prediction parameters (C_{s_app}, C_{crit}) should also be calculated to %/m_{cem}.

The cover thickness of the existing concrete structure need to be measured, preferably at the location where the chloride profile has been measured (i.e., at the location of the largest expected chloride ingress). If the mean cover thickness at the location of the largest expected chloride ingress is significantly higher than at other chloride-exposed location in the concrete structures, it should be considered to sample the chloride profile at locations with the lowest measured mean cover thickness. The predicted lifetime is thus the remaining lifetime of the part of the concrete structure with highest risk of reinforcement corrosion (the highest chloride ingress or the lowest cover thickness).

Making a lifetime predictions then proceeds according to the following steps:

(I.) A regression of the chloride profile(s) will be carried out as explained in Section 2.1.3 (equation 2) to obtain D_{app} and C_{s_app}.

(II.) The ERFC model as described in Section 5.2 (equation 19) will firstly be used for determining the value of the migration coefficient M_{28d}. If M_{28d} has been measured for the concrete in the structure, or can be precisely estimated from concrete composition, then the ERFC model can instead be used to determine the effective ageing factor of the concrete structure or the correlation factor K.

(III.) For the calculation of M_{28d} the following input parameters are required: (i) the age of the concrete structure, or more precisely the chloride exposure duration; (ii) the value of correlation factor K, which can be taken to be 0.5 if the average annual temperature is in the range of 7-9°C. If the annual concrete temperature is significantly lower/higher a new K-value needs to be determined either by a applying a T-correction (see e.g. [STRUREL 2012] or K can be calculated if all other ERFC input parameters are known; (iii) the ageing factor n = 0.45 can be used for Portland cement or Portland cement with relatively small amounts of mineral additions (<20% slag; <15% FA; or <7% SF) and a w/c-ratio <0.5. For relatively porous concrete (w/c> 0.5), chloride ingress by capillary suction may become important, and as a result the ageing factor may go down as was observed in Naxberg. If such behaviour is expected the n-values given in Table 10 can be used to make conservative lifetime predictions. Alternatively, n can also be calculated using equation 19 if all other input parameters are known.

(IV.) With the determined values of M_{28d}, K and n, the ERFC-model can now be used to make future predictions. Firstly, it has to be decided if the apparent surface concentration (C_{s_app}) is taken as a constant or if the time-dependence as measured for Naxberg is used. If the concrete structure is at least 15 years old, it can perhaps be assumed that the maximum C_{s_app} has already been reached, and the C_{s_app} determined in step I is the future C_{s_app}. For example, in settings similar to the Bonaduz and Boras field experiments, and in the absence of the formation of a mountain-shaped profile, this assumption is reasonable. In settings similar to Naxberg or in the cases of a clear mountain-shaped profile, equation 16 (in Table 6) can be used to determine the future C_{s_app}.

(V) By assuming that C_{crit} = 0.05 %/m_{con} or another value for C_{crit}, the remaining corrosion-free lifetime can now be calculated using equation 18. This equation can be implemented in a spreadsheet such as Excel (see Section 2.1.3). All constant parameters

(M_{28d}, K, n, t_0, and cover thickness x_c) are given the assumed or measured values. The time-dependent parameter D_{app} will be repeatedly calculated at different times by means of trial and error until the D_{app} is obtained that produces the critical chloride profile. The critical chloride profile is the profile that has a chloride content equal to C_{crit} at the mean cover depth x_c. If the surface concentration is also assumed to be time-dependent, then both D_{app} and C_{s_app} need to be calculated for each time until the critical chloride profile is obtained.

6.3.2 New concrete structures

For the case of new, to-be-built concrete structures the aim of lifetime calculation is to adjust the input-parameter (and concrete material or structure design) untill the required lifetime is obtained. For this new structures the lifetime prediction procedure is similar to the one described in Section 6.3.1. The main difference is that the development of the (apparent) chloride surface concentration is not known. The choice of C_{s_app} will have a large effect on the predicted lifetime and therefore it should be chosen conservatively, or based on some type of measurement as explained below.

Making a lifetime predictions then proceeds according to the following steps:

(I) Measurement of the migration coefficient at 28 days age. Considering the relatively large scatter of migration coefficient measurement (see [Dalen 2006] a sufficient number of samples has to be measured to obtain a representative average value for M_{28d}. Alternatively, the diffusion coefficient under non-steady-conditions (D_{nss}) can be measured around the age of 28 days, since the M_{nss} and D_{nss} are approximately similar in value (see Section 2.1.3). According to Swiss standard SN EN 206-1 an M_{28d}-value $<10{\cdot}10^{-12}$ m^2/s is required for exposure classes XD1 and XD3. Practically, this usually means that the mean of M_{28d}-value will be $<8{\cdot}10^{-12}$ m^2/s to guarantee that the standard requirement will be fulfilled.

(II) For correlation factor K a value of 0.5 can be used if the annual temperature is 7-9 °C. If the annual concrete temperature is significantly lower/higher the new K-value needs to be obtained by applying a T-correction [STRUREL 2012].

(III) The ageing factor n = 0.45 can be used for Portland cement or Portland cement with relatively small amounts of mineral additions (<20% slag; <15% FA; or <7% SF) and w/c < 0.5 such that M_{28d} $<10{\cdot}10^{-12}$ m^2/s. For concretes with higher contents of slag or fly ash, literature values such as presented in Table 3 can be used if these are believed to represent long-term field ageing. Some of these n-values are determined in short-term laboratory experiments and should therefore not be used in the proposed ERFC-model. In the absence of knowing reliable field ageing factors for concrete with high contents of slag or fly ash, it is probably best to use a lower (0.45) instead of a higher (0.5-0.8) n-values to make the lifetime prediction conservative.

(IV) The apparent surface concentration (C_{s_app}) can be assumed to follow the trend as measured in the Naxberg experiment (equation 20). As shown in Section 5.4 Naxberg represents a rather extreme case of chloride ingress, which may partly be a result of the relatively high porosity of the concrete (w/c = 0.5) compared to the concretes in the field experiments Bonaduz and Boras. The use of equation 20 could therefore lead to (very) conservative lifetime predictions under potentially extreme chloride ingress. An alternative choice of C_{s_app} is to keep this input parameter constant at 0.3 or 0.4 %/m_{con}, if chloride exposure environments as in Bonaduz or Borås are to be expected. A third possibility is to measure the chloride profile in a similarly exposed old concrete in the proximity of the to-be-built structure, and use the profile to determine C_{s_app} of that concrete by regression. The composition of the old concrete may be such that its C_{s_app} value approximately represents the long-term C_{s_app} of the new, to-be-built structure.

(V) By assuming that C_{crit} = 0.05 %/m_{con} or another value for C_{crit}, the corrosion-free lifetime of a given design can now be calculated using equation 18. Alternatively, the reinforced concrete properties required to achieve a given lifetime can be calculated

using equation 18. This equation can be implemented in a spreadsheet such as Excel (see Section 2.1.3). All constant parameters (M_{28d}, K, n, t_0, and cover thickness x_c) are given the assumed, measured or required values. The time-dependent parameter D_{app} will be repeatedly calculated at different times by means of trial and error until the D_{app} is obtained that produces the critical chloride profile. The critical chloride profile is the profile that has a chloride content equal to C_{crit} at the mean cover depth x_c. If the surface concentration is also assumed to be time-dependent, then both D_{app} and C_{s_app} need to be calculated for each time until the critical chloride profile is obtained.

6.4 Future perspectives

From this study it has become clear that the amount of chlorides reaching the concrete surface (represented by C_{s_app}), the ageing factor (n) and critical chloride content (C_{crit}) have a large effect on predicted lifetime. The reliability of a service lifetime prediction will depend a lot on the choice of these three prediction parameters. It would be highly desirable to get a better insight of how chloride surface concentration of concretes (i.e., C_{s_app}) varies with concrete composition, deicing and traffic intensity, microclimatic setting, and distance/height from road. Such insight could be obtained by a large field study in which chloride profiles in old concrete structures are systematically measured or gathered from existing data.

With regard to ageing factor there still exists some questions about how this values may change if concrete contains high amounts of slag, flay ash, silica fume and limestone filler. This would perhaps require setting up a new long-term field experiments in which the actual field performance of such concretes are systematically tested. Alternatively, it could be investigated how ageing factors determined in short-term laboratory experiments relate to ageing factors determined from long-term field experiments. Ageing factors determined in relatively short-term and water-saturated experiments may primarily reflect changes in chloride transport properties due to ongoing cement hydration, and perhaps minor ageing due to chloride binding. Ageing factors obtained by fitting against long-term field experiments, capture long-term material changes due to cement hydration, chloride binding, carbonation and drying. Moreover, when field data are used to fit a DuraCrete-type equation (eq. 19), the ‘mathematical’ meaning of the ageing factor will differ from the laboratory ageing factors, since part of the correlation between M_{28d} and D_{app} is likely to end up in the ageing factor.

Finally, with regard to critical chloride content there are still questions with regard to how to correctly measure this parameter in the laboratory and how the laboratory values relate to C_{crit} for concretes in the field. Another important issue that has not been adressed in this study, is the effect of cracks on chloride ingress and rebar corrosion such as illustrated in Fig. 1c. Does premature rebar corrosion at local crack sites have a significant effect on overall structure lifetime or not?

List of symbols

Symbol	Meaning
C	Chloride concentration
C_0	Chloride concentration at reference time t_0
C_{crit}	Critical chloride concentration (for reinforcement depassivation in concrete)
C_{max}	Maximum chloride concentration in concrete (as measured)
C_s	Chloride concentration at concrete surface (as measured)
C_{s_app}	Apparent chloride concentration at concrete surface (as obtained by regression)
C_p	C_{s_app} at prediction time t_p (see Table 6)
C_m	C_{s_app} at reference time t_m (for a starting chloride profile at t_m – see Table 6)
D	Diffusion coefficient
D_0	Diffusion coefficient at reference time t_0
D_{app}	Diffusion coefficient obtained by regression of a chloride profile
D_{nss}	Diffusion coefficient measured under non-steady-state conditions
D_{ss}	Diffusion coefficient measured under steady-state conditions
D_p	D_{app} at prediction time t_p (see Table 6)
D_m	D_{app} at reference time t_m (for a starting chloride profile at t_m – see Table 6)
E_a	Activation energy
FA	Fly ash
K	Correlation factor in the DuraCrete ERFC-model
k_1	Subcorrelation factor in the DuraCrete ERFC-model
M	Migration coefficient
M_{28d}	Migration coefficient mesured at an age of 28 days
M_{nss}	Migration coefficient measured under non-steady-state conditions
M_{ss}	Migration coefficient measured under steady-state conditions
n	Ageing factor (= exponent describing time-dependence of D or M)
nss	Non-steady-state
ss	Steady-state
SF	Silica fume
SRPC	Sulfate-resistant Portland cement
t	Time
T	Temperature
x	Distance from concrete surface
XD1-XD3	Chloride exposure classes as defined in [SN EN 262-1]
XS1-XS3	Chloride exposure classes as defined in [SN EN 262-1]

References

ACI 2000	ACI Committee 365 (2000) Service Life Prediction : State of the art report. Manual of Concrete Practice, Part 5. American Concrete Institute, Farmington Hills, MI, USA.
Aldred 2014	J.M. Aldred, A. Castel, Chloride penetration after exposure compared with estimates from service life prediction models. RILEM International workshop on performance-based specification and control of concrete durability, 11 - 13 June 2014, Zagreb, Croatia. Page 143-150.
Andrade 1993	C. Andrade, Calculation of chloride diffusion coefficients in concrete from ionic migration measurements. Cement and Concrete Reseach 23 (1993) 724-742.
Andrade 2004	C. Andrade, C. Alonso, Test methods for on-site corrosion rate measurement of steel reinforcement in concrete by means of the polarization resistance method, RILEM TC 154-EMC "Electrochemical Techniques for Measuring Metallic Corrosion", Recommendations, Materials and Structures, Vol. 37, November 2004, pp 623-643.
Andrade 2011	C. Andrade, M. Castellote, R. d'Andrea, Measurement of ageing effect on chloride diffusion coefficients in cementitious matrices. Journal of Nuclear Materials 412 (2011) 209-216.
Andrade 2015	C. Andrade, M.A. Climent, G. de Vera, Procedure for calculating the chloride diffusion coefficient and surface concentration from a profile having a maximum beyond the concrete surface. Materials and Structures (2015) 48:863–869.
Angst 2009	U.M. Angst, et al, Critical chloride content in reinforced concrete – A review. Cement and Concrete Research 39 (2009) 1122-1138.
Angst 2011a	U.M. Angst, Chloride induced reinforcement corrosion in concrete. Concept of critical chloride content - methods and mechanisms. Doctoral thesis 2011:113. 2011: Norwegian University of Science and Technology.
Angst 2011b	U.M. Angst, et al, Probabilistic considerations on the effect of specimen size on the critical chloride content in reinforced concrete. Corrosion Science 53 (2011a) 177-187.
Angst 2011c	U.M. Angst et al, Chloride induced reinforcement corrosion: Electrochemical monitoring of initiation stage and chloride threshold values. Corrosion Science 53 (2011b) 1451-1464.
Angst 2012	U.M. Angst, et al, Present and future durability challenges for reinforced concrete structures. Materials and Corrosion 63 (2012) 1047-1051.
Angst 2015	U.M. Angst, M. Büchler, J. Schlumpf, B. Marazzani. An organic corrosion-inhibiting admixture for reinforced concrete: 18 years of field experience. Materials and Structures (July 2015) 1-12.
Ann 2007	K. Y. Ann, H.W. Song, Chloride threshold level for corrosion of steel in concrete. Corrosion Science 49 (2007) 4113-4133.
Arya 2014	C. Arya, P. Vasie S. Bioubakhsh, Modeling chloride penetration in concrete subjected to cyclic wetting ans drying. Magazine of Concrete Research V66 (2014) 364-376.
Audenaert 2009	K. Audenaert, G. De Schutter, Influence of time dependency of chloride diffusion coefficient on resulting service life of concrete structures. In : Proceedings of the Int. Symp. On Concrete : 21st century Superhero – Building a sustainable future, fib and UK Concrete Society, June 2009, London.
Bažant 1979	Z.P. Bazant. Physical model for steel corrosion in concrete sea structures – Theory. Journal of the Structural Division (June 1979) 1137-1166.
Berke 1990	Corrosion Rates of Steel in Concrete, ASTM STP 1065, Eds.: N.S. Berke, V. Chaker and D. Whiting, American Society for Testing and Materials, Philadelphia, 1990.
Bermudez 2010	M.A., Bermudez, P. Alaejos, Models for chloride diffusion coefficient of concretes in tidal zone. ACI Materials Journal 107 (2010) 3-11.
Bertolini 2013	L. Bertolini, B. Elsener, P. Pedeferri, E. Redaelli, R. Polder. Corrosion of Steel in Concrete: Prevention, Diagnosis, Repair, 2nd edition, Wiley-VCH Verlag, Weinheim, Germany, 2013.
Böhni 2005	H. Böhni, Corrosion of reinforced concrete structures, Woodhead Publishing Ltd., Abington, Cambridge, UK, 2005
Breit 1997	W. Breit, Critical chloride content – Part 1: General. Institüt für Bauforschung Aachen – Kurzbericht 68 (1997) p1-2.
Breit 2001	W. Breit, Critical corrosion inducing chloride content - State of the art and new investigation results, Betontechnische Berichte 1998–2000, Verein Deutscher Zementwerke e.V. Verlag Bau+Technik, Düsseldorf (2001) 145-167.
Broomfield 2007	J.P. Broomfield, Corrosion of steel in concrete – Understanding, investigation and repair, 2nd edition, Taylor and Francis, London, 2007
Castellote 2001	M. Castellote, C. Andrade, C. Alonso, Measurement of the steady and non-steady-state chloride diffusion coefficients in a migration test by means of monitoring the conductivity in the anolyte chamber. Comparison with natural diffusion tests. Cement and Concrete Research 31 (2001) 1411-1420.
Castellote 2006	M. Castellote, C. Andrade, Round-Robin Test on methods for determining chloride transport parameters in concrete. Materials and Structures 39 (2006) 955-990.
Chalee 2008	W. Chalee, C. Jaturapitakkul, Effects of W/B ratios and fly ash finenesses on chloride diffusion coefficient of concrete in marine environment. Materials and Structures 42 (2008) 505-514.
CEN/EN 12390	CEN/EN 12390-11:2013. Testing hardened concrete – Determination of the chloride resistance of concrete, unidirectional diffusion.

Climent 2002	M.A. Climent et al, A test method for measuring chloride diffusion coefficients through nonsaturated concrete. Part I. The instantanous plane source diffusion case. Cement and Concrete Research 32 (2002) 1113-1123.
Collepardi 1970	M. Collepardi, A. Marcialis, R. Turriziani. The kinetics of chloride ion penetration in concrete (in Italian). Il Cemento Vol. 67 (1970) 157-164.
Conciatori 2008	D. Conciatori, H. Sadouki, E. Brühwiler, Capillary suction and diffusion model for chloride ingress into concrete. Cement and Concrete Research 38 (2008) 1401-1408.
Conciatori 2010	D. Conciatori, F. Laferriere, E. Brühwiler, Comprehensive modelling of chloride ion and water ingress into concrete considering thermal and carbonation state for real climate. Cement and Concrete Research 40 (2010) 109-118.
Conciatori 2015	D. Conciatori, E Gregoire, E. Samson, J. Marchand, L. Chouinard, Sensitivity of chloride ingress modelling in concrete to input parameter variability. Materials and Structures (2015) 48:3023–3036.
Costa 1999	A. Costa, J. Appleton. Chloride penetration into concrete in marine environment – Part II : Prediction of long term chloride penetration. Materials and Structures 32 (1999) 354-359.
Dalen 2006	S.M. Dalen, W.J. Bouwmeester, E.A.B. Koenders, M.R. de Rooij, An experimental evaluation of the RCM-method. In : Proceedings of the 2nd fib-International Congress (2006) Naples, Italy.
Delagrave 1996	A. Delagrave, J. Marchand, E. Samson, Prediction of diffusion coefficients in cement-based materials on the basis of migration experiments. Cement and Concrete Research 26 (1996) 1831-1842.
Denarie 2003	E. Denarie, D. Conciatori, E. Brühwiler, Effect of microclimate on chloride penetration into refeinforced concrete. In V.M. Malhotra (ed.) SP-212 6th CANMET/ACI International Conference on Durability of Concrete, Thessaloniki Greece 2003.
De Rooij 2006	M.R. de Rooij, K. van Breugel, R.B. Polder, Remaining service-life predictions : Experiences of Dutch investigation. In: Concrete Repair, Rehabilitation and Reftrofitting – Alexander (ed.). Taylor and Francis Group, London (2006) ISBN 0 415 39654 9.
De Vera 2007	G. de Vera et al, A test method for measuring chloride diffusion coefficients through partially saturated concrete. Part II: The instantaneous plane source diffusion case with chloride binding consideration. Cement and Concrete Research 37 (2007) 714–724.
Eurocode 2002	EN 1990:2002 Eurocode - Basis of structural design.
DuraCrete 2000	DuraCrete R17, DuraCrete Final Technical Report, The European Union – Brite EuRam III, DuraCrete – Probabilistic Performance based Durability Design of Concrete Structures. Document BE95-1347/R17, May 2000; CUR, Gouda, The Netherlands.
Gang 2015	X. Gang, L. Yun-pan, S. Yi-Biao, X. Ke. Chloride ion transport mechanism in concrete due to wetting and drying cycles. Structural Concrete (2015) 289-296.
Gehlen 2000	C. Gehlen, Probabilistische Lebendauerbemessung von Stahlbetonbauwerken – Zuverläsigkeitsbetrachtungen zur wirksamen Vermeidung von Bewehrungskorrosion. Schriftenreihe des Deutschen Ausschusses für Stahlbeton, Heft 519. Beuth-Verlag, Berlin (2000).
Geiker 2007	M. Geiker, E.P. Nielsen, D. Herfort, Prediction of chloride ingress and binding in cement paste. Material and Structures 40 (2007) 405-417.
Goltermann 2004	P. Goltermann, Variation of chloride profiles in homogeneous area. Materials and Structures 37 (2004) 608-614.
Guimarães 2011	A.T.C. Guimarães, et al, Determination of chloride diffusivity through partially saturated Portland cement concrete by a simplified procedure. Construction and Building Materials 25 (2011) 785–790.
Hansson 1990	C.M. Hansson, B. Sørensen. The threshold concentration of chloride in concrete for the initiation of reinforcement corrosion. Philadelphia: American Society for Testing Materials. ASTM 1065, 1990. In: Corrosion rates of steel in concrete (Berke et al, ed.) p. 3-16.
Helland 2010	S. Helland, R. Aarstein, M. In-field performance of North Sea offshore platformas with regard to chloride resistance. Structural Concrete 11 (2010) 15–24.
Hunkeler 1996	F. Hunkeler, The resistivity of pore water solution – a decisive parameter of rebar corrosion and repair methods, Construction and Building Materials, Vol. 10, No. 5, 1996, p. 381-399.
Hunkeler 2002	F. Hunkeler, H. Ungricht, C. Merz, Vergleichende Untersuchungen zum Chloridwiderstand von Betonen. Forschungsauftrag AGB 1998/097 (82/98) auf Antrag der Arbeitsgruppe Brückenforschung (AGB). ASTRA-report 568 (2002).
Hunkeler 2005	F. Hunkeler, Corrosion in reinforced concrete structures: Processes and mechanism in: Corrosion in concrete structures, Ed. H. Böhni, Woodhead Publishing Ltd., Abington, Cambridge, UK, 2005, p. 1-45.
Hunkeler 2006	F. Hunkeler, B. Mühlan, H. Ungricht, Risiko von Betonabplatzungen infolge Bewehrungskorrosion, UVEK/ASTRA, AGB 2002/015, Bericht VSS Nr. 603, Oktober 2006.
Hornbostel 2013	K. Hornbostel, C.K. Larsen, M.R. Geiker, Relationship between concrete resistivity and corrosion rate - A literature review. Cement and Concrete Composites, 2013. 39: p. 60-72.
Kapteina 2011	G. Kapteina, Modell zur Beschreibung des Eindringens von Chlorid in Beton von Verkehrsbauwerken. Dissertation Technische Universität München (2011).
Kopecsko 2009	K. Kopecsko, Effect of slag content of cements on chloride ion binding. In : Proceedings of the Int. Symp. On Concrete : 21st century Superhero – Building a sustainable future, fib and UK Concrete Society, June 2009, London.
Langford 1987	P. Langford, J. Broomfield, Monitoring the Corrosion of Reinforcing Steel, Construction Repair, 1, 1987, Nr. 2, S. 32-36.
Lay 2006	S. Lay, Abschätzung der Wahrscheinlichkeit tausalzinduzierter Bewehrungskorrosion. Dissertation Technische Universität München (2006).

Lindvall 2001	A. Lindvall, L-O Nilsson, Studies on the effect of secondary cementitious materials on chloride ingress. In : Proceedings of Workshop on durability of exposed concrete containing secondary cementitious Materials. November 2001, Hirtshals, Denmark, The Nordic Concrete Federation. 159-178.
Lindvall 2007	A. Lindvall, Chloride ingress data from field and laboratory exposure – Influence of salinity and temperature. Cement and Concrete Composites 29 (2007) 88-93.
Loser 2010	R. Loser, B. Lothenbach, A. Leemann, M. Tuchschmid, Chloride resistance of concrete and ist binding capacity – Comparison between experimental results and thermodynamic modeling. Cement and Concrete Composites 32 (2010) 34-42.
Life-365 2013	Life-365: Service life prediction model and computer program for predicting the service life and life cycle consts of reinforced concrete exposed to chlorides (http://www.life-365.org/consortium.html).
Liu 1998	Y. Liu, R.E. Wyers, Modelling the time-to-corrosion cracking in chloride contami-nated reinforced concrete structures, ACI Materials Journal, November-December 1998, p. 675-681.
Maes 2013	M. Maes, E. Gruyaert, N. de Belie. Resistance of concrete with blast-furnace slag against chlorides, investigated by comparing chloride profiles after migration and diffusion. Materials and Structures 46 (2013) 89-103.
Maheswaran 2004	T. Maheswaran, J.G., Sanjayan, A semi-closed-form solution for chloride diffusion in concrete with time-varying parameters. Magazine of Concrete Research 56 (2004) 359-366.
Marchand 2009	J. Marchand, E. Samson, Predicting the service-life of concrete structures – Limitations of simplified models. Cement and Concrete Composites 31 (2009) 515-521.
Meijers 2005	S.J.H. Meijers, J.M.J.M. Bijen, R. de Borst; A.A. Fraaij, Computational results of a model for chloride ingress in concrete including capillary suction, drying-wetting cycles-and carbonation. Materials and Structures 38 (2005) 145-154.
Nanukuttan 2006	S.V. Nanukuttan, P.A.M. Basheer, D.J. Robinson, W.J. McCarter. Effect of duration and conditions of exposure on chloride diffusion. In: Concrete Repair, Rehabilitation and Reftrofitting – Alexander (ed.). Taylor and Francis Group, London (2006) ISBN 0 415 39654 9.
Nguyen 2009	T.S. Nguyen, S. Lorente, M. Carcasses, Effect of the environment temperature on the chloride diffusion through CEM-I and CEM-V mortars: An experimental study. Construction and Building Materials 23 (2009) 795–803.
Nielsen 2011	E. P. Nielsen, M.R. Geiker, Chloride diffusion in partially saturated cementitious material. Cement and Concrete Research 33 (2003) 133-138.
Nilsson 2011	L-O Nilsson and J.M. Frederiksen (2011): On uncertainties and inaccuracies in empirical chloride ingress modelling, European Journal of Environmental and Civil Engineering, 15:7, 981-990.
Nokken 2006	M. Nokken, A. Boddy, R.D. Hooton, M.D.A. Thomas. Time dependent diffusion in concrete – three laboratory studies. Cement and Concrete Research 36 (2006) 200-207.
Nygaard 2005	P.V. Nygaard, M.R. Geiker, A method for measuring the chloride threshold level required to initiate reinforcement corrosion in concrete. Materials and Structures 38 (2005) 489-494
Oh 2003	B.H. Oh, B.S. Jang. Chloride diffusion analysis of concrete structures considering effect of reinforcements. ACI Materials Journal 100 (2003) 143-149.
Olsson 2013	N. Olsson, V. Baroghel-Bouny, L-Ol Nilsson, M. Thiery, Non-saturated ion diffusion in concrete – A new approach to evaluate conductivity measurements. Cement and Concrete Composites 40 (2013) 40–47.
Oslakovic 2010	I.S. Oslakovic, D. Bjegovic, D., Mikulic., Evaluation of service life design models on concrete structures exposed to marine environment. Materials and Structures 43 (2010) 1397-1412.
Page 1982	C.L. Page, K.W.J. Treadaway, Aspects of the electrochemilry of steel in concrete, Nature, Vol. 297 (1982), May, p.109-115.
Petterson 1993	K. Petterson, The chloride threshold value and the corrosion rate in reinforced mortar specimens. Götenborg: Chalmers University of Technology 1993. Publ. Nr. P-93:1. In: Chloride penetration into concrete structures: Nordic Mini-seminar, January 1993, 338-348.
Phurkhao 2005	P. Phurkhao, M.K., Kassir. Note on chloride-induced corrosion of reinforced concrete bridge deckes. Journal of Engineering Mechanics 131 (2005) 97-99.
Poulsen 2006	E. Poulsen, L. Mejlbro., Diffusion of chloride in concrete : Theory and application. Taylor and Francis London, UK (2006).
Rahimi 2014	A. Rahimi, C. Gehlen, T. Reschke, A. Westendarp, Approaches for modelling the residual service life of marine concrete structures. International Journal of Corrosion, Volume 2014, Article ID 432472. 11 pages.
Raupach 2007	M. Raupach, B. Elsener, B., R. Polder, J. Mietz, Corrosion of Reinforcement in Concrete – Mechanisms, Monitoring, Inhibitors and Rehabilitation Techniques, European Federation of Corrosion Publications Nr. 38, Woodhead Publishing Limited, Cambridge anc CRC Press LLC, 2007.
Sandberg 1998	P. Sandberg, L. Tang, A. Andersen, Recurrent studies of chloride ingress in uncracked marine concrete at various exposure times and elevations. Cement and Concrete Research, Vol. 28, No. 10, pp. 1489–1503, 1998.
Schiegg 2002	Y. Schiegg, H. Böhni, F. Hunkeler, Online-Monitoring of corrosion in reinforced concrete structures, Proc. 1st fib congress, Osaka, Session 15, Monitoring, October 13–19, 2002, pp. 49-58.

Schiegg 2014	Y. Schiegg, H. Ungricht, F. Hunkeler, Massnahmen zur Erhöhung der Dauerhaftigkeit – Fortsetzung des Feldversuches im Naxbergtunnel. In: Neues aus der Brückenfor-schung, SIA Dokumentation D 0247.
Schiessl 1988	Corrosion of Steel in Concrete, Report of the RILEM Technical Committee 60-CSC, Ed.: P. Schiessl, Chapman and Hall, London, 1988.
Siegwart 2003	M. Siegwart, J.F. Lyness, W. Cousins, Advanced analysis of published data on chloride binding in concrete. Magazine of Concrete Research 55 (2003) 41-52.
Sifeng 2012	L. Sifeng, The expression of surface chloride concentration in ecological concrete and serice life prediction. Advanced Materials Research V368-373 (2012) 2204-2210.
Sika/SGK 2013	Jürg Schlumpf, Sika Services AG, Langzeitversuch Sika FerroGard (Bonaduz); Ueli M. Angst, SGK, Zwischenbericht 2013
Skoglund 2008	P. Skoglund, J. Silfwerbrand, J. Holmgren, J. Trägardh, Chloride redistribution and reinforcement corrosion in the interfacial region between substrate and repair concrete – a laboratory study. Materials and Structures 41 (2008) 1001-1014.
Sleiman 2012	H. Sleiman, et al, Chloride transport through unsaturated concrete: chloride profile simulations and experimental validation. Magazine of Concrete Research 64 (2012) 351-359.
SN EN 14629	Swiss Standard SN EN 14629:2007: Produkte und Systeme für den Schutz und die Instandsetzung von Betontragwerken - Prüfverfahren - Bestimmung des Chloridgehaltes von Festbeton.
SN EN 196-1	Swiss Standard SN EN 196-1:2005: Prüfverfahren für Zement - Teil 1: Bestimmung der Festigkeit.
SN EN 480-14	Swiss Standard SN EN 480-14:2006: Zusatzmittel für Beton, Mörtel und Einpressmörtel - Prüfverfahren - Teil 14: Bestimmung des Korrosionsverhaltens von Stahl in Beton - Elektrochemische Prüfung bei gleichbleibendem Potential.
SN EN 206-1	Swiss Standard SN EN 206-1:2000 Beton - Teil 1: Festlegung, Eigenschaften, Herstellung und Konformität.
SIA 262	Swiss Standard SIA 262:2013 Betonbau.
SIA 262/1	Swiss Standard SIA 262/1:2013 Betonbau – Ergänzende Festlegungen. Anhang B: Chloridwiderstand.
Spiesz 2013	P. Spiesz, H.J.H. Brouwers, The apparant and effective chloride migration coefficients obtained in migration tests. Cement and Concrete Research 48 (2013) 116-127.
Stanish 2003	K. Stanish, M. Thomas, The use of bulk diffusion tests to establish time-dependent concrete chloride diffusion coefficients. Cement and Concrete research 33 (2003) 55-62.
Stewart 1998	M.G. Stewart, D.V. Rosowsky, Time-dependet reliability of deteriorating reinforced concrete bridge decks. Structural Safety 20 (1998) 91-109.
STRUREL 2012	STRUREL (2012). Handbuch Durchführung einer Lebensdauermessung mit dem Programmpaket STRUREL (12/074/1.1.1).
Sumranwanich 2004	T. Sumranwanich, S. Tangtermsirikul, A model for predicting time-dependent chloride binding capacity of cement-fly ash cementitious system. Materials and Structures 37 (2004) 387-396.
Tang 1992	L. Tang, L.O. Nilsson: Rapid determination of chloride diffusivity in concreteby applying an electrical field. ACI Materials Journal, Vol. 98, (1992) 49-53.
Tang 1996	L. Tang, Electrically accelerated methods for determining chloride diffusivity in concrete – current development. Magazine of Concrete Research 48 (1996) 173-179.
Tang 1999	L. Tang, Concentration dependence of diffusion and migration of chloride ion. Part 2. Experimental evaluations. Cement and Concrete Research 29 (1999) 1469-1474.
Tang 2005	L. Tang. (2005) Guidline for practical use of methods of testing the resistance of concrete to chloride ingress. Final report of EU-funded research project 'CHLORTEST', Resistance of concrete to chloride ingress.
Tang 2007	L. Tang, P. Utgenannt (2007), Chloride ingress and reinforcement corrosion in concrete under de-icing highway environment – A study after 10 years' field exposure. SP Report 2007: 76.
Tang 2010	L. Tang, et al (2010). Validation of models and test methods for assessment of durability of concrete structures in the road environment. CBI Betonginstitutet report.
Tong 2001	L. Tong, O.E. Gjørv, Chloride diffusivity based on migration testing. Cement and Concrete Research 31 (2001) 973–982.
Truc 2000	O. Truc, J.P. Ollivier, M. Carcassès. A new way for determining the chloride diffusion coefficient in concrete from steady state migration test. Cement and Concrete Research 30 (2000) 217–226.
Tuutti 1982	K. Tuutti, Corrosion of steel in concrete. 1982, Swedish Cement and Concrete Research Institute: Stockholm.
Uji 1990	K. Uji, Y. Matsuoka, T. Maruya. Formulation of an equation for surface chloride content of concrete due to permeation of chloride. Proceedings of 3rd Int. Symp. On Corrosion of Reinforced Concrete, Wishaw, UK (1990) 258-267.
Ungricht 2004	H. Ungricht, Wasserhaushalt und Chlorideintrag in Beton – Einfluss der Exposition und der Betonzusammensetzung. Dissertation Eidgenössischen Technischen Hochschule Zürich (2004).
Ungricht 2006	H. Ungrich, F. Hunkeler, H. Böhni, Water and chloride penetration into concrete – Influence of exposure conditions and concrete quality. In: Proceedings of the 2nd fib-International Congress (2006) Naples, Italy.
Ungricht 2007	H. Ungrich, F. Hunkeler, Instandsetzung von Galerien - Wirkung und Wirksamkeit der ergriffen Massnahmen. ASTRA-Bericht 610 (February 2007).
Ungricht 2008	H. Ungrich, F. Hunkeler, Massnahmen gegen chloridinduzierte Korrosion und zur Erhöhung der Dauerhaftigkeit. ASTRA-Bericht 628 (May 2008).

Vogel 2005	T. Vogel et al (2005) Sicherheit des Verkehrssystems Strasse und dessen Kunstbauten. Teilprojekt AGB 2005/107: Tragsicherheit der bestehenden Kunstbauten. ASTRA-Bericht Nr. 623.
Wegen 2012	G. van der Wegen, R.B. Polder, K. van Breugel, Guideline for service life design of structural concrete - A performance based approach with regard to chloride induced corrosion. HERON 57 (3) (2012) 153-168.
Weng 2012	S-H Weng, C-C Yang, S-W Cho, K-C Yang, The study if chloride ion transport behaviour of mortar under different storing environment temperatures. Journal of Marine Science and Technology 20 (2012) 290-294.
Yang 2002	C.C. Yang, S.W. ChoR. Huang, The relationship between charge passed and the chloride-ion concentration in concrete using steady-state chloride migration test. Cement and Concrete Research 32 (2002) 217–222.
Yang 2009	C.C. Yang, C.H. Liang, The influence of medium–high temperature on the transport properties of concrete by using accelerated chloride migration test. Materials Chemistry and Physics 114 (2009) 670–675.
Yu 2011	H. Yu et al. Effects of concrete mix on initiation of reinforcement corrosion and chloride threshold level. Transportation Research Record: Journal of the Transportation Research Board V2220 (2011) 75-81.
Yuan 2006	Q. Yuan, C. Shi, G. De Schutter, K. Audenaert, Effect of temperature on transport of chloride ions in concrete. In: Concrete Repair, Rehabilitation and Reftrofitting – Alexander (ed.). Taylor and Francis Group, London (2006) ISBN 0 415 39654 9.
Yuan 2009	Q. Yuan et al, Chloride binding of cement-based materials subjected to external chloride environment – A review. Construction and Building Materials 23 (2009) 1-13.
Zhang 2005	T. Zhang, O.E. Gjorv, Effect of chloride source concentration on chloride diffusivity in concrete. ACI Materials Journal 102 (2005) 295-298.
Zheng 2010	J.J. Zheng, X.Z. Zhou, Z.M. Wu. A simple method for predicting the chloride diffusivity of cement paste. Materials and Structures 43 (2010) 99-106.

Aknowledgements

The critical reviews by Dr. Ueli Angst (SGK/ETH) and Dr. Pietro Lura (EMPA/ETH) are highly appreciated and led to significant improvements of this ASTRA-report.

Projektabschluss

Schweizerische Eidgenossenschaft
Confédération suisse
Confederazione Svizzera
Confederaziun svizra

Eidgenössisches Departement für
Umwelt, Verkehr, Energie und Kommunikation UVEK
Bundesamt für Strassen ASTRA

FORSCHUNG IM STRASSENWESEN DES UVEK

Version vom 09.10.2013

Formular Nr. 3: Projektabschluss

erstellt / geändert am: 03.12.2015

Grunddaten

Projekt-Nr.:	AGB 2011/002
Projekttitel:	Modellierung der Initiierung von Korrosion bei chloridbelasteten Stahlbetonbauten
Enddatum:	31.12.2013

Texte

Zusammenfassung der Projektresultate:

Die vorliegende Forschungsarbeit zeigt, wie langfristige Feldversuche genutzt werden können, um den Chlorideintrag in Betonbauteile zu modellieren und Lebensdauermodelle für die Korrosionsinitiierung zu validieren bzw. zu verbessern. Mit der Analyse der 65 gemessenen Chloridprofile aus dem Feldversuch im Naxbergtunnel konnten die Chlorideinträge für verschiedene Betonsorten und weitere Parameter mit Hilfe eines Diffusionsmodells (DuraCrete-Modell) berechnet bzw. prognostiziert werden. Die Daten vom Naxbergtunnel zeigen aber auch, dass Effekte wie starkes kapillares Saugen die generellen Trends beeinflussen und die Voraussagemöglichkeiten einschränken. Der DuraCrete Ansatz wird als Prognose Tool vorgeschlagen, da er problemlos in ein Tabellenkalkulationsprogramm wie z.B. Microsoft Excel implementiert werden kann und demzufolge für Ingenieure einfach verfügbar ist. Zudem hat das Modell den Migrationskoeffizienten als Inputgrösse, der als Parameter in den Schweizer Normen festgelegt ist. Das DuraCrete-Modell wurde in dieser Studie modifiziert und anhand der Ergebnisse von verschiedenen, langfristigen Feldversuchen validiert. Die untersuchten Betonsorten enthalten relativ kleine Mengen (<20%) an Zusatzstoffen (Hüttensand, Flugasche, und Silikastaub) und zeigen keine grossen Unterschiede beim Chlorideintrag. Weitere Untersuchungen sind nötig, um festzustellen, wie der Alterungskoeffizient (ageing factor) durch die Art und Menge des Zusatzstoffes bei einer Expositionsklasse XD3 beeinflusst wird. Es wird vorgeschlagen, für Betone mit CEM I und einer geringen Menge an Zusatzstoffen vorläufig einen universellen Alterungskoeffizienten von 0.45 zu verwenden. Mittels probabilistischer Lebensdauerberechnung wird mit dem DuraCrete-Modell der Zuverlässigkeitsindex für unterschiedliche Bewehrungsüberdeckungen berechnet. Es zeigt sich, dass der in der Schweizer Norm geforderte Grenzwert für den Migrationskoeffizienten für eine lange Nutzungsdauer (> 50 Jahre) unter Umständen keine ausreichende Dauerhaftigkeit garantiert. Weiter wird im Bericht eine neue Methode zur Bestimmung des kritischen Chloridgehaltes für das Auslösen von Lochkorrosion am Betonstahl vorgestellt, die auf Diffusion einer chloridhaltigen Lösung in Mörtelprüfkörpern basiert. Die Ergebnisse zeigen höhere kritische Chloridgehalte, als es der gängigen Praxis entspricht. Grund dürfte die nahezu spaltfreie Umhüllung des Betonstahls mit feinkörniger Mörtelmatrix sein, was bei einem Beton mit Grösstkorn 32 mm nie der Fall sein wird.

Schweizerische Eidgenossenschaft
Confédération suisse
Confederazione Svizzera
Confederaziun svizra

Eidgenössisches Departement für
Umwelt, Verkehr, Energie und Kommunikation UVEK
Bundesamt für Strassen ASTRA

Zielerreichung:

Ziel des Forschungsprojektes war die Schaffung eines anwendungsorientierten Ingenieurmodells, das eine realistische Prognose der Initiierung von Korrosion bei chloridbelasteten Betonbauten ermöglicht. Im Vordergrund stand damit auch das Erarbeiten der erforderlichen Inputgrössen für das vorgeschlagende Modell.
In diesem Forschungsprojekt wurde kein komplett neues Modell entwickelt. Bestehende Modelle wurden kritisch bewertet und folglich wurde der DuraCrete-Ansatz als grundsätzlich geeignet beurteilt. Anhand der Ergebnisse von langfristigen Feldversuchen wurden die Inputparameter für das DuraCrete-Modell festgelegt. Zudem wurde eine neue Methode für die Bestimmung des kritischen Chloridgehaltes für Lochkorrosion, der für die Prognose der Initiierung von Korrosion benötigt wird, entwickelt und erfolgreich geprüft.

Folgerungen und Empfehlungen:

Der DuraCrete-Ansatz eignet sich als Prognosemodell vor allem für relativ dichte Betone, d.h. Betonqualitäten, die für ausreichende Beständigkeit bei der Expositionsklasse XD3 erforderlich sind. In Fällen, wo Transportprozesse hauptsächlich durch kapillares Saugen bestimmt sind (z.B. bei porösen Betonen), ist die Anwendung des DuraCrete-Modells weniger zuverlässig, da die Effekte vom kapillaren Saugen auf den Alterungskoeffizienten (noch) nicht zuverlässig quantifizierbar bzw. prognostizierbar sind.

Das etablierte Modell wurde auch benutzt, um die Normvorgaben für XD3 zu prüfen. Diese Untersuchung hat gezeigt, dass eine geringe Erhöhung der Bewehrungsüberdeckung (von 5 mm) oder eine geringfügige Verringerung des Migrationskoeffizienten die üblicherweise geforderte Dauerhaftigkeit zuverlässiger garantieren würde.

Publikationen:

Vortrag 'Chloride transport in concrete: Long-term field experiments and DuraCrete modelling'. Holcim-Seminar über: Performance Based Specifications of Concrete, worldwide. Status and forecast. Holderbank, 30/11 & 01/12/2015

Vortrag 'Chloride transport in concrete: Long-term field experiments and DuraCrete modelling', ETH-IfB seminar (Prof. R. Flatt), ETH-Zürich, 09/12/2015

Vortrag 'Sind die Bestimmungen der SIA 262 bei chloridinduzierter Korrosion ausreichend? Folgerungen aus einem Forschungsprojekt' 13. Betonkolloquium TFB, Wildegg, 04/05/2016

Eine Publikation in einer englischsprachigen Fachzeitschrift (peer review paper) ist für 2016 geplant

Der Projektleiter/die Projektleiterin:

Name: Schiegg Vorname: Yves

Amt, Firma, Institut: TFB AG, Wildegg

Unterschrift des Projektleiters/der Projektleiterin:

Schweizerische Eidgenossenschaft
Confédération suisse
Confederazione Svizzera
Confederaziun svizra

Eidgenössisches Departement für
Umwelt, Verkehr, Energie und Kommunikation UVEK
Bundesamt für Strassen ASTRA

FORSCHUNG IM STRASSENWESEN DES UVEK

Formular Nr. 3: Projektabschluss

Beurteilung der Begleitkommission:

Beurteilung:

Die Zielsetzungen dieses Forschungsprojektes wurden erfüllt. Die erforderlichen Inputgrössen für eine realistische Modellierung des Schadstoffeintrags konnten identifiziert werden. Durch die Verwendung des bekannten und breit akzeptierten DuraCrete-Modells konnte ein anwendungsorientiertes Ingenieurmodell, das die Realität gut abbildet, entwickelt werden. Die neue Prüfmethode zur Bestimmung des kritischen Chloridgehaltes für verschiedene Betonzusammensetzungen sind vielversprechend. Es braucht aber noch mehr systematische Untersuchungen. Durch die Anwendung eines probabilistischen Ansatzes zur Berechnung der Initiierungszeit (Zuverlässigkeitsindex), der die zeitliche Variabilität der Inputgrössen berücksichtigt, wird ein möglicher Weg zur Bemessung der Dauerhaftigkeit von Betonbauteilen aufgezeigt.

Umsetzung:

Mit den Erkenntnissen dieser Forschungsarbeit und der Entwicklung eines anwendungsorientierten Ingenieurmodells kann der zukünftige Chlorideintrag bei bestehenden Bauteilen relativ genau abgeschätzt werden. Die wenigen erforderlichen Inputgrössen können mit geringem Aufwand ermittelt werden. Auch sind keine komplizierten Modellberechnungen mit Spezialsoftware (z.B. Finite-Element-Programmen) notwendig. Der Bericht enthält ein Kapitel (6.3) mit klaren Richtlinien und genauer Vorgehensweise für die Ausführung einer Lebensdauerberechnung in Excel für bestehende Bauwerke oder Neubauten.

weitergehender Forschungsbedarf:

- Chlorideintrag, Initiierung und Modellierung für heutige Betone mit reduziertem CEM I Gehalt und XD3 Bedingungen
- Bestimmung des Alterungskoeffizienten (ageing factor) von heutigen Betonen mit grösseren Mengen an Zusatzstoffen wie Flugasche, Silikastaub oder Hüttensand
- Chlorid-Oberflächenkonzentrationen in Abhängigkeit der Exposition und der Betonzusammensetzung

Einfluss auf Normenwerk:

Grenzwert für den Chloridwiderstand, Norm SIA 262/1
Bewehrungsüberdeckung, Tabelle 18 der Norm SIA 262

Der Präsident/die Präsidentin der Begleitkommission:

Name: Käser Vorname: Martin

Amt, Firma, Institut: Baudirektion Kt. Zürich

Unterschrift des Präsidenten/der Präsidentin der Begleitkommission:

M. Käs

Verzeichnis der Berichte der Forschung im Strassenwesen

Bericht-Nr.	Projekt Nr.	Titel	Jahr
1522	VSS 2011/106	Normierte gesamtverkehrliche Erschliessungsqualitäten - Grundlagenbericht	2015
1520	ASTRA 2008/013_OBF	Nächtliche Immissionsprognosen von Strassenlärm (Hochleistungsstrassen)	2015
1519	VSS 2009/201	Lärmimmissionen bei Knoten und Kreiseln	2015
1518	SVI 2011/024	Langsamverkehrsfreundliche Lichtsignalanlagen	2015
1517	VSS 2011/103	Bemessungsverkehrsstärken: Ein neuer Ansatz	2015
1516	VSS 2011/711	Forschungspaket Nutzensteigerung für die Anwender des SIS: EP1: Zeitaspekte und Historisierung	2015
1514	VSS 2006/513_OBF	Forschungspaket Brückenabdichtungen: EP3 - Langzeitverhalten des Verbundes	2015
1513	VSS 2005/403	Fliesskoeffizienten von feinen Gesteinskörnungen	2015
1512	SVI 2004/069	Veloverkehr in den Agglomerationen - Einflussfaktoren, Massnahmen und Potenziale	2015
1511	VSS 2012/601	Die Physik zwischen Salz, Schnee und Reifen	2015
1510	VSS 2005/453	Forschungspaket Recycling von Ausbauasphalt in Heissmischgut: EP2: Mehrfachrecycling von Strassenbelägen	2015
1509	ASTRA 2010/022	Markt- und Nutzermonitoring Elektromobilität (MANUEL)	2015
1508	VSS 2011/716	Forschungspaket Nutzensteigerung für die Anwender des SIS: EP6: Schnittstellen aus den Auswertungssystemen SIS (SIS-DWH)	2015
1507	FGU 2007/004	TBM Tunneling in Faulted and Folded Rocks	2015
1506	VSS 2006/512_OBF	Forschungspaket Brückenabdichtungen: EP2 - Flüssigkunststoff-Abdichtungen, Erfassen der Verbundproblematik	2015
1505	VSS 2006/509	Abdichtungssysteme und bitumenhaltige Schichten auf Betonbrücken - Initialprojekt	2014
1504	VSS 2005/504	Druckschwellversuch zur Beurteilung des Verformungsverhaltens von Belägen	2014
1503	VSS 2006/515_OBF	Research Package on Bridge Deck Waterproofing Systems: EP5-Mechanisms of Blister Formation	2014
1502	VSS 2010/502	Road – landside interaction : Applications	2014
1501	VSS 2011/705	Grundlagen zur Anwendung von Lebenszykluskosten im Erhaltungsmanagement von Strassenverkehrsanlagen	2014
1500	ASTRA 2010/007	SURPRICE (Sustainable mobility through road user charging) - Swiss contribution: Equity effects of congestion charges and intra-individual variation in preferences	2015
1499	ASTRA 2011/010	Stauprognoseverfahren und -systeme	2014
1498	VSS 2011/914	Coordinated Ramp Metering Control with Variable Speed Limits for Swiss Freeways	2014
1497	VSS 2009/705	Verfahren zur Bildung von homogenen Abschnitten der Strassenverkehrsanlage für das Erhaltungsmanagement Fahrbahnen	2014
1496	VSS 2010/601	Einfluss von Lärmschutzwänden auf das Raumnutzungs-verhalten von Reptilien	2014
1495	VSS 2009/703	Zusammenhang Textur und Griffigkeit von Fahrbahnen und Einflüsse auf die Lärmemission	2014

Bericht-Nr.	Projekt Nr.	Titel	Jahr
1494	VSS 2010/704	Erhaltungsmanagement der Strassen - Erarbeiten der Grundlagen und Schadenkataloge zur systematischen Zustandserhebung und -bewertung von zusätzlichen Objekten der Strassen	2014
1493	VSS 2006/001	Neue Methoden zur Beurteilung der Tieftemperatureigenschaften von bitumenhaltigen Bindemitteln	2014
1492	SVI 2004/029	Kombiniertes Verkehrsmittel- und Routenwahlmodell	2014
1491	VSS 2007/704	Gesamtbewertung von Kunstbauten	2014
1490	FGU 2004/002	Langzeit-Beständigkeit von Tunnel-Abdichtungssystemen aus Kunststoffen (Best TASK)	2014
1489	VSS 2006/516_OBF	Forschungspaket Brückenabdichtungen: EP6 - Anschlüsse von Brückenabdichtungen	2014
1488	SVI 2007/020	Methodik zur Nutzenermittlung von Verkehrsdosierungen	2014
1487	SVI 2008/001	Erfahrungsbericht Forschungsbündel	2014
1486	SVI 2004/005	Partizipation in Verkehrsprojekten	2014
1485	VSS 2007/401	Anforderungen an Anschlussfugensysteme in Asphaltdecken - Teil 1: Praxiserfahrung	2014
1484	FGU 2010/003	Misestimating time of collision in the tunnel entrance due to a disturbed adaptation	2014
1483	VSS 2005/452	Forschungspaket Recycling von Ausbauasphalt in Heissmischgut: EP1: Optimaler Anteil an Ausbauasphalt	2014
1482	ASTRA 2010/018	SURPRICE: Sustainable mobility through road user charges Swiss contribution: Comprehensive road user charging (RUC)	2015
1481	VSS 2001/702	Application des méthodes de représentation aux données routières	2014
1480	ASTRA 2008/004	Prozess- und wirkungsorientiertes Management im betrieblichen Strassenunterhalt Modell eines siedlungsübergreifenden Unterhalts	2014
1479	ASTRA 2005/004	Entscheidungsgrundlagen & Empfehlungen für ein nachhaltiges Baustoffmanagement	2014
1478	VSS 2005/455	Research Package on Recycling of Reclaimed Asphalt in Hot Mixes - EP4: Evaluation of Durability	2014
1477	VSS 2008/503	Feldversuch mit verschiedenen Pflästerungen und Plattendecken	2014
1476	VSS 2011/202	Projet initial pour la conception multi-usagers des carrefours	2014
1475	VSS 1999/125	Ringversuch "Eindringtiefe eines ebenen Stempels, statische Prüfung an Gussasphalt"	2014
1474	VSS 2009/704	Wechselwirkung zwischen Aufgrabungen, Zustand und Alterungsverhalten im kommunalen Strassennetz-Entwicklung eines nachhaltigen Aufgrabungsmanagement	2014
1473	VSS 2011/401	Forschungspaket "POLIGRIP - Einfluss der Polierbarkeit von Gesteinskörnungen auf die Griffigkeit von Deckschichten - Initialprojekt"	2014
1472	SVI 2010/003	Einfluss der Verlässlichkeit der Verkehrssysteme auf das Verkehrsverhalten	2014
1471	ASTRA 2008/011	Strategien zum wesensgerechten Einsatz der Verkehrsmittel im Güterverkehr Forschungspaket UVEK/ASTRA - Synthese	2014
1470	VSS 2011/907	Initialprojekt für ein Forschungspaket "Kooperative Systeme für Fahrzeug und Strasse"	2014
1469	VSS 2008/902	Untersuchungen zum Einsatz von Bewegungssensoren für fahrzeitbezogene Verkehrstelematik-Anwendungen	2014
1468	VSS 2010/503	Utilisation des géostructures énergétiques pour la régulation	2014

Bericht-Nr.	Projekt Nr.	Titel	Jahr
		thermique et l'optimisation énergétique des infrastructures routières et ouvrages d'art	
1467	ASTRA 2010/021	Sekundärer Feinstaub vom Verkehr	2014
1466	VSS 2010/701	Grundlagen zur Revision der Normen über die visuelle Erhebung des Oberflächenzustands	2014
1465	ASTRA 2000/417	Erfahrungen mit der Sanierung und Erhaltung von Betonoberflächen	2014
1462	ASTRA 2011/004	Ermittlung der Versagensgrenze eines T2 Norm-Belages mit der mobiles Grossversuchsanlage MLS10	2014
1460	SVI 2007/017	Nutzen der Verkehrsinformation für die Verkehrssicherheit	2014
1459	VSS 2002/501	Leichtes Fallgewichtsgerät für die Verdichtungskontrolle von Fundationsschichten	2014
1458	VSS 2010/703	Umsetzung Erhaltungsmanagement für Strassen in Gemeinden - Arbeitshilfen als Anhang zur Norm 640 980	2014
1457	SVI 2012/006	Forschungspaket VeSPA Teilprojekt 5: Medizinische Folgen des Strassenunfallgeschehens	2014
1456	SVI 2012/005	Fotschungspaket VeSPA Teilprojekt 4: Einflüsse des Wetters auf das Strassenunfallgeschehen	2014
1455	SVI 2012/004	Forschungspaket VeSPA Teilprojekt 3: Einflüsse von Fahrzeugeigenschaften auf das Strassenunfallgeschehen	2014
1454	SVI 2012/003	Forschungspaket VeSPA Teilprojekt 2: Einflüsse von Situation und Infrastruktur auf das Strassenunfallgeschehen: Phase 1	2014
1453	SVI 2012/002	Forschungspaket VeSPA Teilprojekt 1: Einflüsse von Mensch und Gesellschaft auf das Strassenunfallgeschehen: Phase 1	2014
1452	SVI 2012/001	Forschungspaket VeSPA: Synthesebericht Phase 1	2014
1450	VSS 2002/401	Kaltrecycling von Ausbauasphalt mit bituminösen Bindemitteln	2014
1448	SVI 2009/008	Anforderungen der Güterlogistik an die Netzinfrastruktur und die langfristige Netzentwicklung in der Schweiz. Forschungspaket UVEK/ASTRA "Strategien zum wesensgerechten Einsatz der Verkehrsmittel im Güterverkehr der Schweiz", Teilprojekt C	2014
667	AGB 2008/004	Résistance au déversement des poutres métalliques de pont	2015
666	AGB 2012/015	Structural Identification for Condition Assessment of Swiss Bridges	2015
665	AGB 2011/001	Wirksamkeit und Prüfung der Nachbehandlungsmethoden von Beton	2014
664	AGB 2009/005	Charges de trafic actualisées pour les dalles de roulement en béton des ponts existants	2014
663	AGB 2003/014	Seismic Safety of Existing Bridges	2014
662	AGB 2008/001	Seismic Safety of Existing Bridges - Cyclic Inelastic Behaviour of Bridge Piers	2014
661	AGB 2010/002	Fatigue limit state of shear studs in steel-concrete composite road bridges	2014
660	AGB 2008/002	Indirekt gelagerte Betonbrücken - Sachstandsbericht	2014
659	AGB 2009/014	Suizidprävention bei Brücken: Follow-Up	2014
658	AGB 2006/015_OBF	Querkraftwiderstand vorgespannter Brücken mit ungenügender Querkraftbewehrung	2014